“TIQXMMI” MILLIY TADQIQOT UNIVERSITETI HUZURIDAGI FUNDAMENTAL VA AMALIY TADQIQOTLAR INSTITUTI HUZURIDAGI ILMIY DARAJALAR BERUVCHI DSc.03/31.03.2022 T/FM.10.04 RAQAMLI ILMIY KENGASH

FUNDAMENTAL VA AMALIY TADQIQOTLAR INSTITUTI

ATAMUROTOV FARRUX SHUXRATOVICH

KOMPAKT OBYEKTLAR ATROFIDAGI PLAZMA MUHITIDA ASTROFIZIK JARAYONLAR

01.03.01-Astronomiya
01.04.02 – Nazariy fizika
(fizika-matematika fanlari)

E’lon qilingan ilmiy ishlar bo’yicha dissertatsiyasiz fan doktori (DSc) ilmiy darajasini olish uchun
TAQDIMNOMA

Toshkent - 2023

UDK 530.12:531.51

Fizika-matematika fanlari doktori (DSc) Taqdimnomasi mundarijasi

Table of Contents of Doctor of Science (DSc) Presentation in Physical and Mathematical Sciences

Содержание Представления доктора физико-математических наук (DSc)

“TIQXMMI” MILLIY TADQIQOT UNIVERSITETI HUZURIDAGI FUNDAMENTAL VA AMALIY TADQIQOTLAR INSTITUTI HUZURIDAGI ILMIY DARAJALAR BERUVCHI DSc.03/31.03.2022 T/FM.10.04 RAQAMLI ILMIY KENGASH

FUNDAMENTAL VA AMALIY TADQIQOTLAR INSTITUTI

ATAMUROTOV FARRUX SHUXRATOVICH

KOMPAKT OBYEKTLAR ATROFIDAGI PLAZMA MUHITIDA ASTROFIZIK JARAYONLAR

01.03.01-Astronomiya
01.04.02 – Nazariy fizika
(fizika-matematika fanlari)

E’lon qilingan ilmiy ishlar bo’yicha dissertatsiyasiz fan doktori (DSc) ilmiy darajasini olish uchun
TAQDIMNOMA

Toshkent –2023

Fizika-matematika fanlari doktori (DSc) dissertatsiyasi mavzusi O‘zbekiston Respublikasi Oliy ta’lim, fan va innovatsiyalar vazirligi huzuridagi Oliy attestatsiya komissiyasida B2023.2.DSc/FM224 raqami bilan ro‘yxatga olingan.

Taqdimnoma “TIQXMMI” Milliy tadqiqot universiteti huzuridagi fundamental va amaliy tadqiqotlar institutida bajarilgan.

Taqdimnoma uch tilda (o‘zbek, ingliz, rus (rezyume)) Ilmiy kengashning internet sahifasida (www.ifar.uz) va “Ziyonet” axborot-ta’lim portalida (www.ziyonet.uz) joylashtirilgan.

Ilmiy maslahatchilar:

Abdujabbarov Ahmadjon Adiljanovich
Fizika-matematika fanlari doktori, professor

Ahmedov Bobomurat Juraevich
Fizika-matematika fanlari doktori, professor

Taqdimnoma “TIQXMMI” Milliy tadqiqot universiteti huzuridagi Fundamental va amaliy tadqiqotlar instituti huzuridagi DSc.03/31.03.2022 T/FM.10.04 raqamli Ilmiy kengashning 2023-yil “_01_” _avgust_ soat _17^{00}_ dagi majlisida bo‘lib o‘tadi. (Manzil: 100000, Toshkent shahri, Qori Niyoziy ko‘chasi 39-uy, Fundamental va amaliy tadqiqotlar instituti, 108-katta majlislar zali; tel.: 71 237-09-61.; e-mail: info@ifar.uz

Taqdimnoma bilan “TIQXMMI” Milliy tadqiqot universiteti huzuridagi fundamental va amaliy tadqiqotlar instituti Axborot-resurs markazida tanishish mumkin (____ raqami bilan ro‘yxatga olingan). (Manzil: 100000, Toshkent shahri, Qori Niyoziy ko‘chasi, 39-uy, Fundamental va amaliy tadqiqotlar instituti, 205- kutubxona; tel.: 71 237-09-61

Dissertatsiya avtoreferati 2023-yil “___” _____ kuni tarqatildi.
(2023-yil “___”_____dagi ___ raqamli reestr bayonnomasi)

A.R. Hayotov
Ilmiy darajalar beruvchi ilmiy
kengash raisi o’rinbosari f.-m.f.d., professor

E. X. Karimbayev
Ilmiy darajalar beruvchi ilmiy
kengash ilmiy kotibi f.-m.f. bo‘yicha PhD

KIRISH (Fan doktori (DSc) taqdimnoma annotatsiyasi)

Mavzuning dolzarbligi. Qora tuynuklar kuchli maydon rejimida tortishish kuchini o‘rganish uchun tajribaviy maydon bo‘lib xizmat qiladi va tadqiqotchilarga fazoviy vaqt tabiati haqida muhim tushunchalarga ega bo‘lish imkonini beradi. Qora tuynuklar yaqinidagi zarralarning harakatini o‘rganish orqali biz uning atrofdagi fazoning tuzilishi haqida yangi ma’lumotlarni ochib bera olamiz. Umumiy nisbiylik nazariyasining yorug’likning gravitatsion egilishi haqidagi tahminlardan birining natijasi bo‘lgan qora tuynuk soyasining mavjudligi ushbu hodisani tekshirish imkoniyatini beradi. Natijada, qora tuynuk soyasini o‘rganishda ushbu fazoda kuchga ega bo‘lmagan geodeziyani tahlil qilish hal qiluvchi ahamiyatga ega bo‘ladi. Qora tuynuklarning yaqin atrofini kesib o‘tuvchi fotonlar yorug’lik halqalari deb nomlanuvchi dumaloq orbitalarni namoyon qiladi. Ushbu yorug’lik halqalari natijasida markaziy qora tuynuk fonda qorong’u disk sifatida paydo bo‘ladi va bu odatda qora tuynuk soyasi deb ataladi.

Qora tuynuklarning massalarini aniqlash masalasi muvaffaqiyatli hal qilindi, natijada qora tuynuklar massalari bo‘yicha to‘rt toifaga bo‘lindi: yulduzsimon, oraliq massali, o‘ta massiv va kichik massali. Biroq, aylanuvchi qora tuynuklarning aylanishini o‘lchash vazifasi hali ham davom etmoqda va qora tuynuk soyalarini o‘rganish bu urinishda yordam berishi mumkin deb ishoniladi. Yaqinda qora tuynuk tizimlarini birlashtirish natijasida chiqarilgan tortishish to‘lqinlarining aniqlanishi va M87* va Sgr A* kabi markaziy supermassiv qora tuynuklar tomonidan olingan soyalarning tasviri qora tuynuk fazo vaqtlarining xususiyatlarini o‘rganish uchun qo‘shimcha ishtiyoq uyg’otdi.

Qora tuynuklar yaqinida fotonlar ko‘pincha plazma muhitini kesib o‘tganda qiziqarli astrofizik vaziyat yuzaga keladi. Ushbu plazma muhitida qora tuynuk soyasining paydo bo‘lgan tasvirining burchak pozitsiyalariga sezilarli darajada ta’sir qilishi mumkin, bu esa kuzatilgan to‘lqin uzunliklarining o‘zgarishiga olib keladi. Natijada, plazma muhitini kiritish qora tuynuk soyalarini tahlil qilishda muhim ahamiyatga ega bo‘ladi. Qora tuynuklar chiqaradigan reaktiv oqimning paydo bo‘lishini o‘rganish uchun tadqiqotchilar qora tuynuk muhitida soddalashtirilgan plazma modelidan foydalanganlar.

Boshqa tarafdan, qora tuynuklar muhim subyektlar sifatida termodinamika sohasida juda qiziq obyektlar sifatida ajralib turadi. Qora tuynuklar fizikasini boshqaradigan printsiplar termodinamika tamoyillariga o‘xshashdir, ular yuza tortishish kuchi, massa-energiya ekvivalenti, harorat va entropiyaga tegishli bo‘lgan fazolar gorizonti maydoni o‘rtasidagi bog’liqlikni o‘rnatadi. Ushbu taqqoslashlar Bekenshteynni fazolar gorizonti maydoni va qora tuynuk entropiyasi o‘rtasidagi miqdoriy bog’liqlikni taklif qilishga olib keldi. Biroq, bu taklif qilingan munosabat termodinamikaning ikkinchi qonuniga zid ko‘rinadi, chunki qora tuynukdan hech qachon hech narsa chiqarib bo‘lmaydi, bu esa qora tuynuklar va issiqlik nurlanish

issiqlik muvozanatga erisha olmasligini ko‘rsatadi. Shunga qaramay, qora tuynuklarning kvant darajasidagi tadqiqotlari Xoking nurlanishi deb ataladigan subatomik zarrachalarning ajralib chiqishini ochib beradi va qora tuynuklarning geometrik xususiyatlari haqida tushuncha beradi. Shunday qilib, kompakt astrofizik obyektlar atrofidagi fazoning strukturaviy va termodinamik xususiyatlarini o‘rganish gravitatsiyaviy o‘zaro ta’sirning tabiatini chuqur tushunishga olib kelishi mumkin.

Ta’kidlash joizki, keyingi yillarda mamlakatimizda fundamental va amaliy tadqiqotlarning dolzarb yo‘nalishlarini rivojlantirishga tobora ko‘proq e’tibor qaratilmoqda. Xususan, istiqbolli yo‘nalishlardan biri bo‘lgan nazariy astrofizik tadqiqotlarni rivojlantirish bugungi kunning muhim masalasidir. Mamlakatimizda ilm-fanni muvaffaqiyatli rivojlantirish bo‘yicha fundamental tadqiqot va ishlanmalarning asosiy yo‘nalishlari va ularni amaliyotda qo‘llash 2022-2026-yillarda O‘zbekiston Respublikasini yanada rivojlantirish bo‘yicha Strategiyada o‘z ifodasini topgan. Shuning uchun plazma muhitida gravitatsiyaviy linzalarning ta’sirini o‘rganish fundamental tadqiqotlar sohasidagi dolzarb masalalardan biri bo‘lib qolmoqda.

Mazkur ilmiy tadqiqot ishi quyidagi davlat me’yoriy hujjatlari bilan belgilangan vazifalarga mos keladi: O‘zbekiston Respublikasi Prezidentining 2017-yil 07-fevraldagi “O‘zbekiston Respublikasini yanada rivojlantirish bo‘yicha harakatlar strategiyasi to‘g’risida”gi PF-4947-son Farmoni, O‘zbekiston Respublikasi Prezidentining 2017-yil 18-fevraldagi “Fanlar akademiyasi faoliyatini yanada takomillashtirish, ilmiy-tadqiqot faoliyatini tashkil etish, boshqarish va moliyalashtirish chora-tadbirlari to‘g’risida”gi PQ-2789-son qarori va boshqalar.

Tadqiqotning Respublika fan va texnikasini rivojlantirishning asosiy ustuvor yo‘nalishlariga muvofiqligi. Dissertatsiya tadqiqoti O‘zbekiston Respublikasi fan va texnikasining ustuvor yo‘nalishlariga muvofiq olib borilgan: II. "Quvvat, energiya va resurslarni tejash".

Muammoni bilish darajasi. Foton harakati va kompakt obyekti atrofidagi tortishish linzalari butun dunyo bo‘ylab turli tadqiqotchilar tomonidan o‘rganilgan (J. Synge, J. Bardeen, X. Falcke, O. Tsupko, V. Bozza, Z. Stuchlik, J, Schee, A. Abdujabborov, B. Ahmedov, V. Morozova, C. Laemmerzal, J. Kunz, A. Grezenbach, L. Amarilla, E. Eiroa, M. Kolos, J. Vrba, N. Dadhich, S. Ghosh, P. Joshi, M. Patil). Biroq, plazmaning kompakt obyekt atrofida foton harakatiga ta’siri turli modellar va nazariyalarda tizimli ravishda o‘rganilmagan.

Kerr-Newman qora tuynugining fotonlar harakat tenglamalari turli mualliflar (Z. Stuchlik, S. Hledik, A. de-Vries va boshqalar) tomonidan to‘g’ri o‘rganilgan. Fotonlar harakat tenglamalari va qora tuynuk soyalari kabi qora tuynuklarning optik xossalarini o‘rganish, aylanuvchi qora tuynuk fazo vaqtlarida faol tadqiqot mavzusi bo‘lib qolmoqda va turli tadqiqotchilar tomonidan o‘rganilgan (A. Belhaj, M. Benali, J. Luminet va boshqalar). Shu bilan birga, plazma muhitining va muqobil

nazariyalarining turli parametrlarining soya va unga bog'liq hodisalarga ta'siri masalasi hali o'rganilmagan.

Qora materiyaning muntazam qora tuynuk atrofidagi astrofizik jarayonlarga ta'siri ham o'rganilmagan. Bunday obyektlar atrofidagi zarrachalar dinamikasini tavsiflovchi matematik modellarni ishlab chiqish va takomillashtirish, modifikatsiyalangan va/yoki muqobil nazariyalarining parametrlari uchun chegara qiymatlarini olishga yordam beradi.

Dissertatsiya mavzusini ushbu mavzuda dissertatsiya olib borilayotgan oliy o'quv yurtlari va ilmiy-tadqiqot muassasalarining ilmiy ishlari bilan bog'lash. Dissertatsiya Innovatsion rivojlanish vazirligi tomonidan moliyalashtirilgan ilmiy loyihalar doirasida bajarilgan. F-FA-2021-510 "Modifikatsiyalangan gravitatsiya nazariyasi doirasida neytron yulduzlardagi yadro moddalarini tadqiq etish".

Tadqiqotning maqsadi plazma mavjud bo'lgan kompakt obyekt atrofida fotonlar va zaif gravitatsion linzalari dinamikasi modelini ishlab chiqish va takomillashtirish, tortishish modellarining parametrlarini kuzatishdan foydalangan holda cheklashdir.

Tadqiqot vazifalari:

Kerr-Newman-Kiselev-Letelier qora tuynuk fazosidagi foton harakatini va unga bog'liq qora tuynuk soyasi hodisalarini o'rganish;

Torli bulut parametri va asosiy mohiyat parametrining foton harakati va qora tuynuk soyasiga ta'sirini tahlil qilish.

Kiselev va torli bulut parametrlari mavjudligida fotonning effektiv potensialini tahlil qilish

Kerr-Newman-Kiselev-Letelier qora tuynugida torli bulut va Kiselev parametrlarining yuqori chegaralarini olish.

Kerr-Newman-Kiselev-Letelier qora tuynugining aylanishini va zaryadining ajraluvchi energiya tezligiga ta'sirini o'rganish.

Torli bulut parametrining Xoking nurlanish jarayoniga ta'sirini o'rganish

qora tuynuk atrofidagi fotonlar va tegishli jarayonlar dinamikasiga mukammal suyuqlik qorong'u materiya parametrining ta'sirini tahlil qilish.

mukammal suyuqlik qorong'u materiya parametri va chiziqli bo'lmagan zaryad mavjudligida nurlanishni o'rganish.

magniztlangan plasmada fonida aylanmaydigan qora tuynuk atrofidagi fotonlar dinamikasiga ta'sirini tahlil qilish.

bir jinsli va bir jinsli bo'lmagan plazmaning fotonlar harakati va gravitatsion obyektlar atrofidagi gravitatsion linzalariga ta'sirini o'rganish.

Bir jinsli plazma, bir jinsli bo'lmagan (singulyar izotermik sfera va non-izotermik sfera) bilan o'ralgan gravitatsion jismlari fonida zaif gravitatsion linzalanish hodisasini tizimli tahlil qilish.

teleparallel tortishish qonuni uchun Xoking haroratining harakatini o'rganish

Nochiziqli elektrodinamikada umumiy nisbiylik bilan bog'langan chiziqli bo'lmagan zaryad va bog'lovchi parametrining yig'ilish samaradorligiga ta'sirini tahlil qilish.

Tadqiqot obyekti bu astrofizik kompakt obyektlar, fotonlar, plazma muhiti.

Tadqiqot predmeti bu plazma ishtirokida kompakt gravitatsion obyektlar yaqinida foton dinamikasini o'rganishning nazariy modellari, differentsial tenglamalarni yechishning raqamli va analitik usullari hisoblanadi.

Tadqiqot metodi bu hisoblash matematikasi metodlari, nazariy astrofizika usullari, matematik fizikaning zamonaviy metodlari, maydon va zarrachalar harakati uchun differentsial tenglamalarni hisoblashning analitik va raqamli metodlaridan iborat.

Tadqiqotning ilmiy yangiligi quyidagilardan iborat:

Kerr-Newman-Kiselev-Letelier qora tuynugining gorizonti kattaligi Kiselev va torli bulut parametrlarining ortishi bilan ortib borishi ko'rsatilgan.

Fotonning effektiv potentsialini tahlil qilish shuni ko'rsatdiki, u Kiselev va torli bulut parametrlarining ortib borayotgan qiymatlari bilan kamayib bormoqda. Kiselev va torli bulut parametrlarining ortib borayotgan qiymatlari uchun foton orbitalarining ham kamayadi.

Torli bulut parametri Xoking radiatsiya jarayonini tezlashtirishi ko'rsatilgan. Ko'rsatilishicha, mukammal suyuqlik qorong'u materiya parametri, zaryad va aylanish parametrlari ortishi bilan effektiv potentsialning cho'qqisi chapga siljiydi.

Yorug'likning nurlanishi ham mukammal suyuqlikning qorong'u materiya parametri va zaryadining kichik qiymati uchun yuqori ekanligi kuzatildi. Ko'rsatilishicha, qora tuynuk soyasining o'lchami katta kuzatuvchi masofasi uchun magnitlangan plasma ortishi bilan kamayib boradi va qizig'i, bu avvalroq bir jinsli bo'lmagan plazma uchun ham ko'rsatilgan.

Bundan tashqari, bir jinsli plazma uchun aksion chastotasi oshishi bilan og'ish burchagi ortadi. Singular izotermik sferalik plasmaning ta'siridagi og'ish burchagi ma'lum darajada Singular bo'lmagan izotermik sferalik plasmaga qaraganda kattaroq ekanligi ko'rsatildi, garchi bu holatda farqni ahamiyatsiz deb hisoblash mumkin.

Qora tuynukda bir jinsli plazma devorlari paydo bo'lganda, fotonlar kattaroq burchak ostida og'ishi ta'kidlangan. Bundan tashqari plazmaning ta'siri natijasida foton sferasi radiusi, og'ish burchagi va kuchli og'ish koeffitsientlari oshishi ko'rsatilgan.

Teleparallel nazariyasi bog'lanish parametri kamayishi bilan Xoking haroratining oshishi ko'rsatilgan. Nochiziqli zaryad va bog'lanish parametrining ortishi bilan to'planish samaradorligi pasayishi ko'rsatilgan.

Tadqiqotning amaliy natijalari quyidagilardan iborat:

Ko'rsatilgandek, soyaning buzilish parametri Kiselev va torli bulut parametrlarining oshishi bilan kamayadi. Tez aylanadigan va yuqori zaryadlangan

qora tuynukning soyasi ko‘proq buzilib ketishi ko‘rsatilgan. Ushbu kuzatish a aylanishning qiymatlarini va qora tuynuklarning zaryadini baholash uchun foydali bo‘lishi mumkin.

Aylanma qora tuynuk holatida soyaning o‘lchami qora tuynuk zaryadi bilan bir qatorda mukammal suyuqlik qorong’u materiya parametri qiymatining oshishi bilan kamayishi kuzatildi.

Hodisalar gorizonti teleskopi (Event Horizon Telescope) hamkorlik ma’lumotlaridan foydalanib, biz Kerr-Newman-Kiselev-Letelier qora tuynuk misolida torli bulut va Kiselev parametrlarining yuqori chegaralarini oldik.

Eynshteyn halqalarining o‘lchami mukammal suyuqlik qorong’u materiya parametrining oshishi bilan kamayishi ko‘rsatilgan.

Tadqiqot natijalarining ishonchliligi bu matematik fizika, hisoblash matematikasi va relyativistik astrofizikaning zamonaviy tasdiqlangan usullarini qo‘llash orqali ta’minlanadi. Natijalar qat’iy ravishda umumiy nisbiylik va nazariy fizikaning matematik apparati doirasida olingan. Hisoblashning zamonaviy raqamli va analitik usullari ham qo‘llaniladi va natijalar mavjud kuzatuv ma’lumotlari va boshqa mualliflarning natijalari bilan taqqoslanadi. Ishning tuzilgan xulosalari kompakt obyektlar astrofizikasining asosiy qoidalariga mos keladi.

Tadqiqot natijalarining ilmiy va amaliy ahamiyati. Tadqiqot natijalarining ilmiy ahamiyati shundaki, tez aylanadigan va zaryadlangan qora tuynuk tomonidan soyaning tahlili aylanishning qiymatlarini va qora tuynuklarning zaryadini baholash uchun foydali bo‘lishi mumkin.

Tadqiqot natijalarining amaliy ahamiyati shundaki, ular o‘zgartirilgan gravitatsion nazariyasi doirasida bulut qatori va Kiselev parametrlarining yuqori chegaralari va cheklovlarini olishda ro’l o‘ynashi mumkin.

Tadqiqot natijalarini amalga oshirish. Plazma ishtirokida kompakt obyektlar atrofidagi fotonlarning dinamikasi uchun ishlab chiqilgan nazariy modellar asosida:

fotonlar harakati bo‘yicha olingan ilmiy natijalar Shanxaydagi Fudan universiteti (FU) olimlari tomonidan qo‘llanildi (FU, Xitoy, 2023 yil 7 iyul ma’lumotnomasi);

kompakt obyektlar atrofidagi gravitation linzalari bo‘yicha natijalar xorijiy tadqiqotchilarning ishlarida, yuqori impakt faktorli xorijiy jurnallarda plazmaning ixcham obyektlar atrofidagi foton harakatiga ta’sirini tasvirlash uchun ishlatilgan (Physical Review D, 2023, 107-jild, 12-son, id.124003, Web-Sc, IF: 5.407 Qirollik Astronomiya Jamiyatining oylik xabarlari, 521-jild, 1-son, 708-716-betlar, Web-Sc, IF: 4.8; Zulmat olam fizikasi, 41-jild, maqola id.101249, Web-Sc, IF:5. Yevropa fizik jurnali C, 83-jild, 5-son, id.426, Web-Sc, IF: 4.4;The European Physical Journal Plus, 138-jild, 3-son, id.192, Web-Sc, IF:3.4. Kosmologiya va astropartikullar fizikasi jurnali, 2021-jild, 10-son, id.013, 26-bet, Web-Sc, IF: 7.28).

Tadqiqot natijalarini nashr etish. DSc tadqiqoti natijalari O‘zbekiston Respublikasi Oliy ta’lim, fan va innovatsiyalar vazirligi huzuridagi Oliy attestatsiya komissiyasi tomonidan tavsiya etilgan nufuzli Q1/Q2 tipdagi ilmiy jurnallarida chop etilgan 24 ta ilmiy maqolalarda taqdim etilgan.

Ishning asosiy tarkibi

I qism.

Plazma bilan o‘ralgan kompakt obyekt fonida gravitatsion linzalarning ta’sirini quyidagi tarzda aniqlangan zaif maydonida olgan holda ko‘rib chiqamiz:

$$g_{\alpha\beta} = \eta_{\alpha\beta} + h_{\alpha\beta} \quad (1)$$

bu yerda $\eta_{\alpha\beta}$ va $h_{\alpha\beta}$ mos ravishda Minkovski fazo-vaqti va g’alayonlangan fazo-vaqtini bildiradi.

$$\begin{aligned} &\eta_{\alpha\beta} = \mathrm{diag}(-1,1,1,1), \\ &h_{\alpha\beta} \ll 1,\ h_{\alpha\beta} \to 0 \ \text{under}\ x^{\alpha} \to \infty, \\ &g^{\alpha\beta} = \eta^{\alpha\beta} - h^{\alpha\beta},\ h^{\alpha\beta} = h_{\alpha\beta}. \end{aligned} \quad (2)$$

Davom etishdan oldin, og’ish burchagining umumiy ifodasini aniqlash uchun (Bisnovatyi-Kogan and Tsupko, Mon. Not. R. Astron. Soc. 2010) da keltirilgan sxemani qisqacha eslaymiz. Statik holatni hisobga olgan holda faza tezligi $\boldsymbol{v}$ va 4-impuls $\boldsymbol{p^{a}}$ o‘rtasidagi korrelyatsiya quyidagicha ifodalanadi:

$$\frac{c^2}{\boldsymbol{v}^2} = n^2 = 1 + \frac{p_\alpha \boldsymbol{p}^\alpha}{\left(\boldsymbol{p}^0\sqrt{-g_{00}}\right)^2} \quad (3)$$

Dispersiv muhitni hisobga olgan holda, Synge (Synge, Relativity 1960) foton traektoriyalarini tasvirlash uchun Fermatning eng kam harakat tamoyilini qayta ishlab chiqdi. Bundan buyon $\partial(\int p_\alpha dx^\alpha) = 0$ o‘zgaruvchanlik printsipi quyidagi shart bilan qo‘llaniladi:

$$H(x^\alpha, \boldsymbol{p}_\alpha) = \frac{1}{2}\left[g^{\alpha\beta}\boldsymbol{p}_\alpha\boldsymbol{p}_\beta - (n^2-1)\left(\boldsymbol{p}_0\sqrt{-g_{00}}\right)^2\right] \quad (4)$$

Yuqoridagi ifoda harakat tenglamalarini quyidagi differensial tenglamalar tizimi $\frac{dx^\alpha}{d\lambda} = \frac{\partial H}{\partial p_\alpha}$, $\frac{dp_\alpha}{d\lambda} = -\frac{\partial H}{\partial x^\alpha}$ bilan boshqaradi, bu yerda λ afin parametrdir. Qora tuynuk yaqinida plazma effektlarini aniq o‘rganish uchun *n* sindirish ko’rsatgichi to‘g’ri aniqlash juda muhim, shuning uchun havolalarga (Bisnovatyi-Kogan and Tsupko, Mon. Not. R. Astron. Soc. 2010) tayanib, biz uni quyidagicha aniqlaymiz:

$$n^2 = 1 - \frac{\omega_e^2}{\left[\omega(x^i)\right]^2},\ \omega_e^2 = \frac{4\pi e^2 N(x^i)}{m} = K_e N\left(x^i\right) \quad (5)$$

Bu yerda *we* plazma elektron chastotasi va $w(x^i)$ foton chastotasi hisoblanadi. *e*, *m* va $N(x^i)$ belgilari mos ravishda electron zaryad, massa va elektron konsentratsiyasini bildiradi. $w^2 > w_e^2$ tengsizligining haqiqiyligi yorug’likning plazma muhiti orqali tarqalishida markaziy o‘rinni egallaydi. Statik muhit bilan aylanmaydigan

gravitatsion maydonini ko‘rib chiqayotganda, foton energiyasi quyidagini bo’ladi (Synge, Relativity 1960)

$$\boldsymbol{p}^0\sqrt{-g_{00}} = -\frac{1}{c}\hbar\omega\left(x^i\right) \tag{6}$$

(5) va (6) tenglamalar foydalanib, skalyar $H(x^\alpha, p_\alpha)$ quyidagi shaklni oladi

$$H(x^\alpha, \boldsymbol{p}_\alpha) = \frac{1}{2}\left[g^{\alpha\beta}\boldsymbol{p}_\alpha\boldsymbol{p}_\beta + \frac{\omega_e^2\hbar^2}{c^2}\right] \tag{7}$$

bu yerda *h* bu Plank doimiysi. Odatda, har qanday ixtiyoriy muhit uchun yassi fazo-vaqtdagi fotonlar to‘g’ri yo‘l bo‘ylab harakatlanadi, boshqa tomondan, egri fazo-vaqtda egilgan traektoriyalar kuzatiladi. Shunday qilib, biz harakatni *z* o‘qi bo‘ylab qabul qilamiz va to‘g’ri yo‘ldan kichik og’ishlarga yo‘l qo‘ymaslik uchun nolga yaqinliklarni (Bisnovatyi-Kogan and Tsupko, Mon. Not. R. Astron. Soc. 2010) olamiz. Bu holda 4-impulsning tarkibiy qismlari quyida keltirilgan:

$$\boldsymbol{p}^\alpha = \left(\frac{\hbar\omega}{c}, 0,0, \frac{n\hbar\omega}{c}\right),\ \boldsymbol{p}_\alpha = \left(-\frac{\hbar\omega}{c}, 0,0, \frac{n\hbar\omega}{c}\right) \tag{8}$$

E’tibor bersangiz, bo‘lajak muhokamada biz quyidagicha maxsus belgilardan foydalanamiz; $\omega(\infty) = \omega$, $\omega_e(\infty) = \omega_0$ va $n(\infty) = \sqrt{1-\omega_0^2/\omega^2}$. Biz diagonal metrikani ko‘rib chiqayotganimiz uchun $g_{\alpha\beta}$ metrik tensorining komponentlari barcha $\alpha \neq \beta$ uchun to’gri keladi. Demak, (7)-tenglamadan foydalangandan so‘ng biz quyidagi tenglamalar to‘plamini olamiz

$$\begin{aligned} \frac{dx^i}{d\lambda} &= g^{ij}\boldsymbol{p}_j, \\ \frac{d\boldsymbol{p}_i}{d\lambda} &= -\frac{1}{2}g_{,i}^{lm}\boldsymbol{p}_l\boldsymbol{p}_m - \frac{1}{2}g_{,i}^{00}\boldsymbol{p}_0^2 - \frac{1}{2}\frac{\hbar^2}{c^2}K_eN, i. \end{aligned} \tag{9}$$

Fotonlar uchun harakat tenglamalarini yaqinlashish (9)-tenglamaga qo‘llanilgandan so‘ng quyidagiga kamayadi:

$$\frac{dz}{d\lambda} = \frac{n\hbar\omega}{c} \tag{10}$$

3 o‘lchovli standart birlik vektor $\boldsymbol{u}^i = \boldsymbol{u}_i = (0,0,1)$ bo‘yicha foton impulsi quyidagicha ifodalanishi mumkin:

$$\boldsymbol{p}_i = \frac{n\hbar\omega}{c}(0,0,1) = \frac{n\hbar\omega}{c}\boldsymbol{u}_i. \tag{11}$$

Yuqoridagi tenglamani (9) ga almashtirib, quyidagini hosil qilamiz:

$$\frac{d}{d\lambda}\left(\frac{n\hbar\omega}{c}\boldsymbol{u}_i\right) = -\frac{1}{2}g_{,i}^{lm}\boldsymbol{p}_l\boldsymbol{p}_m - \frac{1}{2}g_{,i}^{00}\boldsymbol{p}_0^2 - \frac{1}{2}\frac{\hbar^2}{c^2}K_eN, i. \tag{12}$$

Ya’ni, yuqoridagi farazlar tufayli harakat faqat z o‘qi bo‘ylab sodir bo‘ladi, biz faqat birlik vektorining tarqalishning boshlang’ich yo‘nalishiga perpendikulyar bo‘lgan komponentlarini ko‘rib chiqish bilan cheklanamiz. Nihoyat, zaif gravitatsion maydoniga (12)-tenglama qo‘shimcha ravishda fotonlar uchun harakat tenglamlari yaqinlashuvga rioya qilish kabi ko‘rinadi:

$$\frac{d\boldsymbol{u}_i}{dz} = \frac{1}{2}\left(h_{33,i} + \frac{1}{n^2}h_{00,i} - \frac{1}{n^2\omega^2}K_eN_{,i}\right),\ i = 1,2. \tag{13}$$

Og’ish burchagi asosan $a = \mathbf{u}_{+\infty} - \mathbf{u}_{-\infty}$ bilan belgilanadi, shuning uchun (13) bizni quyidagi umumiy ifodaga olib keladi

$$\hat{\alpha}_i = \frac{1}{2}\int_{-\infty}^{\infty}\left(h_{33,i} + \frac{\omega^2}{\omega^2-\omega_e^2}h_{00,i} - \frac{K_e}{\omega^2-\omega_e^2}N,i\right)dz \quad (14)$$

$\hat{\alpha}_i$ ning $\pm$ belgilari mos ravishda markaziy obyekt tomon va undan uzoqlashishni aniqlaydi.

Ushbu formalizmni qo‘llash sifatida D-o‘lchovli Eynshteyn-Gauss-Bonnet nazariyasini qayta aniqlangan bog’lanish doimiysi $\alpha \to \alpha/(D-4)$ bilan hisobga olingan holda, uning harakati quyidagi munosabat bilan ifodalanadi:

$$\mathcal{S} = \frac{1}{16\pi}\int\ d^Dx\sqrt{-g}\left(R + \frac{\alpha}{D-4}\mathcal{G}\right) \quad (15)$$

bu yerda α o‘lchamsiz Gauss-Bonnet (GB) bog’lanish parametri va *G* ifoda bilan aniqlangan Gauss-Bonnet invariantidir.

$$\mathcal{G} = R^{\mu\nu\eta\rho}R_{\mu\nu\eta\rho} - 4R^{\mu\nu}R_{\mu\nu} + R^2 \quad (16)$$

R bu yerda Ricci skalyar, $R_{\mu\nu}$ va $R_{\mu\nu np}$ mos ravishda Ricci va Riemann tensorlarini bildiradi. 4 o‘lchovli tahlildagi S harakati aylanmaydigan 4D-EGB tortishishning chiziqli elementini shaklda beradi

$$ds^2 = -f(r)dt^2 + f^{-1}(r)dr^2 + r^2(d\theta^2 + \sin^2\theta d\phi^2) \quad (17)$$

bu yerda

$$f(r) = 1 + \frac{r^2}{2\alpha}\left(1 - \sqrt{1 + \frac{4\alpha R_s}{r^3}}\right) \quad (18)$$

bu yerda R_s = 2M, GB parametrining qiymati α/M^2 esa [-8,1] oralig’ida yotadi. E’tibor bersangiz, α>1 yalang’och singulyarliklarga mos keladi va α<8 hodisa gorizontining tashqi hududidagi murakkab qiymatli metrikaga olib keladi. Bundan tashqari, Shvartsshild ko‘rsatkichi α→0 bo‘lganda qayta tiklanadi. Batafsilroq baholash uchun biz *f(r)* qatorga yoyamiz va $O(R^3)$ tartibigacha olamiz,

$$f(r) = 1 - \frac{R_s}{r} + \frac{\alpha R_s^2}{r^4} \quad (19)$$

Biz katta masofalarda qaraymiz, shuning uchun qora tuynuk metrikasi quyidagicha yozish mumkin

$$ds^2 = ds_0^2 + \left(\frac{R_s}{r} - \frac{\alpha R_s^2}{r^4}\right)dt^2 + \left(\frac{R_s}{r} - \frac{\alpha R_s^2}{r^4}\right)dr^2 \quad (20)$$

Bu yerda $d(s_0)^2 = -dt^2 + dr^2 + r^2(d\theta^2 + \sin^2\theta d\phi^2)$ ga teng. Dekart koordinatalarida $h_{\alpha\beta}$ komponentlarini quyidagi tarzda yozish mumkin

$$\begin{aligned} h_{00} &= \left(\frac{R_s}{r} - \frac{\alpha R_s^2}{r^4}\right), \\ h_{ik} &= \left(\frac{R_s}{r} - \frac{\alpha R_s^2}{r^4}\right)n_i n_k, \\ h_{33} &= \left(\frac{R_s}{r} - \frac{\alpha R_s^2}{r^4}\right)\cos^2 x, \end{aligned} \quad (21)$$

bu yerda $\cos x = z/\sqrt{b^2+z^2}$ va $r = \sqrt{b^2+z^2}$, *b* esa qora tuynukga fotonlarning eng yaqin yaqinlashishini bildiruvchi ta’sir parametri. (14)-formuladagi yuqorida qayd etilgan ifodalardan foydalanib, plazma bilan o‘ralgan qora tuynuk uchun *b* ga nisbatan yorug’likning og’ish burchagini hisoblash mumkin (Babar et al. PDU 2021)

$$\hat{\alpha}_b = \int_{-\infty}^{\infty} \frac{b}{2r}\left(\partial_r\left(\left(\frac{R_s}{r} - \frac{\alpha R_s^2}{r^4}\right)\cos^2 x\right) + \partial_r\left(\frac{R_s}{r} - \frac{\alpha R_s^2}{r^4}\right)\frac{\omega^2}{\omega^2-\omega_e^2} - \frac{K_e}{\omega^2-\omega_e^2}\partial_r N\right) dz \tag{22}$$

Bir jinsli Plazma. Avvalo, plazma qora tuynuk atrofida bir tekis taqsimlanganda foton geodeziyasini ko‘rib chiqamiz. Bir jinsli plazma muhitida sindirish ko‘rsatkichi *n* ayniqsa w_0 bo‘lgan foton chastotasini doimiy miqdor sifatida hisoblaydi va natijada 1– n << w_0/w ga yaqinlashishiga olib keladi. Oqibatda, tegishli cheklovlar quyidagilarni yo‘q qiladi. $\partial_r N$ atamasi va og’ish burchagi quyidagi shaklni oladi (Babar et al. PDU 2021)

$$\hat{\alpha}_{\text{uni}} = \left(\frac{R_s}{b} - \frac{3\pi\alpha R_s^2}{16b^4}\right) + \left(\frac{R_s}{b} - \frac{3\pi\alpha R_s^2}{4b^4}\right)\frac{1}{\left(1-\frac{\omega_0^2}{\omega^2}\right)}. \tag{23}$$

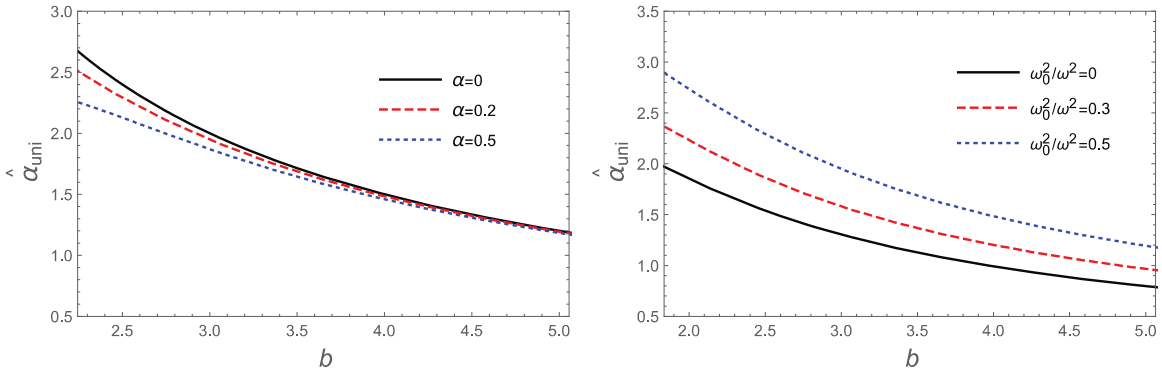

1-rasm: Og’ish burchakning ta’sir paramtri *b* bog’langan grafikini har xil GB paramaetrlari uchun (chap tomonda) va plasma parametri (o‘ng tomonda) uchun keltirilgan.

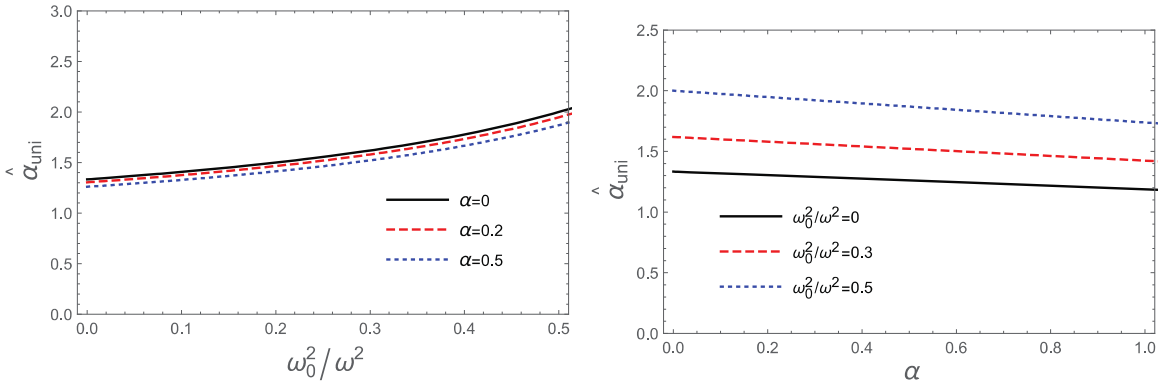

2-rasm: Og’ish burchakning bir jinsli plasma parametri (chap tomonda) va GB parametri (o‘ng tomonda)ga bog’langan grafiki keltirilgan.

(1)-rasmda α (o’ng tomonda) va plazma parametrlari ω_0^2/ω^2 (chap tomonda) uchun *b* ta’sir parametrining funksiyasi sifatida fotonning og’ish burchagi α_{uni} chizmalari

tasvirlangan. *b* ta'sir parametrining kichikroq qiymatlari uchun og'ish burchagida o'sish tekshiriladi, ya'ni qora tuynuk atrofiga juda yaqin o'tadigan massasiz zarracha, asosan, uning og'ish tendentsiyasini kuchaytiradi. 2-rasmda ω_0^2/ω^2 va α ga nisbatan og'ish burchagining aniq tasviri hisoblanadi. Og'ish burchagi yuqori plazma taqsimoti (o'ng tomonda) tufayli maksimal bo'ladi va α (chap tomonda) ortib borayotgan bog'lanish parametriga nisbatan qat'iy pasayganligi ko'rinadi, masalan, α = 0 bo'lsa, Shvartsshild gravitatsiyasi eng yuqori og'ish darajasi α^{uni}ni ta'minlaydi. Kutilganidek, qora tuynuk yaqinida plazma mavjudligi, ω_0^2/ω^2 vakuum holatidan farqli o'laroq, foton harakatiga hissa qo'shadi, deb xulosa qilamiz.

Yakka izotermik sfera. Yakka izotermik sfera (singular isothermal sphere α_{SIS}) gravitatsion linzali fotonlarning o'ziga xos xususiyatlarini tushunish uchun eng qulay modeldir. U birinchi navbatda (Bisnovatyi-Kogan and Tsupko, Mon. Not. R. Astron. Soc. 2010) da galaktikalar va klasterlarning linzalar xususiyatini o'rganish uchun kiritilgan. Umuman olganda, SIS sferik gaz buluti bo'lib, uning markazida zichligi cheksizlikka intiladigan yagona xususiyatga ega. SISning zichlik taqsimoti quyidagi formulalarda tomonidan berilgan:

$$\rho(r) = \frac{\sigma_v^2}{2\pi r^2} \tag{24}$$

Bu yerda σ^2_v bir o'lchovli tezlik dispersiyasiga ishora qiladi. Plazma konsentratsiyasi quyidagi analitik ifodani qabul qiladi

$$N(r) = \frac{\rho(r)}{\kappa m_p} \tag{25}$$

Bu yerda m_p proton massasi va *K* odatda qorong'u materiya olami bilan bog'liq bo'lgan o'lchovsiz doimiy koeffitsientdir. Plazma chastotasidan (5,24,25) foydalanish quyidagi shaklni oladi:

$$\omega_e^2 = K_e N(r) = \frac{K_e \sigma_v^2}{2\pi\kappa m_p r^2}. \tag{26}$$

Biz SISning yuqorida qayd etilgan xususiyatlarini hisobga olamiz va α_{SIS} og'ish burchagini quyidagi tarzda hisoblaymiz (Babar et al. PDU 2021)

$$\hat{\alpha}_{\text{SIS}} = \left(\frac{2R_s}{b} - \frac{15\pi\alpha R_s^2}{16b^4}\right) + \frac{R_s^2\omega_c^2}{b^2\omega^2}\left(\frac{1}{2} - \frac{2R_s}{3b\pi} + \frac{5\alpha R_s^2}{8b^4}\right). \tag{27}$$

Ushbu hisob-kitoblar quyidagi analitik ifodaga ega bo'lgan o'zgarmas ω_0^2 qo'shimcha plazmani olib keladi.

$$\omega_c^2 = \frac{\sigma_v^2 K_e}{2\kappa m_p R_s^2} \tag{28}$$

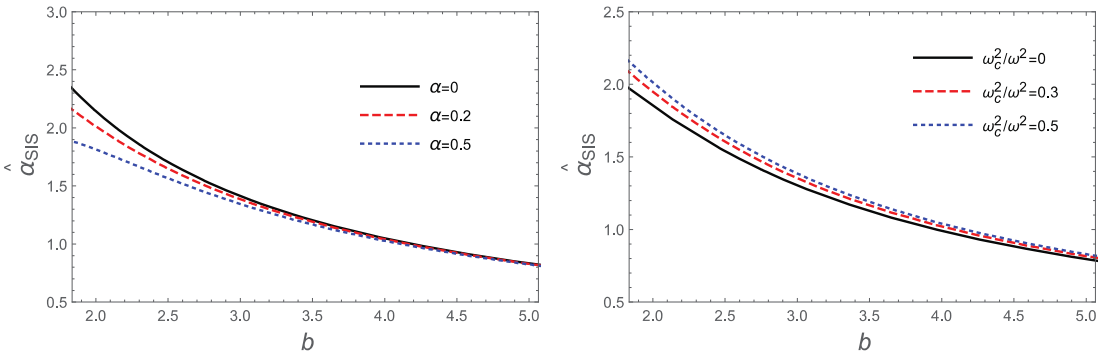

3-rasm. Og'ish burchakning ta'sir paramtri *b* bog'langan grafikini har xil GB paramaetrlari uchun (chap tomonda) va bir jinsli bo'lmagan plasma parametri (o'ng tomonda) uchun keltirilgan.

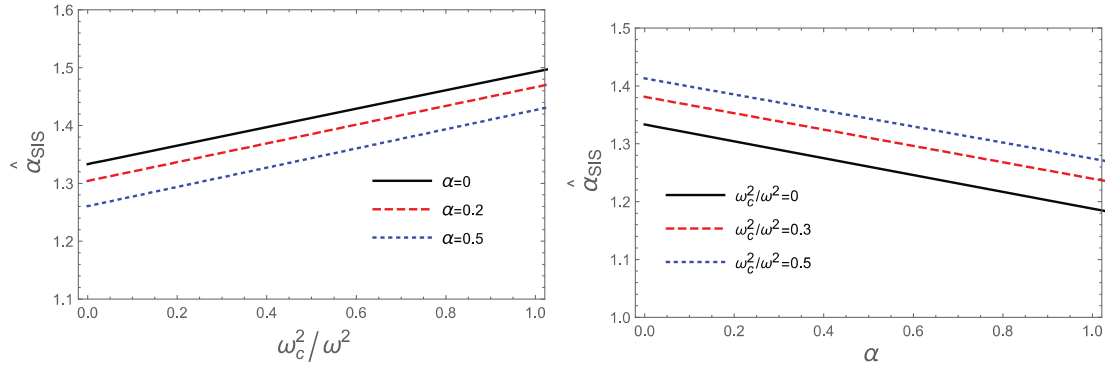

4-rasm. Og'ish burchakning bir jinsli bo'lmagan SIS plasma parametri (chap tomonda) va GB parametri (o'ng tomonda)ga bog'langan grafiki keltirilgan.

SIS ning foton traektoriyasiga ta'sirini o'zlashtirish uchun biz α_{SIS} og'ish burchagini ta'sir parametri *b* funktsiyasi sifatida chizdik (3-rasmga qarang), qiziq tomoni shundaki, biz bir jinsli plazma va SIS muhiti *b* parametriga asoslanganda umumiy xususiyatlarga ega ekanligini ko'ramiz. Shuni esda tutingki, ω_c^2/ω^2 miqdori qora tuynuk yaqinida SIS ning taqsimlanishini aniqlaydi, shuning uchun biz (4-rasm) grafik tahlil yordamida ulanish doimiy parametri α bilan birga belgilangan parametrga foton sezgirligini aniqlaymiz. Biz tekshirib ko'rdikki, ω_c^2/ω^2 ortganda α_{SIS} ortadi (o'ng tomonda) va aksincha, α_{SIS} oshganda (chap tomonda) α kamayadi. Demak, qora tuynuk atrofida SISning mavjudligi ma'lum darajada oraliqdagi massasiz zarrachalarga ta'sir qiladi.

Yakka bo'lmagan izotermik gaz sferasi. Endi biz tahlil uchun yanada oqilona va fizik sozlangan yagona bo'lmagan izotermik sferani (non-singular isothermal sphere – NSIS) hisobga olgan holda fotonlarning harakatini o'rganishni davom ettiramiz. SISdan farqli o'laroq, ushbu obyektiv modelida o'ziga xoslik gaz bulutining kelib chiqishidagi chekli yadro bilan chegaralanadi, bunda zichlik taqsimoti quyidagicha aniqlanadi:

$$\rho(r) = \frac{\sigma_v^2}{2\pi(r^2+r_c^2)} = \frac{\rho_0}{\left(1+\frac{r^2}{r_c^2}\right)},\ \rho_0 = \frac{\sigma_v^2}{2\pi r_c^2} \tag{29}$$

bu yerda yadro radiusi r_c bilan ifodalanadi. NSIS yordamida plazma kontsentratsiyasi (25) quyidagicha bo‘ladi

$$N(r) = \frac{\sigma_v^2}{2\pi\kappa m_p(r^2+r_c^2)} \tag{30}$$

Plazma chastotasini (5,29,30) dan quyidagicha hisoblaymiz

$$\omega_e^2 = \frac{K_e\sigma_v^2}{2\pi\kappa m_p(r^2+r_c^2)} \tag{31}$$

Oxirgi muhokamadagi xususiyatlarga muvofiq NSIS gravitatsion linzalarini o‘rnatishda fotonlarning og’ishi natijasida olingan og’ish burchagi quyidagicha natijaga ega bo’ldik (Babar et al. PDU 2021):

$$\hat{\alpha}_{\text{NSIS}} = \left(\frac{2R_s}{b} - \frac{15\pi\alpha R_s^2}{16b^4}\right) + \frac{R_s^2\omega_c^2}{\omega^2}\left(\frac{R_s}{b\pi r_c^2} + \frac{b}{2\left(\sqrt{b^2+r_c^2}\right)^3}\right.$$
$$- \frac{bR_s\tanh^{-1}\frac{r_c}{\sqrt{b^2+r_c^2}}}{\pi r_c^3\sqrt{b^2+r_c^2}} - \frac{\alpha R_s^2}{r_c^2}\left(\frac{2}{r_c^4} + \frac{3}{4b^4} - \frac{1}{b^2r_c^2}\right.$$
$$\left.\left. - \frac{2b}{r_c^4\sqrt{b^2+r_c^2}}\right)\right). \tag{32}$$

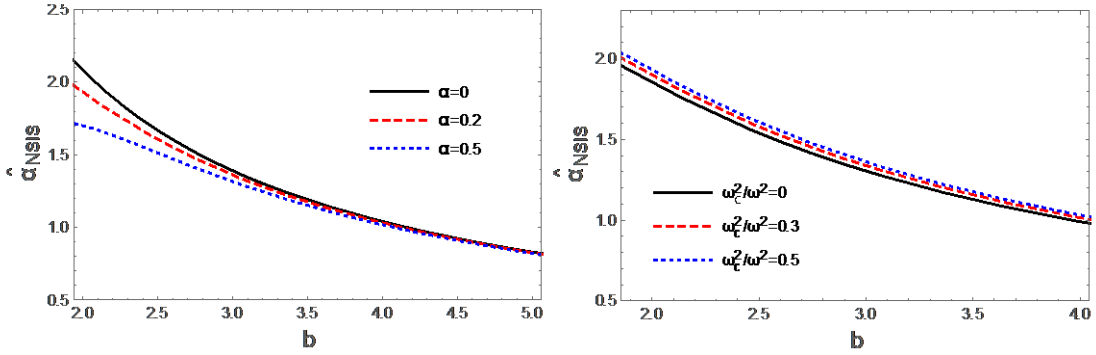

5-rasm. Og’ish burchakning ta’sir paramtri *b* bog’langan grafikini har xil GB paramaetrlari uchun (chap tomonda) va bir jinsli bo’lmagan NSIS plasma parametri (o‘ng tomonda) uchun keltirilgan.

Ilgari bajarilganidek, biz foton harakati bilan bog’liq NSIS xususiyatlarini ochish uchun bir xil grafik talqindan foydalanamiz. Bu erda NSIS ning taqsimlanishi ω_c^2/ω^2 parametri bilan bog’liq. 5, 6-rasmlardan dan aniq ko‘rinib turibdiki, ta’sir parametri b, ulanish konstantasi α va parametr ω_c^2/ω^2 bir xil plazma va SIS korpusi bilan solishtirganda muayyan nuqtai nazardan farqlab bo‘lmaydi. Shunga qaramay, hech bo‘lmaganda og’ish burchagiga eng aniq ta’sir ko‘rsatadigan taqsimotni aniqlash mumkin. 7-rasmda α_{uni}, α_{SIS} va α_{NSIS} ning ta’sir parametri va ulanish konstantasi funktsiyasi sifatida vizual yonma-yon ko‘rsatilgan. Ko‘rinib turibdiki,

qora tuynuk bir jinsli plazma muhiti bilan o‘ralgan bo‘lsa, yorug’likning og’ishi maksimal bo‘ladi. Yakuniy natija shuning uchun $\alpha_{uni} > \alpha_{SIS} > \alpha_{NSIS}$ kabi matematik ifodada ifodalanishi mumkin.

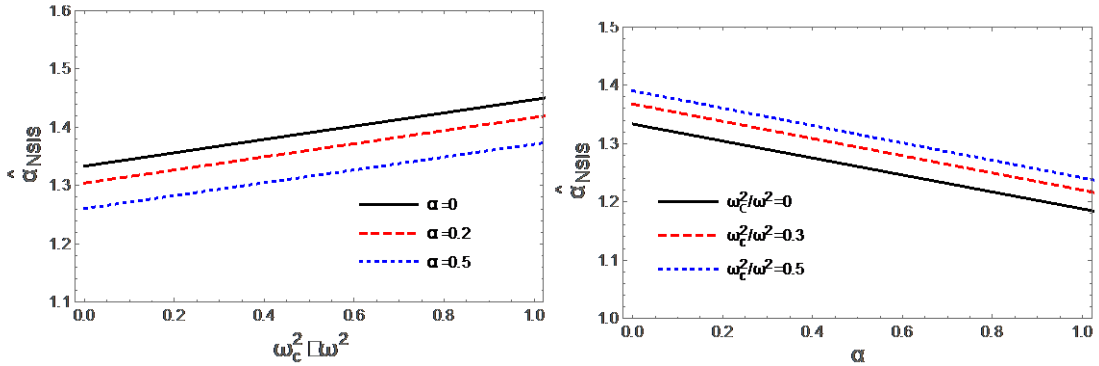

6-rasm. Og’ish burchakning bir jinsli bo’lmagan NSIS plasma parametri (chap tomonda) va GB parametri (o‘ng tomonda)ga bog’langan grafiki keltirilgan.

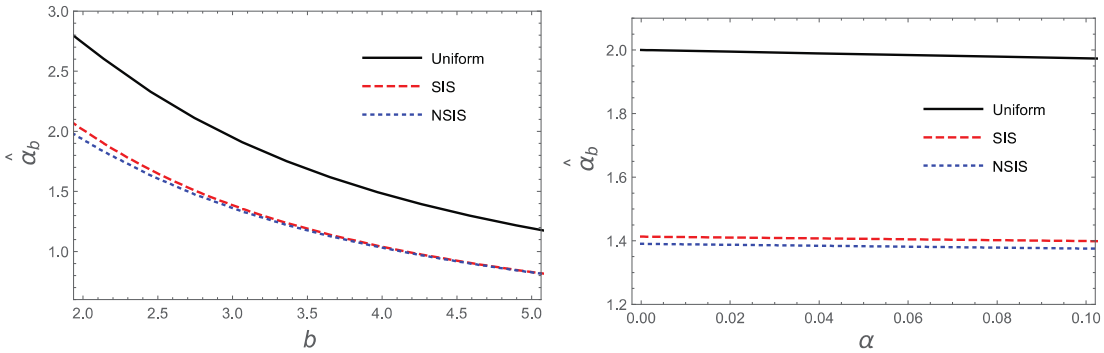

7-rasm: Og’ish burchakning ta’sir parametri (chap tomonda)ga va GB parametri (o‘ng tomonda)ga bog’langan grafiki keltirilgan.

II qism.

Ushbu qismda biz foton harakati va qora tuynukning soyasini muhokama qilamiz. Misol sifatida, biz Kerr-Newman-Kislev-Letelier (KNKL) qora tuynugini nolga teng bo‘lmagan Kiselev (quintessence) va torli bulut (cloud string – CS) parametrini ko‘rib chiqamiz. KNKL qora tuynugi metrikasi quyidagicha ifodalanishi mumkin:

$$ds^2 = -\frac{\Delta}{\Sigma}(dt - a\sin^2\theta d\phi)^2 + \frac{\Sigma}{\Delta}dr^2 + \Sigma d\theta^2 + \frac{\sin^2\theta}{\Sigma}(adt - (r^2 + a^2)d\phi)^2 \quad (33)$$

Tepadagi metrika (33) uchun metrik koeffitsentlari quyidagicha:

$$\Sigma = r^2 + a^2\cos^2\theta \quad (34)$$

$$\Delta = (1-b)r^2 + a^2 + Q^2 - 2Mr - \gamma r^{-3\omega_q+1} \quad (35)$$

Bu yerda KNKL qora tuynuk gorizontlari tuzilishiga Kiselev parametri γ, CS parametr b, spin parametr a va qora tuynukning Q zaryadining ta’sirini muhokama

qilamiz. E'tibor bering, M - massa parametri va tizimning ADM massasini koordinatalarni o'zgartirish orqali olish mumkin.

KNKL qora tuynugining soyasi shakliga ega bo'lish uchun biz birinchi navbatda KNKL qora tuynugining fazoviy geometriyasida nol geodeziyani o'rganamiz. Biz KNKL qora tuynuk fazosining fotonlar harakat tenglamalarini o'rganish uchun Gamilton-Jakobi formalizmini quyidagi tarzda qabul qilamiz

$$\frac{\partial S}{\partial \tau} = -\frac{1}{2} g^{\mu\nu} \frac{\partial S}{\partial x^{\mu}} \frac{\partial S}{\partial x^{\nu}} \tag{36}$$

bu yerda $\boldsymbol{E} = g_{t\mu}\dot{x}^{\mu}$ va $\boldsymbol{L}_z = g_{\phi\mu}\dot{x}^{\mu}$ zarrachaning energiyasi va impulsiga mos keladi, τ afin parametri va $g^{\mu\nu}$ - metrik tensor. Bu yerda S ta'sir funksiyasi quyidagicha ajratiladi:

$$S = \frac{1}{2} m_0^2 \tau - Et + L_z \phi + S_r(r) + S_\theta(\theta) \tag{37}$$

bu yerda m_0 zarrachaning massasi va $S_r(r)$, $S_\theta(\theta)$ faqat r va θ funksiyasi. O'zgaruvchilarni ajratish usulidan foydalanib va 87-tenglamani 36-tenglamaga qo'llash orqali biz foton harakati uchun quyidagi tenglamalarni olamiz ($m_0 = 0$)

$$\mathcal{R} = [(r^2 + a^2)E - aL_z]^2 - \Delta[\mathcal{K} + (L_z - aE)^2] \tag{38}$$

$$\Theta = \mathcal{K} + \cos^2\theta(a^2E^2 - L_z^2 \sin^{-2}\theta). \tag{39}$$

KNKL qora tuynugining fazo-vaqt metrikasida quyidagi geodezik tenglamalarni olamiz:

$$\Sigma \frac{dt}{d\tau} = a(L_z - aE\sin^2\theta) + \frac{r^2 + a^2}{\Delta}(E(r^2 + a^2) - aL_z) \tag{40}$$

$$\Sigma \frac{dr}{d\tau} = \pm\sqrt{\mathcal{R}} \tag{41}$$

$$\Sigma \frac{d\theta}{d\tau} = \pm\sqrt{\Theta} \tag{42}$$

$$\Sigma \frac{d\phi}{d\tau} = (L_z \csc^2\theta - aE) + \frac{a}{\Delta}(E(r^2 + a^2) - aL_z). \tag{43}$$

Endi biz KNKL qora tuynuk soyasining shaklini aniqlaymiz. Buning uchun biz quyidagi $\xi = L_z/E$ va $\eta = K/E^2$ ta'sir parametrlarini aniqlaymiz va shuning uchun bu yangi parametrlar bo'yicha R ni quyidagicha ifodalash mumkin.

$$\mathcal{R} = [(r^2 + a^2) - a\xi]^2 - \Delta[\eta + (\xi - a)^2] \tag{44}$$

Qora tuynuk tomon kelayotgan fotonlar uch turdagi traektoriyalarni kuzatib boradi, ya'ni qora tuynuk ichiga tushishi, qora tuynukdan uzoqlashishi yoki qora tuynuk gorizonti yaqinida beqaror dumaloq orbita bo'ylab harakatlanishi. Ushbu uch turdagi traektoriyalardan qora tuynuk gorizonti yaqinidagi beqaror dumaloq orbitalar qora tuynuk tomonidan tushirilgan soyaning shaklini aniqlash uchun ma'suldir. Beqaror dumaloq foton orbitalarini quyidagi shartlar asosida olish mumkin:

$$\mathcal{R}(r) = 0 = \frac{\partial \mathcal{R}(r)}{\partial r} \tag{45}$$

Ikki parametr ξ va η qora tuynuk tomonidan tushirilgan soyaning shaklini aniqlaydi. (44) va (45) tenglamalarni hisobga oladigan bo‘lsak, KNKL qora tuynuklari uchun bizda ξ va η quyidagicha bo‘ladi

$$\xi = \frac{(a^2 + r^2)\Delta' - 4\Delta r}{a\Delta'} \tag{46}$$

$$\eta = \frac{r^2(16\Delta(a^2 - \Delta) - r^2\Delta'^2 + 8\Delta r\Delta')}{a^2\Delta'^2} \tag{47}$$

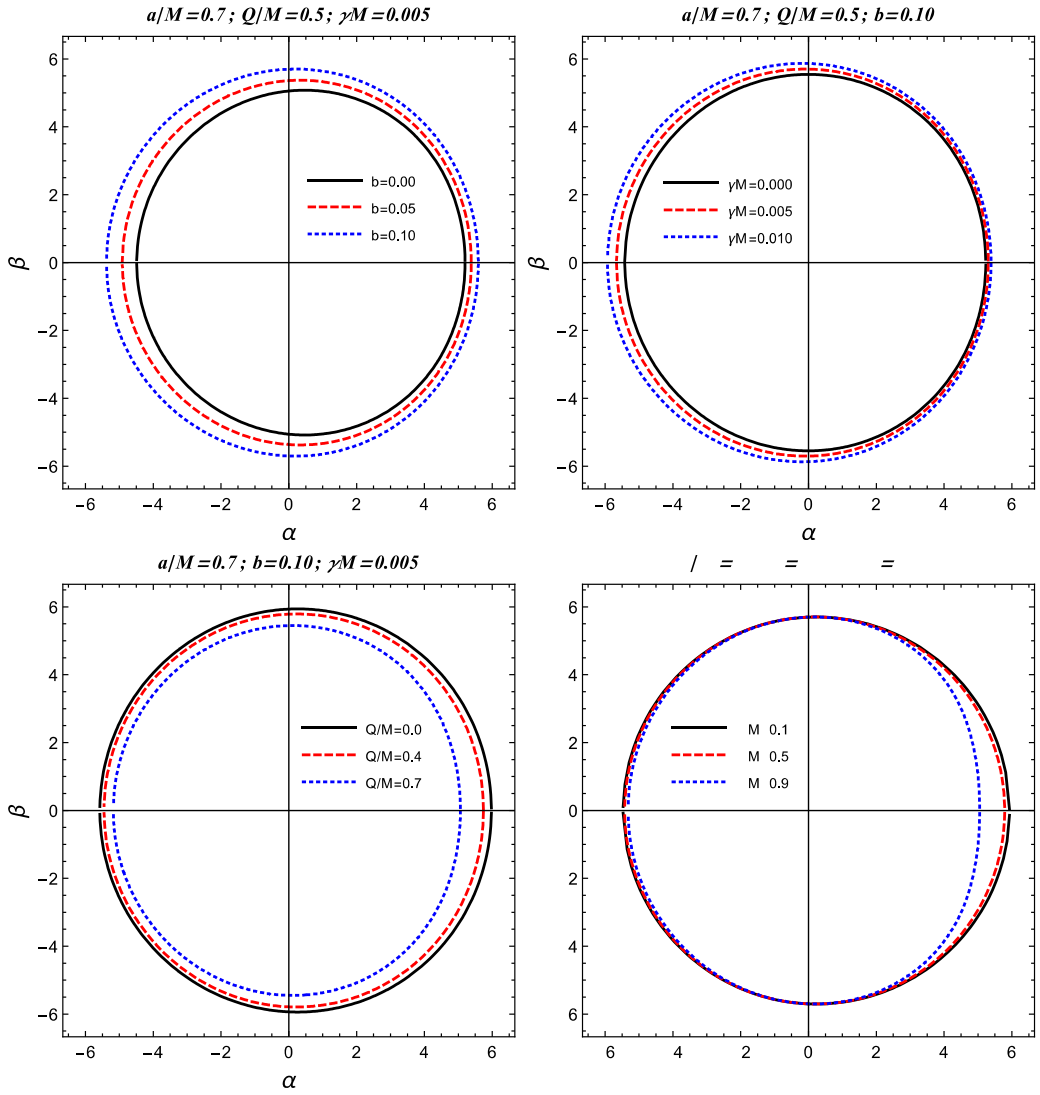

8-rasm. Kerr-Newman-Kiselev-Letelier qora tuynugining soyasi va kuzatilishi mumkin bo‘lgan parametrlar.

KNKL qora tuynugining soyasining geometriyasini muhokama qilish uchun astronomik koordinatalari α va β sifatida aniqlanadi

$$\alpha \quad = -r_0 \frac{P^{(\phi)}}{P^{(t)}}, \tag{48}$$

$$\beta \quad = -r_0 \frac{P^{(\theta)}}{P^{(t)}}. \tag{49}$$

Bu yerda $P^{(\phi)}$, $P^{(\theta)}$ va $P^{(t)}$ foton impulsining tetrad komponentlaridir. r_0 - kuzatilgan masofa va u juda katta, lekin Sgr A* uchun chekli r_0=D=8.3 kpc yoki M87* uchun r_0 = D = 16,8 Mpc hisoblanadi.

Biz kuzatuv burchagi $\theta_0=\pi/2$ bo‘lgan ekvator tekisligidagi KNKL qora tuynugining soyasini aniqlayapmiz, shuning uchun (48) va (49)-tenglamalar quyidagi shaklni oladi

$$\alpha \quad = -\sqrt{-g_{tt}(r_0)}\xi. \tag{50}$$

$$\beta \quad = \pm\sqrt{-g_{tt}(r_0)}\sqrt{\eta}. \tag{51}$$

KNKL qora tuynugiga tushadigan soyaning shakli va ko’rinishini tahlil qilish uchun biz 8-rasmdagi ikkita fazoviy koordinatalarini α va β parametrlarining turli qiymatlari uchun b va γ parametrlarining a aylanuvchi parametrining aniq qiymatlari va qora tuynukning Q zaryadi uchun chizamiz.

Biz b va γ parametrlarining qiymatlarini oshirish uchun KNKL qora tuynuk tomonidan soyasining radiusi ortib borishini kuzatamiz. Xuddi shu 8-rasmda biz α va β koordinatalarini va KNKL qora tuynukning aylanish parametri a va Q zaryadining turli qiymatlari uchun b va γ parametrlarini o‘zgarmagan holda chizamiz. Bu yerda biz a va Q parametrlarining qiymatlari ortib borishi bilan KNKL qora tuynugining soya radiusi kichrayayotganini ko‘ramiz. Shunga qaramay, Kiselev parametrining ham, CSning ham tabiatini KNKL qora tuynuklari tomonidan tushirilgan soya shakllari uchun grafiklarning bunday xatti-harakatidan tasdiqlash mumkin. Bundan tashqari, 8-rasmda biz a aylanish parametrining ortib borayotgan qiymatlari boshqa fazo-vaqt parametrlarining belgilangan qiymatlari uchun KNKL qora tuynuk soyasining buzilishi kuchaytirayotganini kuzatamiz. Shunday qilib, tez aylanadigan qora tuynuk tomonidan tushadigan soya asta-sekin aylanadigan qora tuynuk bilan solishtirganda ko‘proq buziladi. Bu kuzatuv aylanuvchi qora tuynukning aylanishini cheklashda yordam berishi mumkin. Bu yerda biz barcha fazoviy vaqt parametrlari KNKL qora tuynuklari soyasining shakli va o’lchamiga ta’sir qilishini ko‘ramiz.

Bu yerda qora tuynukning soyasining radiusini R_{sh} bilan belgilaymiz va buzilish parametri δ_s quyidagicha ifodalanadi:

$$\delta_s = \frac{D_{cs}}{R_{sh}} \tag{52}$$

bu yerda D_{cs} qora tuynuk tomonidan tushirilgan soyaning o‘ng chekka nuqtalari orasidagi farqni bildiradi. Boshqa kuzatiladigan R_{sh} quyidagicha berilgan:

$$R_{sh} = \frac{(\alpha_t - \alpha_r)^2 + \beta_t^2}{2(\alpha_t - \alpha_r)}. \quad (53)$$

9 va 10-rasmlarda biz kuzatiladigan R_{sh} va δ_s parametrlarini b va γ va zaryad Q parametrlariga bog'liq holda chizamiz. Ko'ramizki, kuzatiladigan R_{sh} esa b va γ parametrlari hamda KNKL qora tuynugi tomonidan tushirilgan soyaning o'lchami bilan ortib boradi. Q zaryadining KNKL qora tuynuk soyasining o'lchamiga ta'siri b va γ parametrlariga qarama-qarshidir. 10-rasmdan biz qora tuynuk tomonidan tushirilgan soya shaklining buzilishi uchun javobgar bo'lgan kuzatilishi mumkin bo'lgan δ_s ham Q, ham a bilan ortib borishini ko'ramiz. Bu paytda parametrning b va γ bilan kamayishi kuzatiladi. Bu kuzatish qora tuynukning zaryadini ham, aylanishini ham cheklashi mumkin.

b va γ parametrlarini M87* va SgrA* uchun EHT tomonidan taqdim etilgan ma'lumotlar bo'yicha qiymatlarini aniqlash

M87 va Somon yo'li galaktikalarining markazidagi o'ta massiv qora tuynuklar CS va Kiselev parameterlari tas'siridagi biz ikkita supermassiv qora tuynuk M87* va SgrA* uchun EHT hamkorligida taqdim etilgan ma'lumotlardan foydalanib, Kiselev parametri γ va SC parametri b bo'yicha yuqori chegaralarni olamiz. Qora tuynuk soyasining ko'rinma burchak diametri, qora tuynukning yerdan masofasi va M87* galaktikasi markazidagi qora tuynukning taxminiy massasi mos ravishda θ_{M87*}= 42 ± 3μas, D = 16,8Mpc va MM87* = 6,5 ± 0,90x10^9M sifatida berilgan. Somon yo'li galaktikasi markazidagi o'ta massali qora tuynuk SgrA* uchun EHT bilan hamkorlikda olingan ma'lumotlar $\theta_{Sgr\ A*}$ = 48,7 ± 7μ, D = 8277 ± 33 pc va $M_{Sgr\ A*}$ = 4,3 ± 0,013. x10^6 M (VLTI)ni tashkil qiladi. EHT hamkorligi tomonidan taqdim etilgan ma'lumotlardan foydalanib, biz qora tuynuk soyasining diametrini, massa birligi uchun quyidagi ifoda yordamida o'rganamiz (Atamurotov et al. EPJC 2022):

$$d_{\rm sh} = \frac{D\theta}{M} \quad (54)$$

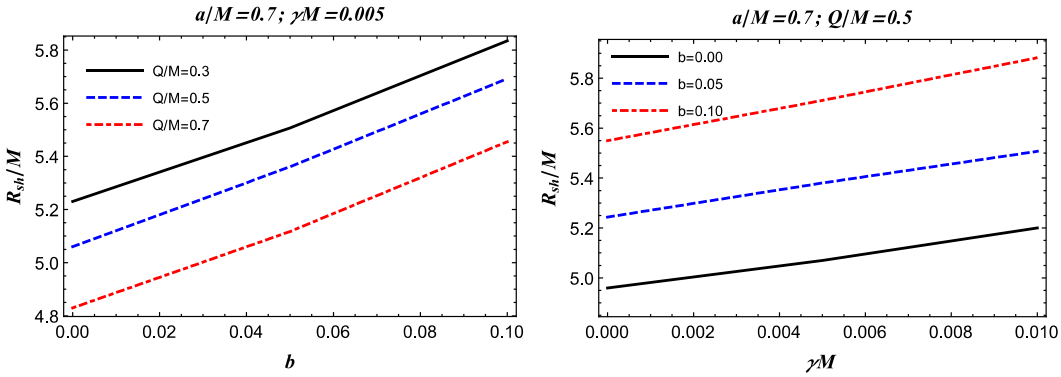

9-rasm. Qora tuynuk soyasining radiusi (Atamurotov et al. EPJC 2022).

Keyin soyaning diametrini $d^{theo}_{sh}=2R_{sh}$ ifodasidan olish mumkin. Shunday qilib, qora tuynuk tomonidan tushirilgan soya tasvirining diametri o‘ta massali qora tuynuk M87* uchun $d^{M87*}_{sh}(11 \pm 1{,}5)M$ va o‘ta massali qora tuynuk Sgr A* uchun $d^{SgrA*}_{sh} = (9{,}5 \pm 1{,}4)M$ ga teng. Somon yo‘li galaktikasining etagida. EHT hamkorligi tomonidan chiqarilgan ma’lumotlarni hisobga oladigan bo‘lsak, bizda biri M87 galaktikasining markazida, ikkinchisi esa Somon yo‘li galaktikasining markazida joylashgan supermassiv qora tuynuklar uchun b va γ parametrlari bo‘yicha cheklovlar mavjud. KNKL qora tuynugining a aylanish va Q zaryadining belgilangan qiymatlari uchun biz natijalarimizni 1-jadvalda ko‘rsatamiz. γ kvintessensiya parametri pasayganda CS parametrining yuqori chegarasi b ortib borishini kuzatamiz. KNKL qora tuynuklari uchun b va γ ikkita parametrini cheklash bo‘yicha ushbu tadqiqot SC ta’siri KNKL qora tuynukining fazoviy vaqt geometriyasiga kvintessensiya ta’siridan kuchliroq bo‘lishi mumkinligini ko‘rsatadi (Atamurotov et al. EPJC 2022).

Ekvatorial va qutbli QNM lar va ularning tipik soya radiusi bilan aloqasi.

Ushbu bo‘limda biz odatiy soya radiusi va QNM o‘rtasidagi munosabatni o‘rganamiz. Ushbu muvofiqliklar qiziqarli va yaqin kelajakda sinovdan o‘tkazilishi mumkin. Xususan, biz bilamizki, QNMlar qora tuynukning pastki aylana fazasi bilan bog’liq va quyidagicha berilishi mumkin

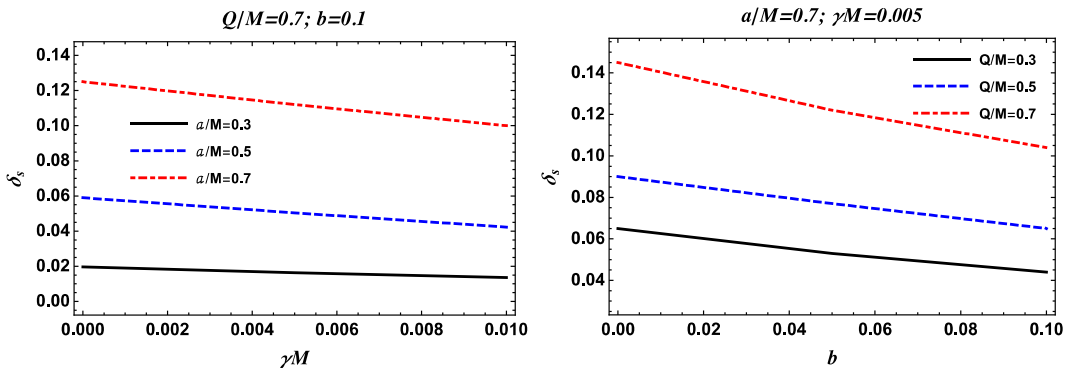

10-rasm. Qora tuynuk soyasining shakli buzilish parametri.

1-jadval: γ va a ning yuqori qiymatlari M87* va Sgr A* galaktikasidagi supermassiv qora tuynuklar uchun jadvalda keltirilgan.E’tibor bering, biz M = 1 ni o‘rnatdik.

	Estimated values of parameters for M87* black hole					
Parameters	$Q = 0.0$ and $a = 0.5$			$Q = 0.5$ and $a = 0.5$		
b	0.0000	0.0200	0.0400	0.0000	0.0200	0.0400
γ	0.0358	0.0297	0.0235	0.0435	0.0386	0.0339
	Estimated values of parameters for Sgr A* black hole					
Parameters	$Q = 0.0$ and $a = 0.5$			$Q = 0.5$ and $a = 0.5$		
b	0.0000	0.0200	0.0345	0.0000	0.0200	0.0400
γ	0.0110	0.0050	0.0000	0.0201	0.0154	0.0104

haqiqiy va tasviriy qismlar nuqtai nazaridan quyidagicha $w=w_R-iw_T$, soya radiusi esa o‘ta massali qora tuynuklar yordamida kuchli tortishish rejimida Umumiy nisbiylikni sinab ko‘rish uchun tegishli. Asimptotik tekis va statik ko‘rsatkichlar uchun burchak tezligi va QNM ning haqiqiy qismi o‘rtasida bog’liqlik mavjudligi ko‘rsatilgan. Xususan, soya radiusi va QNM ning haqiqiy qismini osongina bog’lash mumkin

$$R_{sh} = \frac{l+\frac{1}{2}}{\omega_{\Re}} \tag{55}$$

Biroq, Eynshteyn-Lovelok nazariyasi kabi o‘zgartirilgan tortishish nazariyalarida bu munosabat buzilishi mumkinligiga e’tibor bering. Bundan tashqari, Eikonal chegarasidagi QNM chastotasi o‘qishi ko‘rsatildi

$$\omega_{QNM} = \left(l+\frac{1}{2}\right)\Omega_R - i\gamma_L\left(n+\frac{1}{2}\right) \tag{56}$$

bu yerda

$$\Omega_R = \Omega_\theta + \frac{m}{l+\frac{1}{2}}\Omega_{prec} \tag{57}$$

bunda Ω_θ qutb yo‘nalishidagi orbital chastotani beradi. Bundan tashqari, Ω_{prec} orbita tekisligining Lens-Thiring aniq chastotasi sifatida tanilgan va γ_L orbitaning Lyapunov ko‘rsatkichidir. Ma’lumki, qora tuynukning massasidan tashqari (soya radiusiga proportsional), qora tuynuk aylanishi tufayli soya qiyshayadi va soyaning ko‘rinadigan shakli ko‘rish burchagiga bog’liq bo‘ladi. Shuning uchun soya radiusi uchun yopiq shakl yoki analitik ifodani topish umuman mumkin emas.

$$\Omega_{\text{prec}} = \pm\Omega_\phi \mp \Omega_\theta \tag{58}$$

bilan

$$\Omega_\phi = \frac{-\partial_r g_{t\phi} \pm \sqrt{(\partial_r g_{t\phi})^2 - (\partial_r g_{tt})(\partial_r g_{\phi\phi})}}{\partial_r g_{\phi\phi}}. \tag{59}$$

Kerr kvaznormal rejimlari uchun WKB tahlili bilan bir xil yondashuvni qo‘llash mumkin, keyin $2\int_{-\theta}^{\theta}\sqrt{\Theta}d\theta = 2\pi(L-|L_z|)$ yozish orqali, uni fizik jihatdan Bor-Zommerfeld holati sifatida ko‘rish mumkin va Kerr kvazinormal rejimlari uchun θ yo‘nalishidagi xos qiymat muammosi bilan solishtirish mumkin. (Tafsilotlar uchun 16-havolaga qarang). Bu quyidagicha ta’kidlandi:

$$\mathcal{K} + L_z^2 \simeq L^2 - \frac{a^2E^2}{2}\left(1-\frac{L_z^2}{L^2}\right) \tag{60}$$

va endi oxirgi tenglamani E^2 ga bo‘lsak, quyidagicha olishimiz mumkin:

$$\eta + \xi^2 \simeq \frac{L^2}{E^2} - \frac{a^2}{2}\left(1-\frac{L_z^2}{L^2}\right). \tag{61}$$

Shu nuqtada biz quyidagilardan foydalanishimiz mumkin

$$L_z \quad \Leftrightarrow m \tag{62}$$
$$E \quad \Leftrightarrow \omega_{\Re} \tag{63}$$
$$L \quad \Leftrightarrow l + \frac{1}{2} \tag{64}$$

Bu yerda w_R=$L\Omega_R$ Eikonal chegara deb ham ataladigan m = l >> 1 chegarasida biz m = m/(l + 1/2) = 1 bilan quyidagiga egamiz:

$$\Omega_{prec} = \Omega_{\phi} - \Omega_{\theta} \tag{65}$$

keyin ko‘rsatish mumkin:

$$\Omega_R = \Omega_{\theta} + \Omega_{\text{prec}} = \Omega_{\phi}. \tag{66}$$

Boshqacha qilib aytganda, bu QNMlar Kepler chastotasi bilan bog’liq bo‘lib, uni (Atamurotov et al. EPJC 2022) m = l >> 1 sifatida yozish mumkin.

$$\omega_{\Re}^{\pm} = \left(l + \frac{1}{2}\right) \frac{-\partial_r g_{t\phi} \pm \sqrt{\left(\partial_r g_{t\phi}\right)^2 - \partial_r g_{tt}\, \partial_r g_{\phi\phi}}}{\partial_r g_{\phi\phi}}, \tag{67}$$

bu yerda $\alpha^{\pm}(r_{ph}) = \pm\sqrt{f(r_0)}\xi$ va $\eta(r_{ph}^{\pm}) = 0$ bo‘lgan odatiy soya radiusini belgilash uchun quyidagi ta’rifdan foydalanamiz:

$$\bar{R}_{sh} := \frac{1}{2}\left(\alpha^{+}(r_{ph}^{+}) - \alpha^{-}(r_{ph}^{-})\right) \tag{68}$$

Endi biz 61-tenglamadan foydalansak, bundan kelib chiqadi:

$$\xi^{\pm} = \pm\sqrt{\frac{\left(l+\frac{1}{2}\right)^2}{\omega_{\Re}^2(r_{ph}^{\pm})} - \frac{a^2}{2}(1-\mu^2)} \tag{69}$$

Bu tenglamalarni birlashtirish orqali biz bunga yetib kelamiz:

$$\begin{aligned} \bar{R}_{sh} \quad &= \frac{\sqrt{f(r_0)}}{2}\sqrt{\frac{\left(l+\frac{1}{2}\right)^2}{\omega_{\Re}^2(r_{ph}^{+})} - \frac{a^2}{2}(1-\mu^2)} \\ &+ \frac{\sqrt{f(r_0)}}{2}\sqrt{\frac{\left(l+\frac{1}{2}\right)^2}{\omega_{\Re}^2(r_{ph}^{-})} - \frac{a^2}{2}(1-\mu^2)} \end{aligned} \tag{70}$$

Bu yerda

$$f(r_0) = 1 - b - \frac{2M}{r} + \frac{Q^2}{r^2} - \gamma r^{-3\omega_q - 1}|_{r_0} \tag{71}$$

va r_0 kuzatuvchining joylashuvi. Boshqacha qilib aytganda, CS parametri tufayli fazo-vaqt topologiyasi global konus shaklida va asimptotik tekis emas, shuning uchun uzoq kuzatuvchi tomonidan o‘lchangan soya radiusi o‘zgartiriladi. Agar biz eikonal chegarani hisobga olsak, ya’ni μ=±1 (ya’ni [$(m = \pm \imath)$] ni o‘rnatsak, quyidagi hosildorlik aniq bo‘ladi:

$$\bar{R}_{sh}(\mu=\pm1)=\left(l+\frac{1}{2}\right)\frac{\sqrt{f(r_0)}}{2}\left(\frac{1}{\omega_{\Re}\left(r_{ph}^{+}\right)}-\frac{1}{\omega_{\Re}\left(r_{ph}^{-}\right)}\right) \tag{72}$$

$\omega^{+}=\omega^{-}=\omega_{\Re}$ hosil bo‘lganda statik holatni olishimiz mumkin

$$\bar{R}_{sh}=\sqrt{f(r_0)}\frac{l+\frac{1}{2}}{\omega_{\Re}} \tag{73}$$

Biz asimptotik tekis fazo vaqti uchun $f(r_0)\rightarrow1$ va oxirgi tenglama 27-tenglamaga qisqarishini ko‘ramiz. Metrik funktsiyalardan foydalangan holda va Eikonal chegarasida ba’zi algebraik manipulyatsiyalardan so‘ng biz 67-tenglamadan foydalanishimiz mumkin, uni quyidagicha soddalashtirish mumkin (Atamurotov ey al. EPJC 2022)

$$\omega_{\Re}^{\pm}=\left(l+\frac{1}{2}\right)\frac{1}{a\pm\sqrt{\frac{2r_{ph}^{\pm}}{f'(r)|_{r_{ph}}^{\pm}}}} \tag{74}$$

Oddiy tenglamani olish uchun odatiy soya radiusi tenglamasini qayta yozishimiz mumkin

$$\bar{R}_{sh}=\frac{\sqrt{2f(r_0)}}{2}\left(\sqrt{\frac{r_{ph}^{+}}{f'(r)|_{r_{ph}^{+}}}}+\sqrt{\frac{r_{ph}^{-}}{f'(r)|_{r_{ph}^{-}}}}\right). \tag{75}$$

Oxirgi tenglama ilgari (Atamurotov et al. 2022)-ishda olingan natijadan boshqa narsa emas, bu yerda $r^{\pm}{}_{ph}$ nuqtalari larni yechish orqali aniqlangan (Atamurotov et al. EPJC 2022)

$$r_{ph}^{2}-\frac{2r_{ph}}{f'(r)|_{r_{ph}^{\pm}}}f\left(r_{ph}\right)\mp2a\sqrt{\frac{2r_{ph}}{f'(r)|_{r_{ph}}}}=0. \tag{76}$$

2-jadvalda biz KNKL qora tuynugining ekvatorial QNMlari uchun berilgan parametrlar sohasi uchun raqamli qiymatlarni taqdim etamiz. *l* ortishi bilan biz odatda aniqlikning oshishini kutamiz.

- Holat II: $\theta_0=0$ & $\theta_0=\pi$ burchagini ko‘rish

Bizning ikkinchi misolimiz θ= 0 qutb orbitasini kuzatuvchi uchun ko‘rish burchagi bilan birga ko‘rib chiqishdir: $\theta_0=0$ & $\theta_0=\pi$. Qutbli orbita uchun biz bilamizki, azimutal burchak impulsi nolga teng, ya’ni $L_z=0$. Doiraviy geodeziyadan, ya’ni $\dot{r}^2$ dan foydalanib, bundan quyidagi chiqadi:

$$(r^2+a^2)^2-[r^2f(r)+a^2]R_s^2=0, \tag{77}$$

Bu bilan birga

$$4r(r^2+a^2)-2rf(r)R_s^2-r^2f'(r)R_s^2=0, \tag{78}$$

bunda biz $R^2{}_s=K/E^2+a^2$ ta’sir parametriga egamiz. Endi 77-tenglamadan foydalanib, biz quyidagilarni olamiz

$$R_s^{\pm} = \pm \frac{a^2+r^2}{\sqrt{r^2 f(r)+a^2}}\Big|_{ph}. \tag{79}$$

2-jadval: Ekvatorial rejimlar va qutbli rejimlar uchun QNMlarning real qismining sonli qiymatlari. Biz *M = 1*, *Q/M = 0,5*, *a/M = 0,5*, *= 0,001*, $w_q = -2/3$ va $b = 0{,}001$ ni o‘rnatdik (Atamurotov et al. EPJC 2022).

	Equatorial modes		Polar modes
l	$\omega_{\Re}^{+}$	$\omega_{\Re}^{-}$	$\omega_{\Re}$
1	0.394368035	-0.250600581	0.306612155
2	0.657280058	-0.417667636	0.511020260
3	0.920192081	-0.584734690	0.715428363
4	1.183104105	-0.751801745	0.919836467
5	1.446016128	-0.918868799	1.124244572
6	1.708928152	-1.085935854	1.328652675
7	1.971840175	-1.253002909	1.533060779
8	2.234752199	-1.420069964	1.737468883
9	2.497664222	-1.587137018	1.941876987
10	2.760576245	-1.754204073	2.146285091

Oddiy soya radiusi uchun biz quyidagi ta’rifni qabul qilamiz $\bar{R}_{sh} := (\sqrt{f(r_0)}R_s^{+} - \sqrt{f(r_0)}R_s^{-})/2$, hosila:

$$\bar{R}_{sh} = \sqrt{f(r_0)}\,\frac{a^2+r^2}{\sqrt{r^2 f(r)+a^2}}\Big|_{ph} \tag{80}$$

bu yerda r_{ph} ni quyidagi munosabatni yechish orqali topish mumkin

$$\left(a^2 + r_{ph}^2\right)^2 - \frac{4\left[r_{ph}^2 f(r_{ph})+a^2\right]\left(a^2+r_{ph}^2\right)}{r_{ph} f'(r_{ph})+2f(r_{ph})} = 0. \tag{81}$$

32-tenglamadan foydalanib, $L_z = 0$ ni olib, odatdagi soya radiusi uchun biz quyidagilarni olamiz:

$$\bar{R}_{sh} = \sqrt{f(r_0)}\sqrt{\frac{(l+1/2)^2}{\omega_{\Re}^2(r_{ph})} + \frac{a^2}{2}} \tag{82}$$

Osonlik bilan kuzatish mumkinki, aylanmaydigan holat uchun soya radiusi biz kutganimizdek 45-tenglamaga kamayadi. Boshqa tomondan, agar biz 45- va 52-tenglamalarni birlashtirsak, QNM ning haqiqiy qismini quyidagicha ifodalash mumkin:

$$\omega_{\Re} = \left(l + \frac{1}{2}\right)\sqrt{\frac{2(r^2 f(r)+a^2)}{2(a^2+r^2)^2 - a^2(r^2 f(r)+a^2)}}\Big|_{r=r_{ph}} \tag{83}$$

Nihoyat, 2-jadvalda biz qutbli QNMlar uchun raqamli qiymatlarni taqdim etdik. Biz *l* ning oshishi bilan QNM chastotasi uchun raqamli qiymatlarning aniqligi oshishini kutamiz.

Plazma ishtirokidagi Kerr-Nyuman-Kiselev-Letelier qora tuynugining soyasi. Umumiy nisbiylik nazariyasida asosan muhitning u orqali o‘tadigan yorug’lik nurlariga ta’siri e’tiborga olinmaydi. Shunga qaramay, masalan, Quyosh toji radio signallarining harakat vaqtiga va ularning Quyoshga juda yaqin burilish burchagiga ta’sir qiladi. Bu hodisa bizga ma’lum bo‘lmagan fizikani berishi mumkin bo‘lgan vosita mavjudligini ko‘rsatadi. Shuning uchun plazma muhiti ishtirokida qora tuynuk soyasi kabi astrofizikaviy ahamiyatga ega bo‘lgan jarayonlarni o‘rganish qiziq. Shunday qilib, ushbu bo‘limda biz plazma muhitida KNKL qora tuynugining soyasini o‘rganamiz.

Plazma muhitdagi fotonning dinamikasi. Bu yerda biz plazma bilan o‘ralgan qora tuynuk atrofida harakatlanadigan yorug’lik nuri uchun Gamiltoniandan foydalanamiz va quyidagi ko‘rinishdagi harakat tenglamasini olamiz (Atamurotov et al. PRD 2021):

$$\mathcal{H} = \frac{1}{2}\left[g^{\mu\nu}p_\mu p_\nu + \omega_{\mathrm{p}}(x)^2\right] \tag{84}$$

bu yerda elektron plazma chastotasi w_p sifatida aniqlanadi:

$$\omega_p(x)^2 = \frac{4\pi e^2}{m_e}N_e(x) \tag{85}$$

elektronning zaryadi va massasi mos ravishda e va m_{e} bilan. Elektronlarning son zichligi N_{e} ga teng.

Foton holatida Gamilton-Jakobi tenglamasi quyidagicha berilgan:

$$\mathcal{H}\left(x, \frac{\partial S}{\partial x}\right) = 0 \tag{86}$$

Bu yerda biz o‘zgaruvchilarni ajratish usulini qabul qilamiz va harakatni quyidagi ajratiladigan shaklda yozamiz:

$$S = -\omega_0 t + p_\phi \phi + S_r(r) + S_\theta(\theta), \tag{87}$$

bu yerda zarrachaning burchak impulsi va energiyasi p_ϕ, w_0 bo‘lib, ular saqlangan miqdorlardir. Yaqinda aylanuvchi qora tuynuk uchun plazma chastotasini quyidagi shaklda yozish mumkinligi taqdim etilgan va muhokama qilingan (Badia and Eiroa, PRD 2021):

$$\omega_p(x)^2 = \frac{h(r)+g(\theta)}{\rho^2} \tag{88}$$

bu yerda $h(r)$ va $g(\theta)$ funksiyalari mos ravishda radial va burchak qismlari bilan bog’liq. 86- tenglamada 87 va 88 lardan foydalanamiz va quyidagi ifodani olamiz:

$$\begin{aligned} 0 = {} & \frac{a^2\Delta\sin^2\theta-(r^2+a^2)^2}{\Delta}\omega_0^2 + \frac{4aMre^{-l/r}}{\Delta}\omega_0 p_\phi + \\ & \Delta(S_r')^2 + (S_\theta')^2 + \frac{\Delta-a^2\sin^2\theta}{\Delta\sin^2\theta}p_\phi^2 + h(r) + g(\theta), \end{aligned} \tag{89}$$

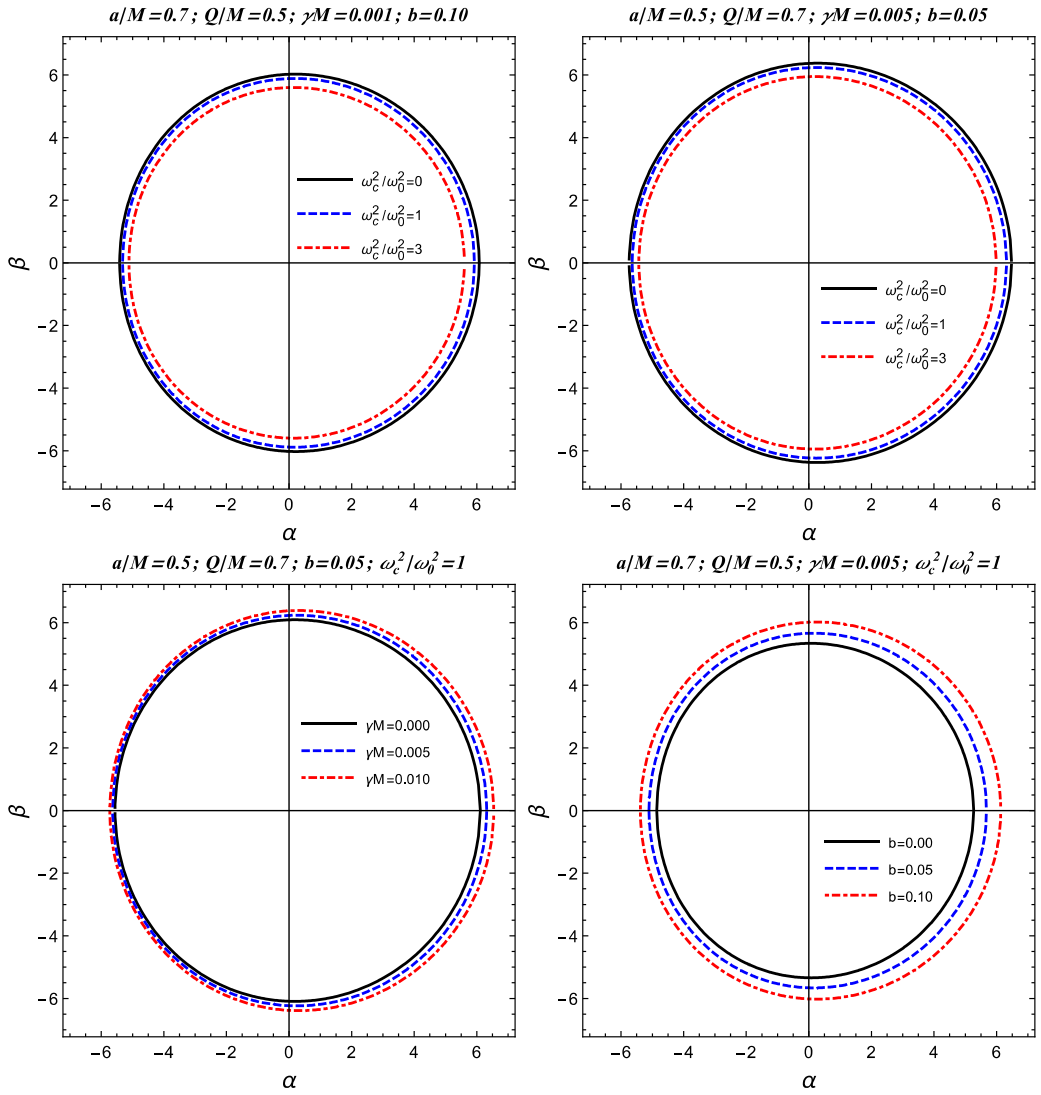

11-rasm: Plazma ishtirokidagi KNKL qora tuynugining soyasi (Atamurotov et al. EPJC 2022).

plazma muhiti bilan KNKL qora tuynuk fazoda. Keyin biz tenglamani quyidagi ikki qismga ajratish uchun Karter doimiysi K dan foydalanamiz:

$$(S_\theta')^2 + \left(a\omega_0 \sin\theta - \frac{p_\phi}{\sin\theta}\right)^2 + g(\theta) \quad = \mathcal{K} \tag{90}$$

$$\frac{1}{\Delta} - \Delta(S_r')^2 \left((r^2+a^2)\omega_0 - a p_\phi\right)^2 - h(r) \quad = \mathcal{K} \tag{91}$$

89-tenglamadan foydalanib, plazma muhiti bilan KNKL qora tuynukning fazo vaqtidagi harakat tenglamasini quyidagicha olishimiz mumkin:

$$\rho^2 \frac{dt}{d\tau} = a\left(p_\phi - a\omega_0 \sin^2\theta\right) + \frac{r^2 + a^2}{\Delta} P(r), \quad (92)$$

$$\rho^2 \frac{dr}{d\tau} = \pm\sqrt{\mathcal{R}}, \quad (93)$$

$$\rho^2 \frac{d\theta}{d\tau} = \pm\sqrt{\Theta}, \quad (94)$$

$$\rho^2 \frac{d\phi}{d\tau} = \frac{p_\phi}{\sin^2\theta} - a\omega_0 + \frac{a}{\Delta} P(r), \quad (95)$$

Bu yerda *P(r)* quyidagicha berilgan:

$$P(r) = (r^2 + a^2)\omega_0 - a p_\phi, \quad (96)$$

R va Θ funktsiyalari mos ravishda harakatning radial va burchak tenglamalari bilan bog'liq va quyidagicha ifodalanadi:

$$\mathcal{R} = P(r)^2 - \Delta\left[\mathcal{Q} + \left(p_\phi - a\omega_0\right)^2 + h(r)\right] \quad (97)$$

$$\Theta = \mathcal{Q} + \cos^2\theta\left(a^2\omega^2 - p_\phi^2 \sin^{-2}\theta\right) - g(\theta) \quad (98)$$

Bu yerda Q = K − $(p_\phi - a\omega_0)^2$.

Plazmaning ishtirokidagi Kerr-Newman-Kiselev-Letelier qora tuynugining soyasi

Qora tuynuklarning soyalarini muhokama qilish uchun biz yorug'lik nurlarining chegarasini baholaymiz. Fotonlarning aylana orbitalarining radiusi *r* bo'yicha harakat konstantalarini olish uchun *R =0= R'* sifatida berilgan shartlardan foydalanamiz:

$$\mathcal{Q} = \frac{\left(a p_\phi - \omega_0(a^2 + r^2)\right)^2}{\Delta} - \left(p_\phi - a\omega_0\right)^2 - h(r) \quad (99)$$

$$p_\phi = \frac{\omega_0}{a}\left[r^2 + a^2 - \frac{\Delta}{a\Delta'}\left(\sqrt{4r^2 - \frac{h'(r)\Delta'(r)}{\omega_0}} + 2r\right)\right]. \quad (100)$$

Endi biz plazma borligida qora tuynuk tomonidan tushirilgan soya siluetini ko'rsatish uchun fazo koordinatalaridan foydalanamiz. U quyidagi shaklda ifodalanishi mumkin:

$$\alpha = -\frac{p_\phi}{\omega_0 \sin\theta_0}\sqrt{f(r_0)}, \quad (101)$$

$$\beta = \pm\frac{\sqrt{f(r_0)}}{\omega_0}\sqrt{\mathcal{Q} + \cos^2\theta_0\left(a^2\omega_0^2 - \frac{p_\phi^2}{\sin^2\theta_0}\right) - g(\theta_0)}. \quad (102)$$

O'lchami va shaklini fazo-vaqt parametrlarining funktsiyalari sifatida ko'rib chiqish uchun biz cheksizlikda tinch holatda bo'lgan va birinchi bo'lib Shapiro tomonidan plazma uchun ishlatilgan changning mashhur holatini ko'rib chiqamiz.

Aylanadigan fazoda massa zichligi va 132-tenglama bo‘yicha kvadrat plazma chastotasi θ dan mustaqil bo‘lib, juda yaxshi yaqinlikka $r^{-3/2}$ ga o‘tadi. Biroq, bunday plazma taqsimotini 88-tenglama tomonidan berilgan ajraladigan shaklga keltirish mumkin emas. Shuning uchun, qo‘shimcha burchakka bog’liqlikka ega bo‘lish chastotasini olamiz:

$$h(r) = \omega_c^2\sqrt{M^3 r} \tag{103}$$

$$g(\theta) = 0, \tag{104}$$

Bundan esa quyidagi kelib chiqadi

$$\omega_p^2 = \omega_c^2 \frac{\sqrt{M^3 r}}{r^2 + a^2\cos^2\theta} \tag{105}$$

Bu yerda w_c o‘zgarmas hamda M esa qora tuynukning massasini ifodalaydi. KNKL qora tuynugining soyasini olish uchun ekvator tekisligida 101, 102, 103 va 104-tenglamalarni birlashtiramiz va 11-rasmdagi chizmalar fazo va vaqtning turli qiymatlari uchun qora tuynuk soyasini va plazma parametrlarini ko‘rsatadi. 11-rasmdan biz plazma parametrining oshishi bilan KNKL qora tuynuk soyasining o‘lchami kamayishini kuzatamiz, boshqa barcha fazo-vaqt parametrlarining belgilangan qiymatlari uchun. Bundan tashqari, plazma parametrini va boshqa fazo-vaqt parametrlarini barqaror ushlab tursak, γ va b parametrlarining ortib borayotgan qiymatlari uchun KNKL qora tuynuk soyasi ortib borishini ko‘ramiz. Demak, plazmaning mavjudligi KNKL qora tuynugiga tushadigan soyani qisqartiradi. Bundan tashqari, γ va b parametrlarining tabiati hatto plazma muhiti mavjud bo‘lganda ham itaruvchidir (Atamurotov et al. EPJC 2022).

Aksion-plazmon muhiti ishtirokida Qora tuynukga tushadigan gazdan iborat bo‘lgan juda oddiy o‘sish modelini ko‘rib chiqamiz. Garchi real rasm ancha murakkab bo‘lsa-da, u yig’ish modelining o‘lchami va shakli yoki Qora tuynuk atrofidagi magnit maydonlarning tarqalishi kabi bir qator tarkibiy qismlarga bog’liq. Biz kiruvchi va radiatsiya gazi tufayli ko‘rinadigan soyani topish uchun "Orqaga nurlanish" deb nomlanuvchi raqamli texnikadan foydalanmoqchimiz. Qora tuynukdan uzoqda kuzatilgan $I_{\nu 0}$ o‘ziga xos intensivlikni aniqlashimiz kerak bo‘lgan birinchi miqdor quyidagi ifoda bilan berilgan (Bambi, PRD 2013):

$$I_{obs}(\nu_{obs}, X, Y) = \int_\gamma \mathrm{g}^3 j(\nu_e) dl_{\mathrm{prop}} \tag{106}$$

Bu yerda $g=\nu_{obs}/\nu_e$ qizil siljish omili va ν_e emitentning ortib qolgan ramkasida o‘lchanadigan foton chastotasini beradi. Umumiy oqimni hisoblash uchun (Bambi, PRD 2013)-adabiyotdan foydalanish mumkin

$$F_{obs}(X, Y) = \int_\gamma I_{obs}(\nu_{obs}, X, Y) d\nu_{obs} \tag{107}$$

Radiatsiya qiluvchi gaz erkin tushish holatida bo‘lib, uning to‘rt tezlikli komponentlari tomonidan quyidagicha berilgan

$$u_e^t = \frac{1}{f(r)}, u_e^r = -\sqrt{1 - f(r)}, u_e^\theta = u_e^\phi = 0. \tag{108}$$

Umumiy oqimni hisoblash uchun biz to‘rt tezlikli fotonning radial va vaqt komponentlari o‘rtasidagi munosabatni aniqlashimiz kerak

$$k^r = \pm k^t f(r)\sqrt{f(r)\left(\frac{1}{f(r)} - \frac{b^2}{r^2}\right)}. \tag{109}$$

Yuqoridagi tenglamadagi +(–) belgilarining fizik ma’nosi quyidagicha: Foton Qora tuynukga yaqinlashishi yoki undan uzoqlashishi mumkin. E’tibor bering, ta’sir parametri b magnitlangan plasma effektini kodlaydi va u quyidagini topiladi (Atamurotov, PRD 2021):

$$b = r\sqrt{\frac{1}{f(r)} - \frac{\omega_{\mathrm{p}}^2(r)}{\omega_0^2}\left(1 + \frac{\tilde{B}^2}{1-\tilde{\omega}_\varphi^2}\right)}. \tag{110}$$

Bundan tashqari, (Bambi, PRD 2013)-adabiyot bilan hisoblanishi mumkin bo‘lgan g qizil siljish funktsiyasidan foydalanishimiz mumkin

$$\mathrm{g} = \frac{k_\alpha u_o^\alpha}{k_\beta u_e^\beta} \tag{111}$$

O‘sish modelimizda biz yana bir taxminni qo‘llaymiz, ya’ni tenglama bilan berilgan o‘ziga xos ajralib chiqish uchun monoxromatik va $1/r^2$ radial profildan foydalanamiz

$$j(\nu_e) \propto \frac{\delta(\nu_e - \nu_\star)}{r^2} \tag{112}$$

bunda δ Dirac delta funksiyas. To‘g’ri uzunlikni munosabat bilan ifodalashimiz mumkin

$$dl_{\mathrm{prop}} = k_\alpha u_e^\alpha d\lambda = -\frac{k_t}{\mathrm{g}|k^r|}dr \tag{113}$$

Nihoyat, biz barcha kuzatilgan chastotalar bo‘yicha intensivlikni integrallagandan so‘ng, 107-tenglama bilan berilgan jami oqimni qayta yozishimiz mumkin

$$F_{obs}(X,Y) \propto -\int_\gamma \frac{\mathrm{g}^3 k_t}{r^2 k^r}dr \tag{114}$$

Biz (Atamurotov, PRD 2021) da keltirilgan raqamli texnikani diqqat bilan kuzatib boramiz va natijada magnitlangan plasma effektlari bilan qora rangning soyali tasvirlari 12-rasmda tasvirlangan. Xususan, biz bir xil plazma muhiti va quvvat qonuni plazma muhitini ko‘rib chiqdik. Uzoqda joylashgan kuzatuvchi tomonidan ko‘rilganda vakuum holatiga nisbatan biz intensivlikdagi farqni va soya radiuslarini aniq ko‘rishimiz mumkin. Bir jinsli plazma holatida ta’sir kuchliroq. Qora tuynukdan uzoqda kuzatilgan intensivliklarning farqi yorug’likning burilish burchagiga plazma ta’sir qilishi bilan izohlanadi. Yagona plazma uchun og’ish burchagi ortib borayotganligi sababli, intensivlik cheksizda kichikroq bo‘ladi, chunki Qora tuynuk tomonidan ko‘proq fotonlar ushlanadi. Ushbu ishda biz foton sferasini garchi ufq va foton sferasi o‘rtasidagi mintaqadan keladigan kichik hissa yoki amalda e’tibordan chetda qoladigan effekt mavjud bo‘lsada raqamli ravishda birlashtirdik.

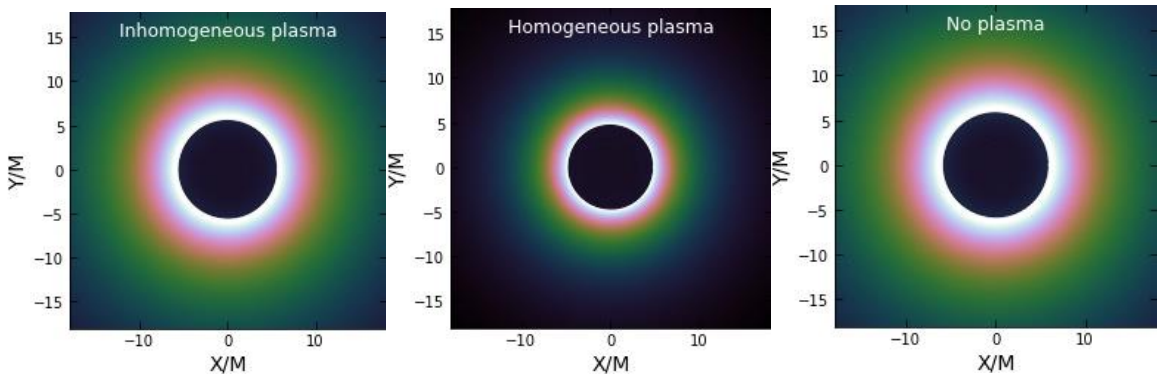

12-rasm: Plazma ishtirokisiz hamad plazma muhitidagi Qora tuynuk uchun soya tasvirlari.

III qism.

Zarrachalarning tezlashishi. Eynshteyn-Born-Infeld (EBI) nazariyasida maydon tenglamalariga olib keladigan harakatni hisobga olsak va gravitatsion maydoni chiziqli bo‘lmagan Born-Infeld elektrodinamikasiga o‘lchovlar (3 + 1) bo’lganda quyidagicha yoziladi:

$$I = \int d^4x\sqrt{-g}\left(\frac{R}{16\pi G} + \mathcal{L}(\mathcal{F})\right) \tag{115}$$

bu yerda *R* skalyar egrilik va $g = \det|g_{\mu\nu}|$. Lagrangian *L(F)* quyidagicha aniqlanadi:

$$\mathcal{L}(\mathcal{F}) = \frac{\beta^2}{4\pi G}\left(1 - \sqrt{1 + \frac{2\mathcal{F}}{\beta^2}}\right) \tag{116}$$

$\mathcal{F} = \frac{1}{4}F_{\mu\nu}F^{\mu\nu}$, $F_{\mu\nu}$ elektromagnit maydon-tenzorini bildiradi. β belgisi Born-Infeld parametri bo‘lib, elektromagnit maydon intensivligining maksimal qiymatiga teng. Eynshteyn maydon tenglamalari va elektromagnit maydon tenglamalari mos ravishda (115) dan quyidagicha tuzilgan:

$$R_{\mu\nu} - \frac{1}{2}g_{\mu\nu}R = kT_{\mu\nu}, \tag{117}$$

$$\nabla_\mu\left(F^{\mu\nu}\mathcal{L}_{,\mathcal{F}}\right) = 0. \tag{118}$$

T_{uv} energiya impulse quyidagini ifodalanadi:

$$T_{\mu\nu} = \mathcal{L}g_{\mu\nu} - F_{\mu\eta}F_\nu^\eta \tag{119}$$

$L_{,F}$ bu *L* ning *F* ga nisbatan hususiy hosilasini ifodalaydi. EBI nazariyasida *M* massali va *Q* nochiziqli elektromagnit manbali statik va sferik simmetrik kompakt obyektning fazo-vaqti birinchi navbatda Hoffman tomonidan o‘rganilgan. EBI fazo-vaqt metrikasi quyidagicha ifodalanadi (Babar et al, PRD 2021):

$$\begin{aligned} ds^2 &= -f(r)dt^2 + f(r)^{-1}dr^2 + r^2(d\theta^2 + \sin^2\theta d\phi^2) \\ f(r) &= \left(1 - \frac{2GM}{r} + \frac{Q^2(r)}{r^2}\right) \end{aligned} \tag{120}$$

xolbuki, $Q^2(r)$ bu quyidagilarddan tashkil topgan: qora tuynuk zaryadi *Q*, β va *r* Born-Infeld parametri va quyidagicha yoziladi

$$Q^2(r) = \frac{2\beta^2r^4}{3}\left(1 - \sqrt{1 + \xi^2(r)}\right) + \frac{4Q^2}{3}F\left(\frac{1}{4}, \frac{1}{2}, \frac{5}{4}, -\xi^2(r)\right), \tag{121}$$

bu yerda F Gauss gipergeometrik funksiyasini bildiradi va $\xi^2(r)$ parametri $Q^2/(\beta^2 r^4)$ bilan xarakterlanadi. Aylanadigan EBI nazariyasi Newman-Janis algoritmini statik sferik metrikaga (120) qo‘llash orqali olinadi.

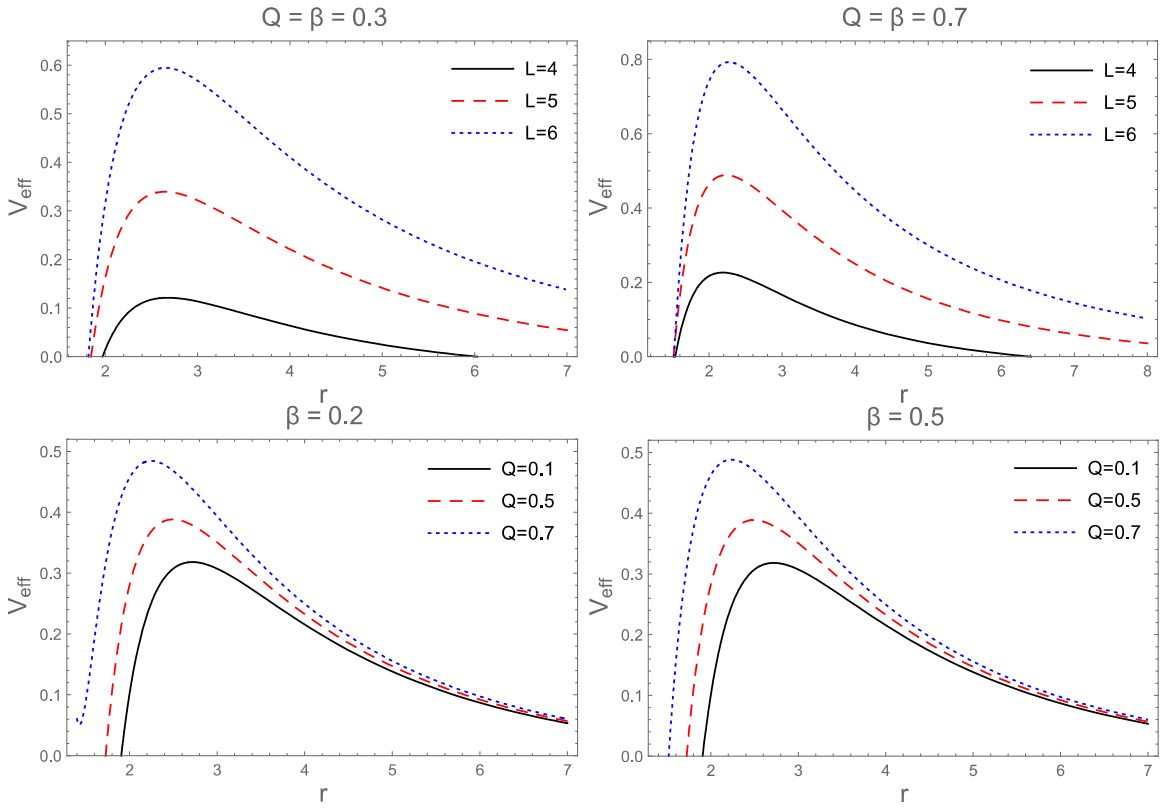

13-rasm: Effektiv potensialning radial koordinataga bog’lanishi.

Endi biz EBI gravitatsiyasi fonida zarrachalarning tezlashishini tekshirish uchun to’liq tahlil qilamiz. Ekstremal va ekstremal bo‘lmagan zaryadlangan qora tuynukni hisobga olgan holda fazolar gorizonti yaqinida ikki zarracha to‘qnashuvi natijasida hosil bo‘lgan markaziy massa (CM) energiyasini aniq o‘rganamiz. Biz dastlab cheksizlikda joylashgan ikkita relyativistik bo‘lmagan zarralar qora tuynuk tomon erkin tushishi va oxir-oqibat gorizont yaqinida katta to‘qnashuvga duch keladigan senariyni ilgari surdik. Bu yerda biz to‘qnashuv nuqtasi uchun noyob tanlov qildik, chunki cheksizlikdan tushgan zarralar gorizontda cheksiz ko‘k siljish bilan paydo bo‘ladi va shuning uchun cheksiz katta miqdorda energiya ishlab chiqaradi.

Test massasi m_0 bo‘lgan zarrachaning $\theta=\pi/2$ qutb tezligi nolga aylanadigan ekvator tekisligida harakatini ko‘rib chiqamiz. Aylanadigan zaryadlangan qora tuynukning fazo vaqtidagi zarrachaning implusi quyidagicha ifodalanadi:

$$P_t = g_{tt}\dot{t} + g_{t\phi}\dot{\phi} \tag{122}$$

$$P_\phi = g_{\phi\phi}\dot{\phi} + g_{t\phi}\dot{t} \tag{123}$$

bu yerda P_t va P_ϕ harakat konstantalari. Asosan, ikkita P_t va P_ϕ kattaliklari simmetriya o‘qi bo‘ylab harakat qiluvchi mos ravishda E energiyasi va L burchak impulsi sifatidagi zarrachaga mos keladi. Ortiqcha nuqta hususiy vaqt τ ga nisbatan farqlashni bildiradi. Massiv zarrachaning harakat tenglamalari (122,123) dan $u_\mu u^\mu = -m^2$, normallashtirish sharti bilan quyidagi tarzda hisoblab chiqiladi:

$$\dot{t} = \frac{1}{r^2}\left[\frac{(a^2+r^2)}{\Delta}(E(a^2+r^2)-aL) + a(L-aE)\right], \quad (124)$$

$$\dot{\phi} = \frac{1}{r^2}\left[\frac{a}{\Delta}(E(a^2+r^2)-aL)+(L-aE)\right], \quad (125)$$

$$\dot{r} = \pm\frac{\sqrt{(aL-(a^2+r^2)E)^2-\Delta(m_0^2r^2+(L-aE)^2)}}{r^2}. \quad (126)$$

(126) + va – belgilari mos ravishda chiquvchi va kiruvchi geodeziyaga tegishli. Sinov zarrasining EBI gravitatsiyasi yaqinidagi harakatini to‘liq tushunish uchun biz (126) yordamida to‘g’ridan-to‘g’ri ishlab chiqilgan effektiv potentsialni baholashimiz kerak.

$$\frac{1}{2}\dot{r}^2 + V_{\text{eff}} = 0, \quad (127)$$

$$V_{\text{eff}} = -\frac{(aL-(a^2+r^2)E)^2-\Delta(m_0^2r^2+(L-aE)^2)}{2r^4}. \quad (128)$$

Tezlashtirilgan zarracha qora tuynukga yetib borsa, u katta ehtimol bilan fazo-vaqtida harakatini davom ettirishi mumkin.

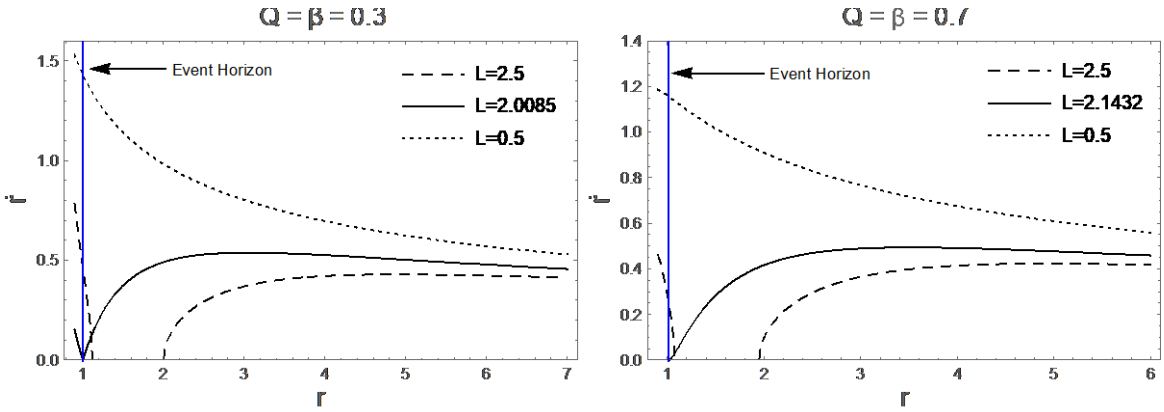

14-rasm: $\dot{r}$ ning radial koordinataga bog’lanishi.

13-rasmda effektiv potentsial $Q = \beta$ uchun kiruvchi sinov zarrasining burchak impulsini o‘zgartirish orqali ko‘rsatilgan. L ning kattaroq qiymatlari uchun potentsial to‘siq ko‘tariladi, bu esa kuchaygan zarracha qora tuynukni tezda aylana boshlashi mumkin. Bundan tashqari, agar elektr maydonining intensivligi maksimalga erishsa, qora tuynuk atrofida zarrachaning harakatlanishining ehtimolligi ortadi.

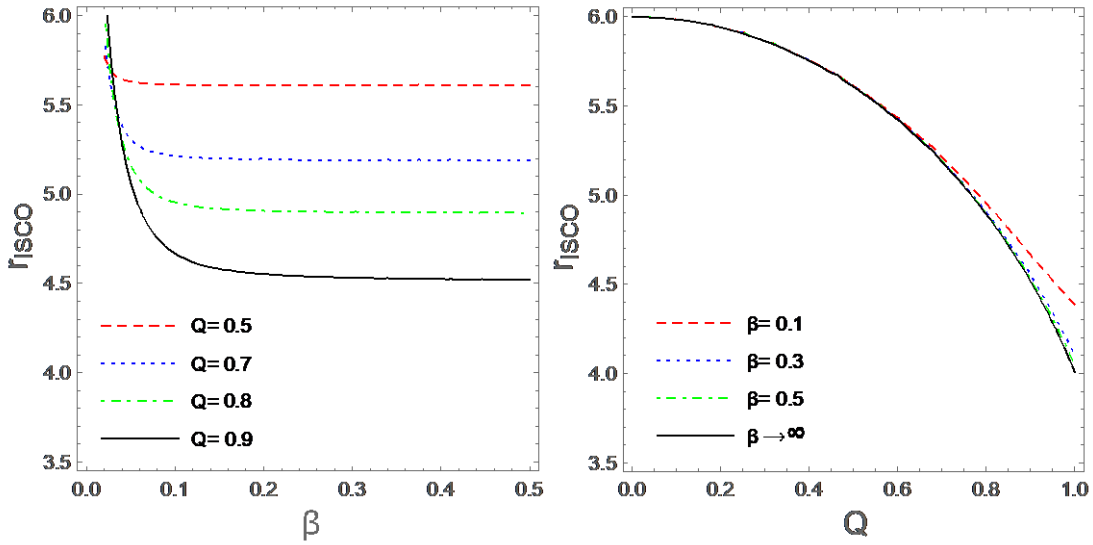

15-rasm. Massali zarrachaning orbitasini qora tuynuk parametrlariga bog'liqligi.

Zarracha impulsining kattaligi uning geodeziyasini gravitatsion fazo-vaqtda harakatida muhim rol o'ynaydi. Shunday qilib, burchak implusining kritik qiymatini (124) dan olish mumkin, qachonki $r \to r_H^E$ teng bo'lsa, ya'ni $L_c = (a^2 + (r_H^E)^2)E/a$ bo'lsa. 14-rasmda EBI fazo-vaqtida geodeziyaning tushunarli namoyishi berilgan. L <Lc bo'lgan zarracha har doim qora tuynukning maydoni bilan ushlanadi va L=Lc, shunga qaramasdan L >Lc bo'lsa, gorizontga to'g'ri tushadi. Geodeziya hech qachon qora tuynuk ichiga tushmaydi.
Bir vaqtning o'zida $\partial_r V_{\text{eff}} = \partial^2 V_{\text{eff}} = 0$ tenglamalarining yechimi zarrachaning eng ichki barqaror aylana orbitasini r_{ISCO} ni aniqlaydi. 15-rasmda Born-Infeld parametri va qora tuynukning Q zaryadini o'zgartirish orqali statik aylanmaydigan EBI gravitatsiyasi uchun r_{ISCO} tasvirlangan. β va Q oshgani sayin orbitalarning radiusi kichrayishi kuzatilmoqda, ammo qora tuynuk zaryadlanganda pasayish nisbatan yuqoriroq bo'ladi. Aniqroq qilib aytishimiz mumkinki, EBI qora tuynukning zaryadi cheksiz tortishish kuchi bilan bir qatorda uning yaqinidagi kiruvchi zarrachani ushlash qobiliyatini sezilarli darajada oshiradi va buning natijasida ISCO zaryad miqdorini oshirib, qora tuynukga yaqinlashadi. Bu qonuniyat (Zaslavskii, EPJC 2015) da Kerr-Newman fazo vaqti uchun tekshirilgan narsani eslatadi.

Hodisalar gorizontidagi zarralar to'qnashuvi. Endi biz EBI qora tuynugining gorizonti yaqinida ikki zarracha to'qnashuvi natijasida hosil bo'lgan o'ta yuqori energiyani tahlil qilamiz. Bir xil massali m_0 va turli to'rt tezlikli u_1 va u_2 bo'lgan zarralarni ko'rib chiqamiz. Ikki zarrachaning radial koordinatasidagi to'qnashuvining CM energiyasi $E_{c.m}$ quyidagi ifoda bilan ifodalanadi (Banados et al. PRD 2009),

$$E_{\text{c.m}} = m_0\sqrt{2}\sqrt{1 - g_{\mu\nu}\mathrm{u}_1{}^{\mu}\mathrm{u}_2{}^{\nu}}. \qquad (129)$$

Yuqorida aytib o‘tilgan energiya ramkasida (124-126) o‘rnini bosish orqali biz quyidagini olamiz:

$$\frac{E_{\text{c.m}}^2}{2m_0^2} = -\frac{\mathcal{K}}{r^2\Delta}, \tag{130}$$

Bu yerda *K* pastda berilgan,

$$\begin{aligned}\mathcal{K} \quad &= -2r^4 + 2r^3 - r^2(2a^2 + Q^2(r) - L_1L_2) \\ &-2a^2r + 2r[a(L_1 + L_2) - L_1L_2] \\ &+Q^2(r)(a - L_1)(a - L_2) \\ &+\sqrt{(a^2 + r^2 - aL_1)^2 - \Delta[r^2 + (a - L_1)^2]} \\ &\times \sqrt{(a^2 + r^2 - aL_2)^2 - \Delta[r^2 + (a - L_2)^2]}\end{aligned} \tag{131}$$

3-jadval: Aylanadigan EBI qora tuynuklarining turli ekstremal holatlari uchun burchak impulslarining cheklovchi qiymatlari (Babar, PRD 2021).

Q	β	$Q(r)_{\text{E}}$	a_{E}	r_{H}^{E}	L_1	L_2
0	0	0	1	1	-4.82843	2
0.2	0.2	0.19792	0.98021707	1.00141	-4.80013	2.00327
0.3	0.3	0.296864	0.95491506	1.00304	-4.76386	2.0085
0.4	0.4	0.39579	0.91832659	1.00512	-4.71127	2.01845
0.5	0.5	0.494701	0.86903103	1.00751	-4.64012	2.03709
0.6	0.6	0.593595	0.80470045	1.01008	-4.54673	2.07259
0.7	0.7	0.692477	0.72132723	1.01274	-4.42477	2.1432

Bizning muhokamamizda ishtirok etuvchi zarralar bir xil o‘ziga xos xususiyatlarga ega va asosan L_1 va L_2 burchak implusiga keltiruvchi bilan ajralib turadi. Bu yerda soddalik uchun $E_1/m_0=E_2/m_0=1$ saqlangan energiyalarni olamiz. Shuni aytib o‘tish joizki, qora tuynukka yaqinlashib kelayotgan sinov zarrachasi L_c kritik burchak implusi ega bo‘lganda, to‘xtovsizlik bilan yuqori energiya miqdori olinadi (Babar, PRD 2021).

4-jadval: Aylanadigan EBI qora tuynuklarining turli ekstremal bo‘lmagan holatlari uchun burchak impulsining cheklovchi qiymatlari (Babar, PRD 2021).

Q	β	a	r_{H}^{-}	r_{H}^{+}	L_1	L_2
0.2	0.2	0.9	0.663948	1.38792	-4.74224	2.56572
0.3	0.3	0.8	0.632149	1.52037	-4.64939	2.78645
0.4	0.4	0.7	0.638054	1.59260	-4.54509	2.93519
0.5	0.5	0.6	0.653747	1.62586	-4.42765	3.04241
0.6	0.6	0.5	0.674623	1.62645	-4.29465	3.11902
0.7	0.7	0.3	0.686800	1.65050	-4.04668	3.33159

Ekstremal va ekstremal bo‘lmagan EBI fazo vaqti uchun mos keladigan aylanish parametrlari va gorizontlari bilan birga burchak implusining cheklovchi qiymatlari mos ravishda (3,4) jadvallarda keltirilgan. Q=β ning turli qiymatlari

uchun ekstremal qora tuynuk gorizonti yaqinida to‘qnashuv natijasida hosil bo‘lgan $E_{c.m}$ 16-rasmda ko‘rsatilgan. Zaryadlangan Kerr-Newman gravitatsiyasi juda o‘xshash, kiruvchi zarracha harakatning kretik parametrlari bilan ta’minlangan bo‘lsa, CM energiyasi bir zumda EBI gorizonti yaqinida ajralib chiqadi, boshqa tomondan, $L<L_c$ ni qabul qiluvchi zarralar faqat chekli $E_{c.m}$. Shunga qaramay, agar biz ekstremal bo‘lmagan fazo-vaqt fonida to‘qnashuvni ko‘rib chiqsak, biz hodisa joyidan qat’i nazar, cheklangan $E_{c.m.}$ ga erishamiz, 17-rasmga qarang.

Termodinamikalar.

Bizning ishimizning ushbu qismida *f(Q)* nazariyasi uchun ta’sirni ko‘rib chiqamiz, bu quyidagi orqali beriladi:

$$S = \int \sqrt{-g} d^4x \left[\frac{1}{2} f(Q) + \lambda_\alpha^{\beta\mu\nu} R^\alpha_{\beta\mu\nu} + \lambda_\alpha^{\mu\nu} T^\alpha_{\mu\nu} + L_m\right] \qquad (132)$$

$g_{\mu\nu}$ ning determinanti g bilan belgilanadi, *f(Q)* metrik bo‘lmagan Q funksiyasi, λ Lagranj uchun ko‘paytmasi, L_m esa materiyaning Lagranj zichligini bildiradi. Endi *f(Q)* gravitatsion maydon tenglamalari yechimini $f(Q) = Q + \alpha Q^2$ ansatsi uchun 4-o‘lchovli sferik simmetrik va statsionar fazo vaqt sifatida ko‘rib chiqamiz, bunda bog’lanish doimiysi α bilan belgilanadi. O‘zgartirilgan *f(Q)* nazariyasidagi Qora tuynukning tegishli chiziqli elementi quyidagicha yoziladi

$$ds^2 = g_{tt}dt^2 - g_{rr}dr^2 - r^2 d\theta^2 - r^2 \sin^2\theta d\phi^2 \qquad (133)$$

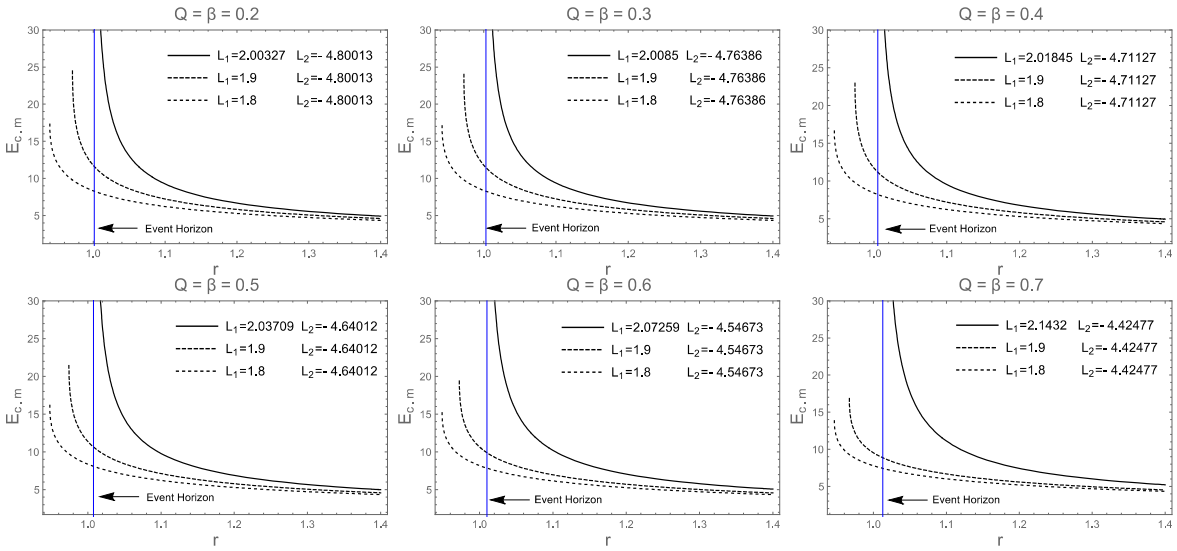

16-rasm: Ekstrimal qora tuynuk uchun markaziy massa energiyasining radial koordinataga bog’liqligi bog’liqligi.

bu yerda tegishli metrik komponent ($g_{tt} = 1/g_{rr}$) sifatida aniqlanadi

$$g_{tt} = -\frac{\alpha c_2 + \alpha^2(c_3 - 16(3c_6 + c_7)m^2) + 2m}{r} - \frac{(\alpha^2\mu)\log\left(\frac{r}{R}\right)}{r} + 1, \qquad (134)$$

c_1, c_2, c_3 va c_4 real integrallovchi domiylar. Bu yerda m Shvartsshild qora tuynukining massasini ifodalaydi. Bu yerda ulanish doimiysi α bilan belgilanadi va uning qiymatlari fizik jihatdan maqbul konfiguratsiya uchun |α|<1 talabiga mos kelishi kerak. Ushbu qo‘lyozmada biz α ning kerakli diapazon bo‘yicha qiymatlarini ham |α|< 1 sifatida ko‘rib chiqdik. Logarifmada o‘lchamsiz argumentni olish uchun $\mu = 48m^2c_7$ sifatida kiritilgan yangi masshtab parametri va doimiy $c_6 \rightarrow c_6 - 48m^2c_7$ $\log(R)$ ni siljitish uchun R shkalasi qo‘llaniladi. α = 0 uchun umumiy nisbiylik nazariyasida Shvartsshild yechimiga keltiriladi.

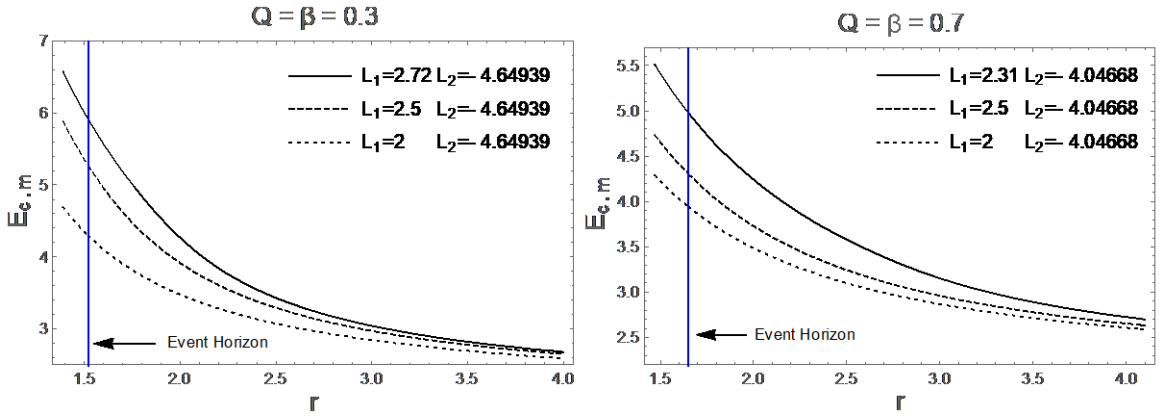

17-rasm: Ekstrimal bo’lmagan qora tuynuk uchun markaziy massa energiyasining radial koordinataga bog’liqligi bog’liqligi.

134-tenglamada aniqlangan metrik funktsiyali 133-tenglamada berilgan chiziq elementi nazariyaning aniq yechimi emas, u faqat beqaror yechimdir. Shu munosabat bilan metrik funktsiyani quyidagicha qayta yozamiz:

$$\mathcal{J}(r) = g_{\mathrm{tt}}|_{\alpha=0} + \alpha\epsilon g_{\mathrm{tt},\alpha} + \alpha^2\epsilon^2 g_{\mathrm{tt},\alpha\alpha}, \qquad (135)$$

bu yerda ε <<1 kuzatuv parametri. Metrik funktsiyaning hosilasini va doimiyning ikkinchi darajali hadlargacha ko‘rib chiqamiz. Demak, yuqorida aniqlangan ansatz bilan ko‘rib chiqilgan geometriyaning yechimi sifatida mos keladigan metrik funktsiya quyidagicha bo‘ladi:

$$\begin{aligned}\mathcal{J}(r) \quad &= 1 - \frac{2m}{r} + \frac{\alpha\epsilon}{r}\left(-2\alpha(c_3 - 16(3c_6 + c_7)m^2) - c_2 - 2\alpha\mu\log\left(\frac{r}{R}\right)\right) \\ &+ \frac{\alpha^2\epsilon^2}{r}\left(-2(c_3 - 16(3c_6 + c_7)m^2) - 2\mu\log\left(\frac{r}{R}\right)\right)\end{aligned} \qquad (136)$$

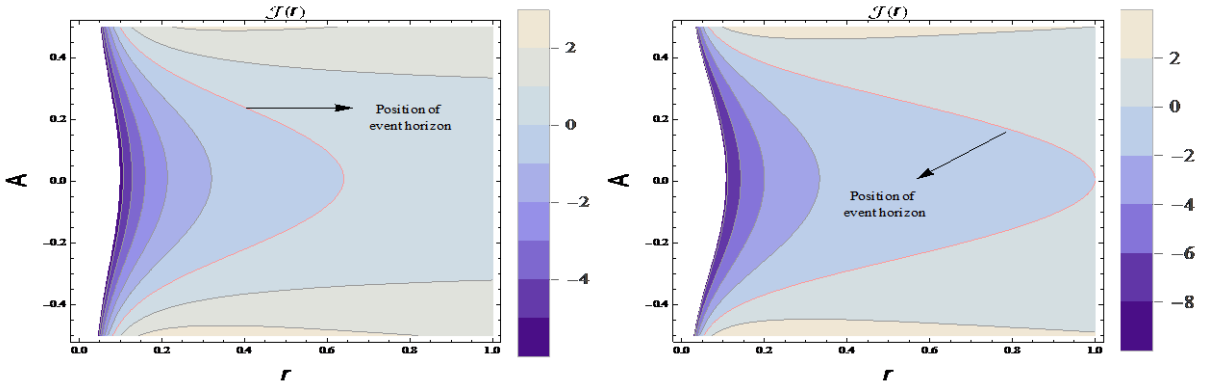

18-rasm: Bog'lanish parametri α ning radial koordinataga va potensial funksiyaga bog'lanish.

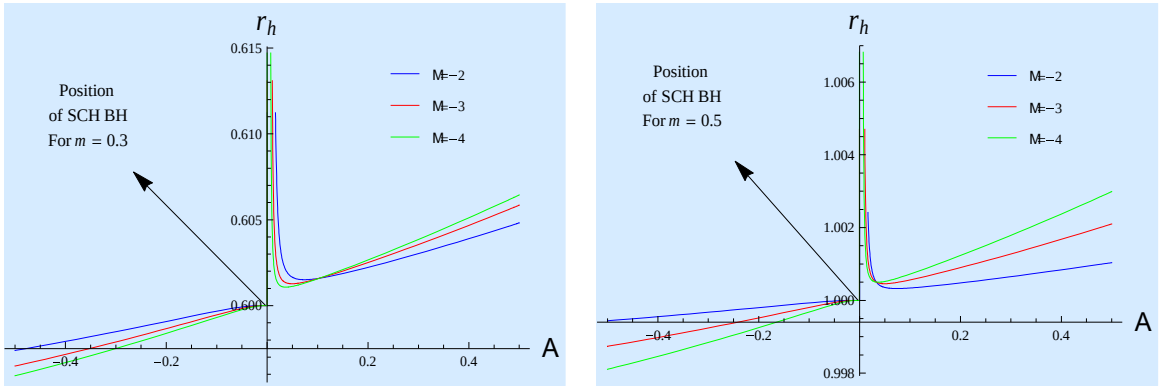

19-rasm. Hodisalar gorizontining radial koordinataga bog'langanligi.

α= 0 uchun u Umumiy nisbiylik nazariyasida Shvartsshild yechimiga keltiriladi va tuzatish shartlari r ning katta qiymatida Shvartsshild yechimidan chetlanishga olib kelishi mumkin. *J(r) = 0* ni qabul qilib, hodisa gorizontining holatini quyidagi shaklda hisoblaymiz:

$$r_h = 2m + \alpha\epsilon\left(Re^{-\frac{c_2}{2\alpha\mu}-\frac{c_3}{\mu}+\frac{16(3c_6+c_7)m^2}{\mu}}\right) + \alpha^2\epsilon^2\left(Re^{\frac{16(3c_6+c_7)m^2}{\mu}-\frac{c_3}{\mu}}\right). \quad (137)$$

18-rasmda fizik parametrlarning turli qiymatlari uchun metrik funktsiyaning grafik harakati ko‘rsatilgan. Ta’kidlanishicha, metrik funktsiya α ulanish konstantasining musbat va manfiy qiymatlari bo‘yicha simmetrik harakatni ko‘rsatadi. Metrik funktsiyaning harakati salbiydan musbatga r ga o‘tadi va o‘sadi, α esa salbiy yoki ijobiy ortadi. Qora tuynuk massasi oshgani sayin hodisa gorizontining qiymati ortadi. 19-rasmning chap va o‘ng chizmalarida Shvartsshild qora tuynuk massasining turli qiymatlari uchun hodisa gorizontining joylashuvining grafik harakati ko‘rsatilgan. Bu yerda shuni ta’kidlash juda joizki, Shvartsshild hodisa gorizontining qiymati ($r_h = 2m$) α= 0 uchun tiklanadi, ya’ni m= 0.3 va 0.5 uchun biz mos ravishda $r_h = 0.6$ va $r_h = 1$ ni olamiz. Ta’kidlanishicha, hodisalar gorizonti α o‘sishi bilan ortadi.

Endi biz qora tuynukning termodinamik miqdorlarini, ya'ni Xoking(Hawking) haroratini Qora tuynuk massasi va issiqlik sig'imi bo'yicha hisoblaymiz. Ushbu miqdorlar Qora tuynuk strukturasining termodinamik barqaror xususiyatlarini o'rganish uchun ishlatiladi. Buning uchun $J(r) = 0$ ni qo'yamiz, so'ngra r_h bo'yicha qora tuynuk massasi quyidagicha berilgan:

$$m = \frac{\frac{1}{2}\sqrt{128\alpha^2\left(3c_6+c_7\right)\epsilon(\epsilon+1)\left(\alpha\epsilon\left(2\alpha c_3(\epsilon+1)+c_2\right)+2\alpha^2\mu\epsilon(\epsilon+1)\log\left(\frac{r_h}{R}\right)-r\right)+4}+1}{32\alpha^2\left(3c_6+c_7\right)\epsilon(\epsilon+1)}. \tag{138}$$

Qora tuynuk sirtidagi gravitatsiyasi ($k = 0.5\, d\mathcal{J}(r)/dr$) Xoking haroratini aniqlash uchun ishlatiladi (Hawking, Nature 1974). Ko'rib chiqilayotgan tuzilma uchun u quyidagi shaklga ega:

$$\kappa = \frac{\alpha\epsilon\left(2\alpha(\epsilon+1)\left(c_3-16\left(3c_6+c_7\right)m^2\right)+c_2\right)+2\left(\alpha^2\mu(-\epsilon)(\epsilon+1)+m+\alpha^2\mu\epsilon(\epsilon+1)\log\left(\frac{r_h}{R}\right)\right)}{2r_h^2}.$$

Demak, biz Xoking haroratini ($\mathbb{T} = k/2\pi$) sifatida olamiz.

$$\mathbb{T} = \frac{\alpha\epsilon(2\alpha(\epsilon+1)(c_3-16(3c_6+c_7)m^2)+c_2)+2\left(\alpha^2\mu(-\epsilon)(\epsilon+1)+m+\alpha^2\mu\epsilon(\epsilon+1)\log\left(\frac{r_h}{R}\right)\right)}{4\pi r_h^2}. \tag{139}$$

20-rasmning chap grafigi Xoking haroratini ifodalaydi va T ning musbat/manfiy oshgani sayin kamayishi va yirik qora tuynuklar uchun kamayishi aniqlandi. Harorat ulanish doimiysi α ning musbat va manfiy qiymatlari uchun simmetrik harakatni ko'rsatadi.

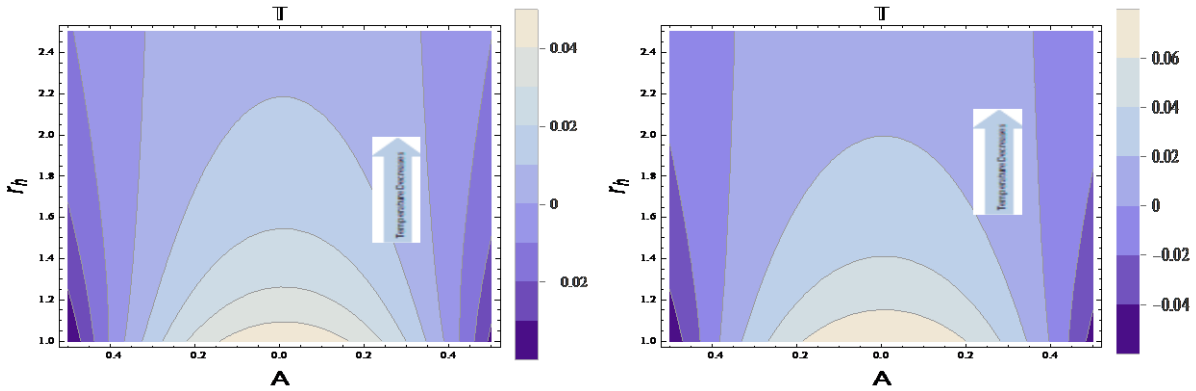

20-rasm. Hodisalar gorizontining bog'lanish parametri va temperaturaga bog'lanishi.

Tizimning entropiyasi Bekenshteynning maydon entropiyasi munosabati orqali hisoblanadi. Bu quyidagicha beriladi:

$$\mathbb{S} = \int_0^{2\pi}\int_0^{\pi}\sqrt{g_{\theta\theta}g_{\phi\phi}}d\theta d\phi = \pi r_h^2. \tag{140}$$

XULOSA

“Kompakt obyektlar atrofidagi plasma muhitida astrofizik jarayonlar” mavzusida olib borilgan tadqiqotlar asosida quyidagi xulosalar kelindi:

1. Kerr-Newman-Kiselev-Letelier qora tuynugining hodisalar gorizontining kattaligi Kiselev va torli bulut parametrlarining oshishi bilan ortib borishi topildi. Kiselev va torli bulut parametrlari qiymatining oshishi bilan foton orbitalarining radiusi ham kamayadi. Qora tuynuk soyasining buzilish parametri Kiselev va torli bulut parametrlarining ortishi bilan kamayishi ham ko‘rsatilgan. Torli bulut va Kiselev parametrlarinign yuqori chegaralari EHT (Event Horizon Telescope) hamkorligidan olingan so‘nggi kuzatuv ma’lumotlari bilan batafsil taqqoslash yordamida baholanadi.
2. Torli bulut parametri Xoking nurlanish jarayonini tezlashtirishi isbotlangan. Mukammal suyuqlik qorong‘u materiya parametrlari, zaryad va aylanish parametrlarining ortishi bilan effektiv potentsialning cho‘qqisi markaziy obyektga siljishi topildi. Qora tuynuk soyasining o‘lchami mukammal suyuqlik qorong‘u materiya parametri qiymatining oshishi, shuningdek qora tuynukning zaryadi va soya shaklining buzilishi bilan kamayishi kuzatildi. Shunga ko‘ra, Eynshteyn halqalarining o‘lchami mukammal suyuqlik qorong‘u materiya parametrining oshishi bilan kamayadi.
3. Qora tuynuk soyasining o‘lchami uzoqdagi kuzatuvchi uchun magnitlangan plasma ortishi bilan kamayib borishi ko‘rsatildi. Bir jinsli plazmaning foton sferasi radiusiga, shuningdek qora tuynuk soyasining radiusiga ta’siri bir jinsli bo’lmagan plazmaning ta’siridan ko‘ra aniqroq ekanligi ko‘rsatilgan. Bundan tashqari, bir jinsli plazma uchun plasma chastotasi oshishi bilan og’ish burchagi ortadi.
4. Garchi farqni ahamiyatsiz deb hisoblash mumkin bo‘lsada, yagona izotermik sfera(SIS)ning mavjudligida og’ish burchagi yagona bo‘lmagan izotermik sfera(NSIS)ga mavjudligiga qaraganda ma’lum darajada katta ekanligi ko‘rsatildi. Qora tuynukda bir jinsli plazma bo‘lganda fotonlar kattaroq burchakka og‘ishi ta’kidlangan. Bundan tashqari plazmaning ta’siri natijasida foton sferasi radiusi, og’ish burchagi va kuchli burilish koeffitsientlari ortishi ko‘rsatilgan.
5. Bundan tashqari, qora tuynuk aylanishining ortishi bilan plazmaning kuchli gravitatsion linzalariga ta’siri orbitasida aylanish parametri ortishi bilan kichikroq bo‘lishi ko‘rsatilgan.

6. Teleparallel gravitatsiya parametri kamayishi bilan qora tuynukning Hawking harorati ortishi aniqlandi. Nochiziqli zaryad va teleparallel gravitatsiya parametrining ortishi bilan akkretsiyalanish samaradorligi pasayishi ko'rsatildi. Nurlanish oqimi singulyar nuqta atrofida pasayadi va kuchli maydon yaqinida singulyarlikdan uzoqda maksimal qiymatga erishadi.

SCIENTIFIC COUNCIL DSc.03/31.03.2022.T/FM.10.04 ON AWARD OF SCIENTIFIC DEGREE AT INSTITUTE OF FUNDAMENTAL AND APPLIED RESEARCH "TIIAME" NATIONAL RESEARCH UNIVERSITY

INSTITUTE OF FUNDAMENTAL AND APPLIED RESEARCH

ATAMUROTOV FARRUH SHUHRATOVICH

ASTROPHYSICAL PROCESSES AROUND COMPACT OBJECTS IN PLASMA ENVIRONMENT

01.03.01 – Astronomy
01.04.02 – Theoretical Physics
(physical and mathematical sciences)

PRESENTATION
on awarding the scientific degree of Doctor of Science (DSc) on the basis of published papers without a dissertation

Tashkent – 2023

The theme of the doctor of science (DSc) researche is registered by Supreme Attestation Commission of Higher Education, Science and Innovations of Republic of Uzbekistan under B2023.2.DSc/FM224.

The esearch work has been carried out at the Institute of Fundamental and Applied Research under “TIAMEE” National Research University.

The presentation was posted in three (Uzbek, English, Russian (resume)) languages on the website of the Scientific Council (www.ifar.uz) and on the information and education portal at "Zionet" (www.ziyonet.uz).

Scientific consultants:

Abdujabbarov Ahmadjon Adiljanovich
Doctor of physical and mathematical sciences, professor

Ahmedov Bobomurat Juraevich
Doctor of physical and mathematical sciences, professor

Presentation of the research will be held on “_01_” _august_ 2023 at _17^{00}_ in the meeting of the Scientific Council No. DSc.03/31.03.2022 T/FM.10.4 at the Institute of Fundamental and Applied Research under the National Research University "TIIAME" (Address: 100000, Tashkent city, Qori Niyazov Street 39, Institute of Fundamental and Applied Research, Hall 108; tel.: 71 237-09-61.; e-mail: info@ifar.uz

The presentation can be looked through at the Information Resource Center of the Institute of Fundamental and Applied Research under the National Research University "TIIAME" (registered under № ____). (Address: 100000, Tashkent city, 39 Qori Niyazov str., Institute of Fundamental and Applied Research, hall 205; ph.: 71 237-09-61

The presentation was distributed on "___" _____, 2023.

(Registry record № ___ dated "___"_____, 2023)

A. R. Hayotov
Vice Chairman of the Scientific Council
on Award of Scientific Degrees,
D. Ph.-M.S., Professor

E. Kh. Karimbayev
Scientific Secretary of Scientific Council
on Award of Scientific Degrees
PhD in Ph.-M.S.

INTRODUCTION (presentation abstract)

Relevance and necessity of the topic. Black holes serve as an experimental setting to examine gravity in the strong field regime, allowing researchers to gain valuable insights into the nature of spacetime. By studying particle behavior near black holes, we can uncover new information about the structure of the surrounding space. The presence of a black hole shadow, a consequence of one of General Relativity's predictions concerning the gravitational bending of light, offers an opportunity to investigate this phenomenon. Consequently, the analysis of null geodesics in these spacetimes becomes crucial in studying the black hole shadow. Photons traversing the immediate vicinity of black holes exhibit circular orbits known as light rings. As a result of these light rings, the central black hole appears as a dark disc in the sky, commonly referred to as the black hole shadow.

The matter of determining the masses of black holes has been successfully resolved, resulting in the classification of black holes into four categories based on their masses: stellar, intermediate, supermassive, and miniature. However, the task of measuring the spin of rotating black holes is still ongoing, and it is believed that studying black hole shadows can assist in this endeavor. The recent detection of gravitational waves emitted by merging black hole systems and the imaging of the shadows cast by central supermassive black holes like M87* and Sgr A* have generated additional enthusiasm for investigating the properties of black hole spacetimes.

In the vicinity of black holes, an intriguing astrophysical situation arises where photons often traverse a plasma medium. This plasma medium can significantly influence the angular positions of the resulting image of the black hole shadow, leading to variations in observed wavelengths. Consequently, the inclusion of the plasma medium becomes an important consideration in the analysis of black hole shadows. To investigate the generation of jets emitted by black holes, researchers have utilized a simplified plasma model within black hole environments.

On the other hand, black holes, as significant entities, stand out as highly intriguing objects within the realm of thermodynamics. The principles governing black hole physics bear similarities to the principles of thermodynamics, which establish connections between surface gravity, mass-energy equivalence, temperature, and the horizon area as it pertains to entropy. These comparisons led Bekenstein to propose a quantifiable relationship between the horizon area and the entropy of a black hole. However, this proposed relation appears to contradict the second law of thermodynamics, as nothing can ever be extracted from a black hole, thereby suggesting that black holes and thermal radiation cannot achieve thermal equilibrium. Nevertheless, quantum-level investigations of black holes reveal the emission of subatomic particles called Hawking radiation, providing insights into the geometric properties of black holes. Thus, the study of the structural and

thermodynamical properties of the spacetime around compact astrophysical objects may lead to look deep insight of the nature of gravitational interaction.

It is worth to note that in recent years, in our country, more and more attention has been paid to the development of current directions of fundamental and applied research. In particular, the development of theoretical astrophysical research, which is one of the promising areas, is an important issue today. The main directions of fundamental research and development and their practical application for the successful development of science in our country are reflected in the Strategy[1]for the further development of the Republic of Uzbekistan from 2022-2026. Therefore, the research of effect of gravitational lemsing in the plasma environment remains one of the urgent issues in the field of fundamental research.

This research work corresponds to the tasks by the following state regulatory documents: Decree of the President of the Republic of Uzbekistan No. PD-4947 "On the Strategy of Actions for the Further Development of the Republic of Uzbekistan" dated February 07, 2017, Resolution of the President of the Republic of Uzbekistan No. PR-2789 "On measures for further improvement of the activities of the Academy of Sciences, organization, management and financing of research activities" dated February 18, 2017 and others.

Conformity of the research to the main priorities of science and technology development of the Republic. The dissertation research has been carried out in accordance with the priority areas of science and technology in the Republic of Uzbekistan: II. “Power, energy and resource-saving”.

The degree of knowledge of the problem. The photon motion and gravitation lensing around compact gravitating object have been investigated by the different researcher worldwide (J. Synge, J. Bardeen, H. Falke, O. Tsupko, V. Bozza, Z. Stuchlik, J, Schee, A. Abdujabbarov, B Ahmedov, V. Morozova,C. Laemmerzahl, J. Kunz, A. Grezenbach, L. Amarilla, E. Eiroa, M. Kolos, J. Vrba, N. Dadhich, S. Ghosh, P. Joshi, M. Patil). However, the effect of plasma on photon motion around compact object in different models and theories have not been systematically studied.

The null geodesic of the Kerr–Newman black hole is properly studied by different authors (Z. Stuchlik, S. Hledik, A. de-Vries, etc). The investigation of null geodesics and the associated optical properties of black holes, such as black hole shadows, have been remain an active topic of research in rotating black hole spacetimes and have been studied by various researchers (A. Belhaj, M. Benali, J. Luminet, etc.). However, the question of effect of different parameters of alternative theories of gravity and plasma environment on shadow and related phenomenon have not been studied yet.

[1] Decree No. PF-60 of the President of the Republic of Uzbekistan dated January 1, 2022 “On the Development Strategy of New Uzbekistan for 2022-2026”

The influence of dark matter on the astrophysical processes around a regular black hole also remains unexplored. The development and improvement of mathematical models describing the dynamics of particles around such objects contribute to obtaining limit values for the parameters of modified and/or alternative theories of gravity.

Connection of the topic of the dissertation topic to the scientific works of higher education and research institutions, where the dissertation is carried out. The dissertation was done in the framework of the scientific projects funded by the Ministry of Innovative Development. F-FA-2021-510 "Investigations of nuclear matter of neutron stars in modified gravity".

The aim of the research is the development and improvement of model for the dynamics of photons and weak gravitational lensing around compact object in the presence of plasma, constraints on the parameters of the gravity models using observation.

The tasks of the research:

to study the photon motion and the related phenomena of black hole shadow in the Kerr–Newman–Kiselev–Letelier black hole spacetime;

to analyze the influence of the cloud of string parameter and the quintessence parameter on the photon motion and the black hole shadow;

to analyze the effective potential for the photon in the presence of the quintessence and cloud string parameters;

to obtain the upper limits on the cloud string and quintessence parameters in the case of the Kerr–Newman–Kiselev–Letelier black hole;

to study the effect of the spin and charge of the Kerr–Newman–Kiselev–Letelier black hole on the emission energy rate;

to study the effect of cloud string parameter on the Hawking radiation process;

to analyze the effect of perfect fluid dark matter parameter on the dynamics of photons and related processes around black hole;

to study the rate of emission in the presence of perfect fluid dark matter parameter and nonlinear charge;

to analyze the effect of axion-plasmon on the dynamics of photons around nonrotating black hole;

to study the effect of homogenous and inhomogeneous plasma on the photon motion and gravitational lensing around gravitating objects;

to perform the systematic analysis of the weak-field lensing phenomenon in the background of a gravitating objects environed by a uniform plasma, singular isothermal sphere and non-singular isothermal sphere;

to investigate the behavior of the Hawking temperature for the teleparallel gravity;

to analyze the effect of the nonlinear charge and coupling parameter in nonlinear electrodynamics coupled to general relativity on the efficiency of accretion;

The object of the research are astrophysical compact objects, photons, plasma environment.

The subject of the research are theoretical models for studying photon dynamics near compact gravitational objects in the presence of plasma, numerical and analytical methods for solving differential equations.

The methods of the research are methods of computational mathematics, methods of theoretical astrophysics, modern methods of mathematical physics, analytical and numerical methods of calculating differential equations for field and particle motion.

The scientific novelty of the research is the following:

It has been shown that the size of the horizon of the Kerr–Newman–Kiselev–Letelier black hole increases with the increase of parameters of quintessence and cloud string.

The analysis of the effective potential for the photon have shown that it is decreasing with the increasing values of the quintessence and cloud string parameters. For the increasing values of the quintessence and cloud string parameters the unsuitability of the photon circular orbits also decreases.

It has been shown that cloud string parameter accelerates the Hawking radiation process. It has been shown that with the increase of perfect fluid dark matter parameter, charge and rotation parameter the peak of the effective potential is shifting towards the left.

It has been observed that the rate of emission is higher for the small value of both perfect fluid dark matter parameter and charge. It has been shown that the size of the black hole shadow decreases with increasing axion-plasmon for a large observer distance, and interestingly, this was also shown earlier for the case of an inhomogeneous plasma.

It has been also stated that for a homogeneous plasma, the deflection angle increases as the axion frequency increases. It has been shown that the singular isothermal sphere deflection angle is greater to a certain extent than that of the non-singular isothermal sphere, even though the difference could be regarded as negligible.

It has been stated that the photons deviate at a larger angle when a uniform plasma walls in the black hole. It has been further shown that the effect of plasma result in the increase of the photon sphere radius, the deflection angle and the strong deflection coefficients.

It has been shown that the Hawking temperature increases as coupling parameter of the teleparallel gravity decreases. It has been shown that with the increasing the nonlinear charge and coupling parameter the efficiency of accretion decreases.

The practical results of the research are the following:

It has been shown that the distortion parameter of shadow decreases with the increase quintessence and cloud string parameters. It has been shown that the shadow cast by a fast rotating and highly charged black hole would be more distorted. This observation may be helpful for estimating the values of the spin a and the charge of black holes.

It has been observed that the size of the shadow in case of non rotating black hole decreases with the increase the value of perfect fluid dark matter parameter as well as black hole's charge.

Using the data of the Event Horizon Telescope collaboration we have obtained the upper limits on the cloud string and quintessence parameters in the case of the Kerr–Newman–Kiselev–Letelier black hole.

It has been shown that the size of Einstein rings decreases with the increase of the perfect fluid dark matter parameter.

The reliability of the research results provided by applying modern proven methods of mathematical physics, computational mathematics, and relativistic astrophysics. The results were obtained strictly within the mathematical apparatus of general relativity and theoretical physics. Modern numerical and analytical methods of calculation are also used, and the results are compared with available observational data and the results of other authors. The structured conclusions of the thesis correspond to the basic rules of astrophysics of compact objects.

The scientific and practical significance of the research results. The scientific significance of the research results is found that the analysis of the shadow cast by a fast rotating and charged black hole may be helpful for estimating the values of the spin a and the charge of black holes.

The practical significance of the research results is that they can play a role in the obtaining the upper limits and constraints on the cloud string and quintessence parameters within modified theory of gravity.

Implementation of the research results. Based on the developed theoretical models for the dynamics of the photons around compact objects in the presence of plasma:

scientific results obtained on the motion of photons have been used by scientists from Fudan University (FU) in Shanghai (FU, China, July 7, 2023 reference);

results on the gravitational lensing around compact have been used in the works of foreign researchers, in foreign journals with a high impact factor (Physical Review D, 2023, Volume 107, Issue 12, article id.124003, Web-Sc, IF: 5.407; Monthly Notices of the Royal Astronomical Society, Volume 521, Issue 1, pp.708-716, Web-Sc, IF: 4.8; Physics of the Dark Universe, Volume 41, article id. 101249, Web-Sc, IF: 5.5; The European Physical Journal C, Volume 83, Issue 5, article id.426, Web-Sc, IF: 4.4; The European Physical Journal Plus, Volume 138, Issue 3, article id.192, Web-Sc, IF:3.4; Journal of Cosmology and Astroparticle Physics,

Volume 2021, Issue 10, id.013, 26 pp, Web-Sc, IF: 7.28) to describe the effects of plasma on photon motion around compact objects.

Publication of research results. The results of DSc research have been presented in 24 peer-reviewed articles published in prestigious Q1/Q2 quartile scientific journals recommended by Supreme Attestation Commission at the Ministry of higer education, science and innovations of the Republic of Uzbekistan.

Main content of the work.

Part I

Consider the effects of gravitational lensing in the background of compact object surrounded by a plasma considering a weak-field approximation defined as follows,

$$g_{\alpha\beta} = \eta_{\alpha\beta} + h_{\alpha\beta} \tag{1}$$

where $\eta_{\alpha\beta}$ and $h_{\alpha\beta}$ connote the Minkowski metric and perturbation metric, respectively.

$$\begin{aligned} &\eta_{\alpha\beta} = \text{diag}(-1,1,1,1), \\ &h_{\alpha\beta} \ll 1,\ h_{\alpha\beta} \to 0 \text{ under } x^{\alpha} \to \infty, \\ &g^{\alpha\beta} = \eta^{\alpha\beta} - h^{\alpha\beta},\ h^{\alpha\beta} = h_{\alpha\beta}. \end{aligned} \tag{2}$$

Before proceeding any further we shall briefly recall the layout presented in (Bisnovatyi-Kogan and Tsupko, Mon. Not. R. Astron. Soc. 2010) to elicit the general expression of the angle of deflection. The correlation between the phase velocity $\boldsymbol{v}$and the 4-momentum $\boldsymbol{p}^{\alpha}$ considering a static case is expressed as

$$\frac{c^2}{\boldsymbol{v}^2} = n^2 = 1 + \frac{p_{\alpha}\boldsymbol{p}^{\alpha}}{\left(\boldsymbol{p}^0\sqrt{-g_{00}}\right)^2} \tag{3}$$

By taking into account a dispersive medium, Synge (Synge, Relativity 1960) remodeled the Fermat's least ac tion principle to describe the photon trajectories. Henceforth, the variational principle $\partial(\int p_{\alpha}dx^{\alpha}) = 0$ was applied with the condition,

$$H(x^{\alpha}, \boldsymbol{p}_{\alpha}) = \frac{1}{2}\left[g^{\alpha\beta}\boldsymbol{p}_{\alpha}\boldsymbol{p}_{\beta} - (n^2-1)\left(\boldsymbol{p}_0\sqrt{-g_{00}}\right)^2\right] \tag{4}$$

The above expression governs the equations of motion by the following system of different equations $\frac{dx^{\alpha}}{d\lambda} = \frac{\partial H}{\partial p_{\alpha}}, \frac{dp_{\alpha}}{d\lambda} = -\frac{\partial H}{\partial x^{\alpha}}$, here λ is the affine parameter. It is of utmost importance to define the refractive index *n* properly in order to study the plasma effects clearly in theblack hole vicinity, therefore by the implication of (Bisnovatyi-Kogan and Tsupko, Mon. Not. R. Astron. Soc. 2010) we define it as

$$n^2 = 1 - \frac{\omega_e^2}{[\omega(x^i)]^2},\ \omega_e^2 = \frac{4\pi e^2 N(x^i)}{m} = K_e N(x^i) \tag{5}$$

Here, ω_e is the plasma electron frequency and $\omega(x^i)$ is a space coordinate function termed as the photon frequency. The notations e, m and N (x^i) denote the charge, mass and electron concentration, correspondingly. The validity of the inequality, $\omega^2 > \omega_e^2$ is central to the propagation of light through the plasma medium. While considering a non-rotating gravitational field with a static medium, the photon energy reads (Synge, Relativity 1960)

$$\boldsymbol{p}^0\sqrt{-g_{00}} = -\frac{1}{c}\hbar\omega(x^i) \tag{6}$$

Using (6) and (5) the scalar $H(x^\alpha, \boldsymbol{p}_\alpha)$ takes the form

$$H(x^\alpha, \boldsymbol{p}_\alpha) = \frac{1}{2}\left[g^{\alpha\beta}\boldsymbol{p}_\alpha\boldsymbol{p}_\beta + \frac{\omega_e^2\hbar^2}{c^2}\right] \tag{7}$$

where $\hbar$ is the Planck's constant. Generally, for any arbitrary medium, photons in a flat space- time move along a straight path, while on the other hand, bent trajectories are followed in a curved space-time. Thus, we assume the motion specifically along z-axis and take in the null approximations (Bisnovatyi-Kogan and Tsupko, Mon. Not. R. Astron. Soc. 2010) to avoid any small deviations from the straight path. In this case the components of the 4-momentum are as below

$$\boldsymbol{p}^\alpha = \left(\frac{\hbar\omega}{c}, 0, 0, \frac{n\hbar\omega}{c}\right),\ \boldsymbol{p}_\alpha = \left(-\frac{\hbar\omega}{c}, 0, 0, \frac{n\hbar\omega}{c}\right) \tag{8}$$

Note that, in the forthcoming discussion we shall utilize special notations at infinity; $\omega(\infty) = \omega$, $\omega_e(\infty) = \omega_0$ and $n(\infty) = \sqrt{1 - \omega_0^2/\omega^2}$. Since we are considering a diagonal metric therefore the components of the metric tensor $g_{\alpha\beta}$ dissolves for all $\alpha \neq \beta$. Hence, after using (7) we get the following set of equations

$$\begin{aligned} \frac{dx^i}{d\lambda} &= g^{ij}\boldsymbol{p}_j, \\ \frac{d\boldsymbol{p}_i}{d\lambda} &= -\frac{1}{2}g_{,i}^{lm}\boldsymbol{p}_l\boldsymbol{p}_m - \frac{1}{2}g_{,i}^{00}\boldsymbol{p}_0^2 - \frac{1}{2}\frac{\hbar^2}{c^2}K_e N, i. \end{aligned} \tag{9}$$

After applying the null approximation (9) reduces to

$$\frac{dz}{d\lambda} = \frac{n\hbar\omega}{c} \tag{10}$$

The photon momentum in terms of 3-dimensional standard unit vector $\boldsymbol{u}^i = \boldsymbol{u}_i = (0, 0, 1)$ can be expressed as

$$\boldsymbol{p}_i = \frac{n\hbar\omega}{c}(0,0,1) = \frac{n\hbar\omega}{c}\boldsymbol{u}_i \tag{11}$$

By substituting the above equation in (9) we get,

$$\frac{d}{d\lambda}\left(\frac{n\hbar\omega}{c}\boldsymbol{u}_i\right) = -\frac{1}{2}g_{,i}^{lm}\boldsymbol{p}_l\boldsymbol{p}_m - \frac{1}{2}g_{,i}^{00}\boldsymbol{p}_0^2 - \frac{1}{2}\frac{\hbar^2}{c^2}K_e N, i \tag{12}$$

Owing to the preceding assumption made i.e, the motion takes place only along z axis, we are confined to consider only those components of the unit vector which are perpendicular to the initial direction of propagation. Finally, complying with the the null approximationin addition to a weak gravitational field (12) appears as

$$\frac{d\boldsymbol{u}_i}{dz} = \frac{1}{2}\left(h_{33,i} + \frac{1}{n^2}h_{00,i} - \frac{1}{n^2\omega^2}K_e N_{,i}\right),\ i = 1,2 \tag{13}$$

The deflection angle is basically defined by $\hat{a} = \boldsymbol{u}_{+\infty} - \boldsymbol{u}_{-\infty}$, thus, (13) leads us to a general expression for it as below

$$\hat{\alpha}_i = \frac{1}{2}\int_{-\infty}^{\infty}\left(h_{33,i} + \frac{\omega^2}{\omega^2-\omega_e^2}h_{00,i} - \frac{K_e}{\omega^2-\omega_e^2}N,i\right)dz \tag{14}$$

The $\pm$ signs of $\hat{\alpha}_i$ determines the deflection towards and away from the central object, respectively. As an application of this formalism consider D-dimensional Einstein-Gauss-Bonnet theory with a redefined coupling constant $\alpha \to \alpha/(D-4)$ the action of which is expressed by the relation

$$\mathcal{S} = \frac{1}{16\pi}\int d^D x\sqrt{-g}\left(R + \frac{\alpha}{D-4}\mathcal{G}\right) \tag{15}$$

where α is a dimensionless Gauss-Bonnet (GB) coupling parameter and G is the Gauss-Bonnet invariant defined by the expression

$$\mathcal{G} = R^{\mu\nu\eta\rho}R_{\mu\nu\eta\rho} - 4R^{\mu\nu}R_{\mu\nu} + R^2 \tag{16}$$

R is the Ricci scalar, $R_{\mu\nu}$ and $R_{\mu\nu\eta\rho}$ denote, respectively, the Ricci and Riemann tensors. The action S in a 4-dimensional analysis yields the line-element of a non-rotating 4D-EGB gravity in the form

$$ds^2 = -f(r)dt^2 + f^{-1}(r)dr^2 + r^2(d\theta^2 + \sin^2\theta d\phi^2) \tag{17}$$

where

$$f(r) = 1 + \frac{r^2}{2\alpha}\left(1 - \sqrt{1 + \frac{4\alpha R_s}{r^3}}\right) \tag{18}$$

Here $R_s = 2M$, the value of GB parameter α/M^2 lies in the range [-8,1]. Note that, $\alpha > 1$ corresponds to naked singularities and $\alpha < -8$ leads to complex-valued metric in the outer region of the event horizon. Moreover, Schwarzschild metric is recovered when $\alpha \to 0$. We shall take the series expansion of $f(r)$ upto order $O(R^3)$ for a more exhaustive evaluation,

$$f(r) = 1 - \frac{R_s}{r} + \frac{\alpha R_s^2}{r^4} \tag{19}$$

At large r we have, thereby the black hole metric is approximated to

$$ds^2 = ds_0^2 + \left(\frac{R_s}{r} - \frac{\alpha R_s^2}{r^4}\right)dt^2 + \left(\frac{R_s}{r} - \frac{\alpha R_s^2}{r^4}\right)dr^2 \tag{20}$$

Where $d(s_0)^2 = -dt^2 + dr^2 + r^2(d\theta^2 + \sin^2\theta d\phi^2)$. In the Cartesian coordinates the components $h_{\alpha\beta}$ can be written as

$$\begin{aligned} h_{00} &= \left(\frac{R_s}{r} - \frac{\alpha R_s^2}{r^4}\right), \\ h_{ik} &= \left(\frac{R_s}{r} - \frac{\alpha R_s^2}{r^4}\right) n_i n_k, \\ h_{33} &= \left(\frac{R_s}{r} - \frac{\alpha R_s^2}{r^4}\right) \cos^2 x, \end{aligned} \tag{21}$$

where $\cos x = z/\sqrt{b^2 + z^2}$ and $r = \sqrt{b^2 + z^2}$, b is the impact parameter signifying the closest approach of the photons to the black hole. Using the above mentioned expressions in the formula (14) one can compute the light deflection angle with respect to b for a black hole surrounded by plasma (Babar et al. PDU 2021)

$$\hat{\alpha}_b = \int_{-\infty}^{\infty} \frac{b}{2r}\left(\partial_r\left(\left(\frac{R_s}{r} - \frac{\alpha R_s^2}{r^4}\right)\cos^2 x\right) + \partial_r\left(\frac{R_s}{r} - \frac{\alpha R_s^2}{r^4}\right)\frac{\omega^2}{\omega^2 - \omega_e^2} - \frac{K_e}{\omega^2 - \omega_e^2}\partial_r N\right) dz \tag{22}$$

Uniform Plasma. First of all, we consider the photon geodesics when plasma is uniformly distributed in the black hole surroundings. In homogenous plasma medium the refractive index n particulary counts on the photon frequency with ω_0 as a constant quantity which ultimately leads to the approximation $1 - n << \omega_0/\omega$. Subsequently, the corresponding constraints annihilate the term $\partial_r N$ and the angle of deflection takes the form (Babar et al. 2021)

$$\hat{\alpha}_{\text{uni}} = \left(\frac{R_s}{b} - \frac{3\pi\alpha R_s^2}{16b^4}\right) + \left(\frac{R_s}{b} - \frac{3\pi\alpha R_s^2}{4b^4}\right)\frac{1}{\left(1 - \frac{\omega_0^2}{\omega^2}\right)}. \tag{23}$$

Fig. (1) illustrates the plots of the photon deflection angle as a function of the impact parameter b for various coupling constant α (right panel) and plasma parameters (left panel). An increase is examined in the deflection angle for smaller values of the impact parameter b, which means that a massless particle passing too close to the black hole surroundings basically enhances its deviating tendency. Fig. (2) is a visualization of the deflection angle distinctively with respect to ω_0^2/ω^2 and α. The deflection angle is maximum due to high plasma distribution (right panel) and is seen to be strictly decreasing against an increasing coupling parameter α (left panel), for instance, taking α = 0, the Schwarzschild gravity ensures the highest degree of deviation. We deduce that, as expected, the existence of plasma in the black hole vicinity, contrariwise to the vacuum case ω_0^2/ω^2 contributes to the photon motion.

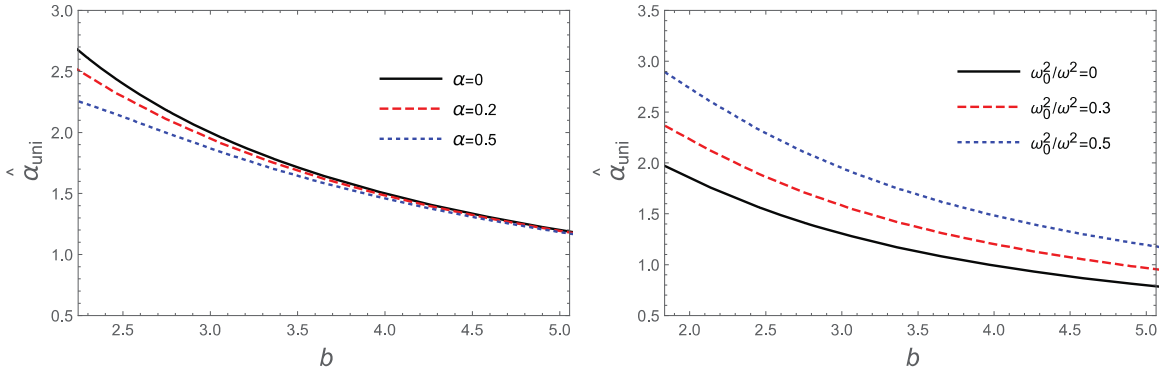

Figure 1. Plot of the deflection angle as a function of the impact parameter *b* for different values of GB parameter (left panel) and uniform plasma parameter (right panel).

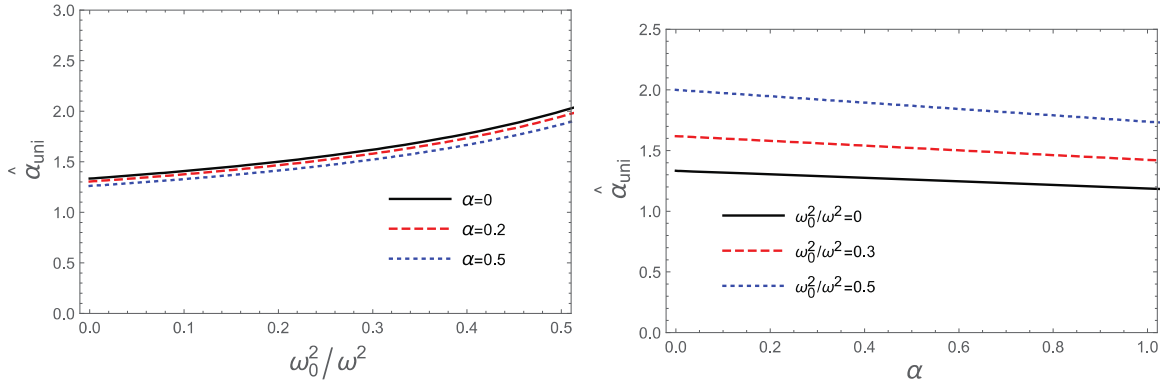

Figure 2. Plot of the deflection angle as a function of the uniform plasma parameter (left panel) and GB parameter (right panel).

Singular Isothermal sphere. A singular isothermal sphere (SIS) is the most favourable model to comprehend the peculiar features of gravitational lensed photons. It was primarily introduced in (Bisnovatyi-Kogan and Tsupko, Mon. Not. R. Astron. Soc. 2010) to explore the len's property of the galaxies and clusters. Generally, SIS is a spherical gas cloud with a singularity located at its center where the density tends to infinity. The density distribution of a SIS is given by

$$\rho(r) = \frac{\sigma_v^2}{2\pi r^2} \tag{24}$$

where σ^2_v refers to a one-dimensional velocity dispersion. The plasma concentration admitsthe following analytic expression

$$N(r) = \frac{\rho(r)}{\kappa m_p} \tag{25}$$

here m_p is the proton mass and κ is a dimensionless constant coefficient generally associatedto the dark matter universe. Utilizing (5,24,25) the plasma frequency takes the form

$$\omega_e^2 = K_e N(r) = \frac{K_e \sigma_v^2}{2\pi\kappa m_p r^2}. \tag{26}$$

We reckon with the above mentioned properties of the SIS and compute the angle of deflection $\hat{\alpha}_{\rm SIS}$ as below (Babar et al. PDU 2021)

$$\hat{\alpha}_{\rm SIS} = \left(\frac{2R_s}{b} - \frac{15\pi\alpha R_s^2}{16b^4}\right) + \frac{R_s^2\omega_c^2}{b^2\omega^2}\left(\frac{1}{2} - \frac{2R_s}{3b\pi} + \frac{5\alpha R_s^2}{8b^4}\right). \tag{27}$$

These calculations brings up a supplementary plasma constant ω^2 which has the following analytic expression

$$\omega_c^2 = \frac{\sigma_v^2 K_e}{2\kappa m_p R_s^2} \tag{28}$$

In order to assimilate the influence of SIS on the photon trajectory we plotted the deflec-tion angle $\hat{\alpha}_{\rm SIS}$ as a function of the impact parameter b, see Fig. (3), interestingly, we see that the uniform plasma and SIS medium share common features regarding the parameter b. Note that, the quantity ω_c^2/ω^2 identifies the distribution of SIS in the black hole vicinity, thus we detect the photon sensitivity to the specified parameter along with the coupling constantparameter α, by means of a graphical analysis in Fig. (4). We examined that $\hat{\alpha}_{\rm SIS}$ increases when ω_c^2/ω^2 increases (upper panel) and, conversely, $\hat{\alpha}_{SIS}$ decreases when α increases (lower panel). Hence, the presence of SIS in the black hole surroundings to some extent affects theintervening massless particles.

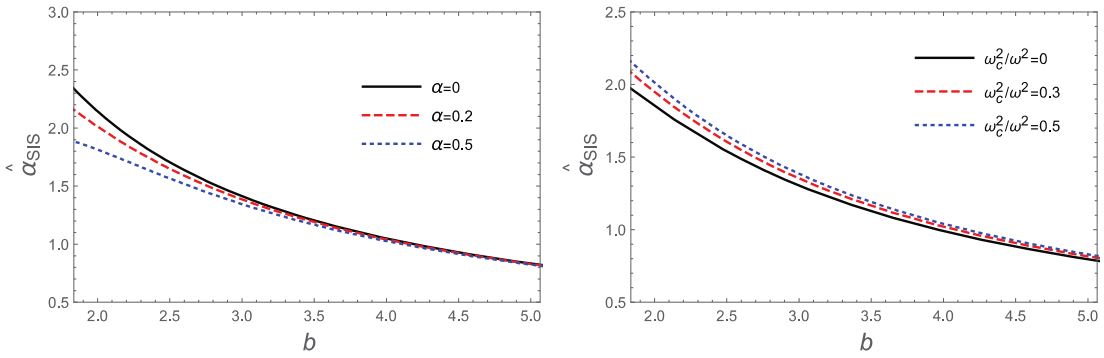

Figure 3: Plot of the deflection angle as a function of the impact parameter b for non-uniform plasma (right panel) and GB parameter (left panel).

Non-Singular Isothermal gas sphere. Now we further proceed to study the motion of photons considering a non-singular isothermal sphere (NSIS) which is a more reasonable and physical setup for the analysis. Unlike the SIS, in this lens model the singularity is bounded by a finite core at the origin of the gas cloud whereby the density distribution is defined as

$$\rho(r) = \frac{\sigma_v^2}{2\pi(r^2+r_c^2)} = \frac{\rho_0}{\left(1+\frac{r^2}{r_c^2}\right)},\ \rho_0 = \frac{\sigma_v^2}{2\pi r_c^2} \tag{29}$$

here the core radius is represented by $r_{\rm c}$. The plasma concentration for NSIS using (25)becomes

$$N(r) = \frac{\sigma_v^2}{2\pi\kappa m_p\left(r^2+r_c^2\right)} \tag{30}$$

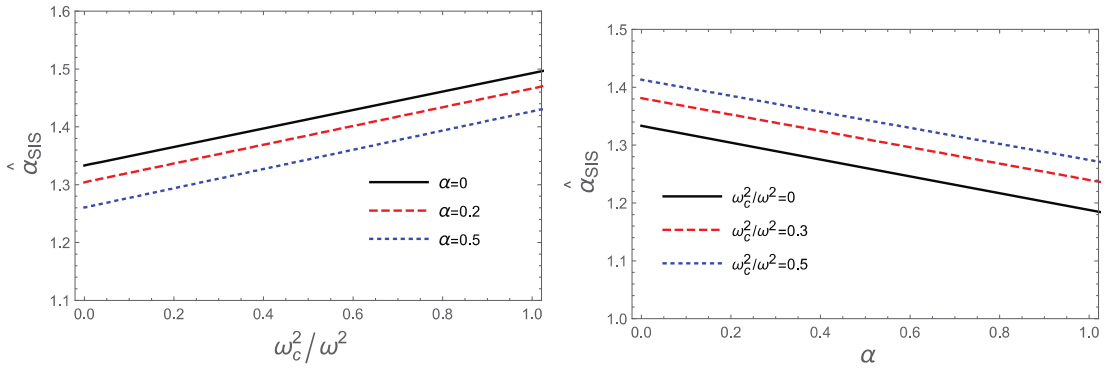

Figure 4: Plot of the deflection angle as a function of non-uniform plasma (right panel) and GB (left panel).

We compute the plasma frequency from (5,29,30) as follows

$$\omega_e^2 = \frac{K_e\sigma_v^2}{2\pi\kappa m_p\left(r^2+r_c^2\right)} \tag{31}$$

The angle of deflection obtained by the deviation of photons in NSIS gravitational lens setup

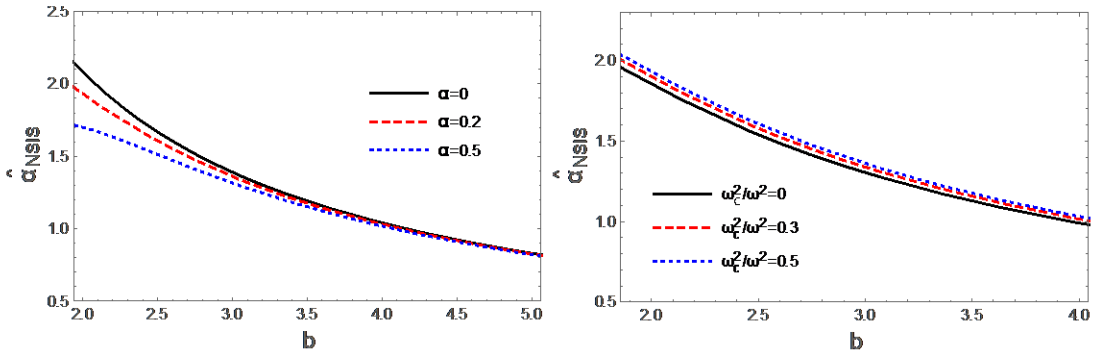

Figure 5: Plot of the deflection angle as a function of the impact parameter b for non-uniform plasma (right panel) and GB parameter (left panel).

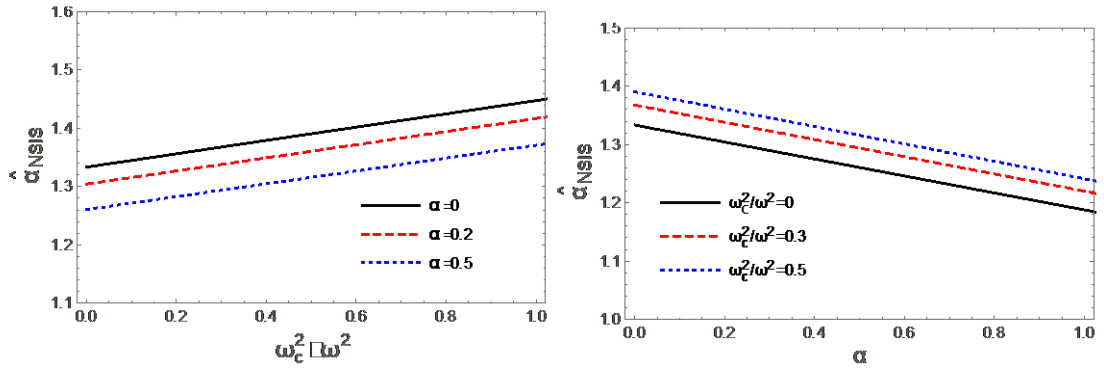

Figure 6: Plot of the deflection angle as a function of non-uniform plasma (right panel) and GB (left panel).

in accordance with the properties in the latter discussion is as below (Babar et al. PDU 2021)

$$\hat{\alpha}_{\text{NSIS}} = \left(\frac{2R_S}{b} - \frac{15\pi\alpha R_S^2}{16b^4}\right) + \frac{R_S^2\omega_c^2}{\omega^2}\left(\frac{R_S}{b\pi r_c^2} + \frac{b}{2\left(\sqrt{b^2+r_c^2}\right)^3}\right. \\ \left. - \frac{bR_S\tanh^{-1}\frac{r_c}{\sqrt{b^2+r_c^2}}}{\pi r_c^3\sqrt{b^2+r_c^2}} - \frac{\alpha R_S^2}{r_c^2}\left(\frac{2}{r_c^4} + \frac{3}{4b^4} - \frac{1}{b^2r_c^2}\right.\right. \\ \left.\left. - \frac{2b}{r_c^4\sqrt{b^2+r_c^2}}\right)\right). \tag{32}$$

As previously executed we employ the same graphical interpretation to unfold the proper-ties of NSIS concerning the photon motion. Here, the distribution of NSIS is associated with the parameter ω_c^2/ω^2. It is evidently revealed from Fig. (5,6) that the behavior of the impact parameter b, coupling constant α and the parameter ω_c^2/ω^2 cannot be distinguished from a specific point of view when brought in comparison with the uniform plasma and SIS case. Neverthe-less, one can at least figure out the distribution which has the most pronounced effect on the deflection angle. Fig. (7) is a visual juxtaposition of the $\hat{\alpha}_{\text{uni}}$, $\hat{\alpha}_{\text{SIS}}$ and $\hat{\alpha}_{\text{NSIS}}$ as a function of the impact parameter and the coupling constant. It is quite obvious that the deflection is maximum when the black hole is surrounded by a uniform plasma medium. The final result can therefore be encaspulated in a mathematical expression as, $\hat{\alpha}_{\text{uni}} > \hat{\alpha}_{\text{SIS}} > \hat{\alpha}_{\text{NSIS}}$.

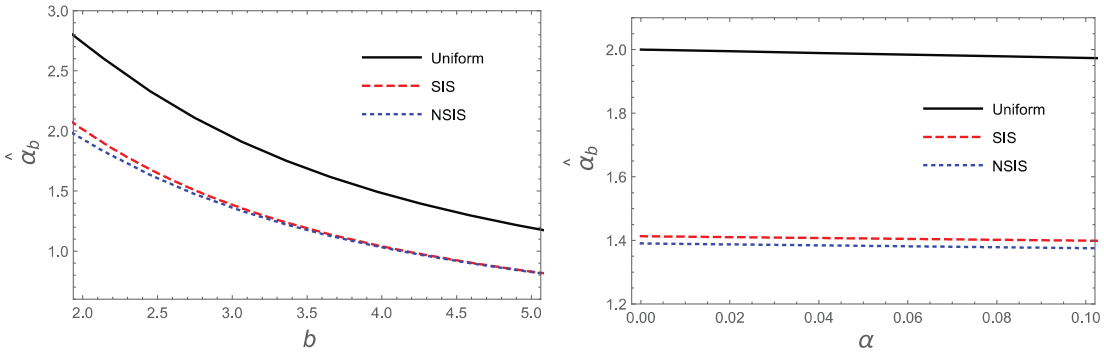

Figure 7: Plot of the deflection angle as a function of the impact parameter (right panel) and GB parameter (left panel).

Part II.

In this part we discuss the photon motion and the shadow cast by black hole. As an example we consider the Kerr-Newman-Kislev-Letelier (KNKL) black hole with nonzero quintessence and cloud string (CS) parameter. The KNKL black hole metric can be presented as

$$ds^2 = -\frac{\Delta}{\Sigma}(dt - a\sin^2\theta d\phi)^2 + \frac{\Sigma}{\Delta}dr^2 + \Sigma d\theta^2 + \frac{\sin^2\theta}{\Sigma}(adt - (r^2 + a^2)d\phi)^2 \quad (33)$$

For the above metric (33), the metric coefficients are

$$\Sigma = r^2 + a^2\cos^2\theta \quad (34)$$

$$\Delta = (1-b)r^2 + a^2 + Q^2 - 2Mr - \gamma r^{-3\omega_q+1} \quad (35)$$

Here we discuss the effect of quintessence parameter γ, CS parameter b, spin parameter$a$ and charge Q of the black hole on the structure of the horizons of the KNKL black hole. Note that M is the mass parameter and the ADM mass of the system can be obtained by rescaling the coordinates.

In order to have the shape of the shadow cast by the KNKL black hole we first investigatenull geodesics in the spacetime geometry of the KNKL black hole. We adopt the Hamilton- Jacobi formalism to study the null geodesic structure of the KNKL black hole spacetime, as follows

$$\frac{\partial S}{\partial \tau} = -\frac{1}{2}g^{\mu\nu}\frac{\partial S}{\partial x^\mu}\frac{\partial S}{\partial x^\nu} \quad (36)$$

where $\boldsymbol{E} = g_{t\mu}\dot{x}^\mu$ and $\boldsymbol{L}_z = g_{\phi\mu}\dot{x}^\mu$ correspond to the energy and momentum of the particle, τ is the affine parameter and $g^{\mu\nu}$ is the metric tensor. Here the action S is separated as

$$S = \frac{1}{2}m_0^2\tau - Et + L_z\phi + S_r(r) + S_\theta(\theta) \quad (37)$$

where m_0 isthe mass of the particle and $S_r(r)$, $S_\theta(\theta)$ are the function of r and θ only. Using the method of separation of variables and utilizing Eq. (87) into the Eq. (36), we obtain the following equations for the motion of photon ($m_0 = 0$)

$$\mathcal{R} = [(r^2 + a^2)E - aL_z]^2 - \Delta[\mathcal{K} + (L_z - aE)^2] \quad (38)$$

$$\Theta = \mathcal{K} + \cos^2\theta(a^2E^2 - L_z^2\sin^{-2}\theta). \quad (39)$$

We obtain the following geodesic equations in the spacetime metric of the KNKL black hole

$$\Sigma\frac{dt}{d\tau} = a(L_z - aE\sin^2\theta) + \frac{r^2 + a^2}{\Delta}(E(r^2 + a^2) - aL_z) \quad (40)$$

$$\Sigma\frac{dr}{d\tau} = \pm\sqrt{\mathcal{R}} \quad (41)$$

$$\Sigma\frac{d\theta}{d\tau} = \pm\sqrt{\Theta} \quad (42)$$

$$\Sigma\frac{d\phi}{d\tau} = (L_z\csc^2\theta - aE) + \frac{a}{\Delta}(E(r^2 + a^2) - aL_z). \quad (43)$$

Now we determine the shape of the shadow of the KNKL black hole. For this we define the following impact parameters $\xi = L_z/E$ and $\eta = K/E^2$, and therefor, the R in terms of these new parameters can be expressed as

$$\mathcal{R} = [(r^2 + a^2) - a\xi]^2 - \Delta[\eta + (\xi - a)^2] \quad (44)$$

Photons coming towards a black hole follow three types of trajectories, i.e., falling inside the black hole, scattering away from the black hole or moving in unstable circular orbit in the vicinity of the horizon of the black hole. Out of these three types of trajectories, the unstable circular orbits near the horizon of a black hole are responsible for determining the shape of the shadow cast by the black hole. The unstable circular photon orbits can be obtained from the following conditions

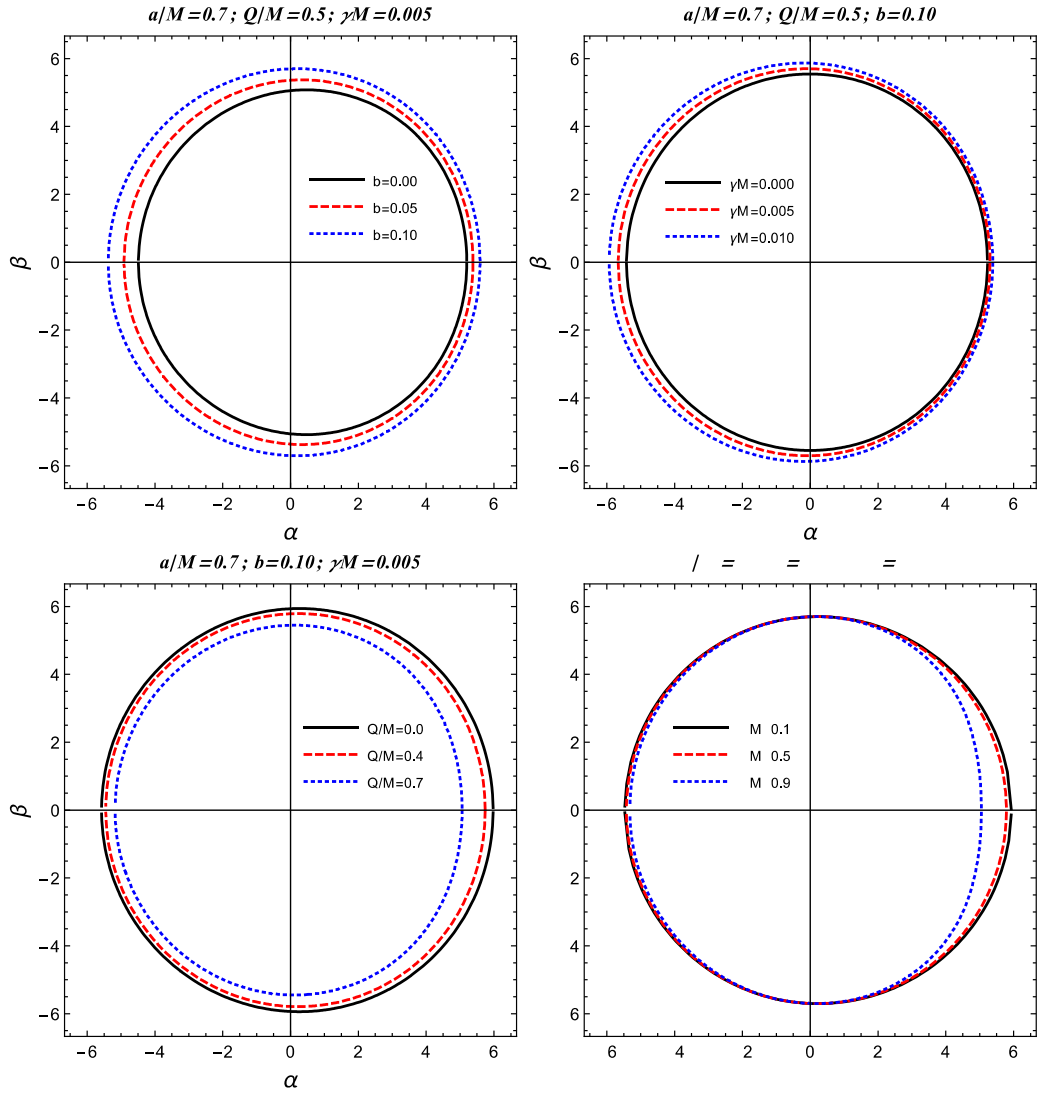

Figure 8: Shadow cast by the Kerr-Newman-Kiselev-Letelier black hole and the observables.

$$\mathcal{R}(r) = 0 = \frac{\partial \mathcal{R}(r)}{\partial r} \quad (45)$$

The two parameters ξ and η determine the shape of the shadow cast by a black hole. Con-sidring Eqs. (44) and (45), for the KNKL black hole we have ξ and η as

$$\xi = \frac{(a^2 + r^2)\Delta' - 4\Delta r}{a\Delta'} \tag{46}$$

$$\eta = \frac{r^2(16\Delta(a^2 - \Delta) - r^2\Delta'^2 + 8\Delta r\Delta')}{a^2\Delta'^2} \tag{47}$$

To discuss the geometry of the shadow cast by the KNKL black hole the celestial coordinates α and β are defined as

$$\alpha = -r_0 \frac{P^{(\phi)}}{P^{(t)}}, \tag{48}$$

$$\beta = -r_0 \frac{P^{(\theta)}}{P^{(t)}}. \tag{49}$$

where $P^{(\phi)}$, $P^{(\theta)}$, and $P^{(t)}$ are the tetrad components of the photon momentum with respect to locally nonrotating reference frame. The r_0 is the observed distance and it is very large but finite $r_0 = D = 8.3$ kpc for the Sgr A* or $r_0 = D =$ 16.8 Mpc for the M87*. We are determining the shadow of the KNKL black hole in the equatorial plane for which the angle of the inclination is $\theta_0 = \pi/2$, therefore, Eqs. (48) and (49) assumes the following form

$$\alpha = -\sqrt{-g_{tt}(r_0)}\xi. \tag{50}$$

$$\beta = \pm\sqrt{-g_{tt}(r_0)}\sqrt{\eta}. \tag{51}$$

To analyse the shape and size of the shadow cast by the KNKL black hole we plot the two celestial coordinates α and β for different values of the parameters b and γ for fixed values of the spin parameter a and charge Q of the black hole in Fig. 8. We observe that for increasing values of the parameters b and γ the radius of the shadow cast by the KNKL black hole increases. In the same Fig. 8 we plot the coordinates α and β for different values of the spin parameter a and charge Q of the KNKL black hole, keeping the parameters b and γ fixed. Here we notice that the shadow radius for the KNKL black hole gets smaller as the values of the parameters a and Q go on increasing. Again the repulsive nature of both the quintessence and CS can be confirmed from this behaviour of the graphs for the shapes of the shadow cast by the KNKL black hole. Further, form the Fig. 8 we observe that the increasing values of the spin parameter a enhances the distortion of the shadow of the KNKL black hole, for fixed values of the other spacetime parameters. Thus the shadow cast by a fast rotating black hole would be more distorted as compared to the one cast by a slowly rotating black hole.

This observation may be helpful in constraining the spin of a rotating black hole. Here we see that all the spacetime parameters have an influence on the shapeand size of the shadow cast by the KNKL black hole.
Here we denote the radius of the circular shadow of the black hole by R_{sh} and the distortion parameter δ_s is given by

$$\delta_s = \frac{D_{cs}}{R_{sh}} \tag{52}$$

here D_{cs} denotes the difference between the right endpoints of the shadow cast by the blackhole. The other observable R_{sh} is given as

$$R_{sh} = \frac{(\alpha_t-\alpha_r)^2+\beta_t^2}{2(\alpha_t-\alpha_r)}. \tag{53}$$

In the Figs. 9 and 10, we plot the observable R_{sh} and δ_s as a function of the parameters $b$and γ and charge Q. We see that the observable R_{sh} increase with the parameters b and $\gamma$and hence the size of the shadow cast by the KNKL black hole increases. While the effect ofthe charge Q on the size of the shadow of the KNKL black hole is just opposite to that of the parameters b and γ. From the Fig. 10 we notice that the observable δ_s which is responsiblefor the distortion in the shape of the shadow cast by the black hole increases with both $Q$and a. While it decreases with the parameters b and γ. This observation may constrain boththe charge and spin of the black hole.

Constraints on the parameters b and γ from the data provided by the EHT for M87* and SgrA*. With the assumption that the supermassive black holes at the centre of the galaxies M87 and Milky way are surrounded by the CS and quintessence, we obtain upper limits on the quintessence parameters γ and the CS parameter b, using the data provided by the EHT collaboration for the two supermassive black holes M87* and SgrA*. The angular diameter of the black hole shadow, the distance of the black hole from earth and the estimated massof the black hole at the centre of the galaxy M87*, are given as $\theta_{M87*} = 42 \pm 3\,\mu$as, D = 16.8Mpc and $M_{M87*} = 6.5 \pm 0.90\text{x}10^9\,M_\odot$, respectively. For the supermassive black hole SgrA* at the centre of the Milky way galaxy, the data obtained by the EHT collaboration isas $\theta_{\text{Sgr A*}} = 48.7 \pm 7\,\mu$, $D = 8277 \pm 33$ pc and $M_{\text{Sgr A*}} = 4.3 \pm 0.013\text{x}10^6\,M_\odot$ (VLTI).
Utilising the data provided by the EHT collaboration, we explore the diameter of the shadow

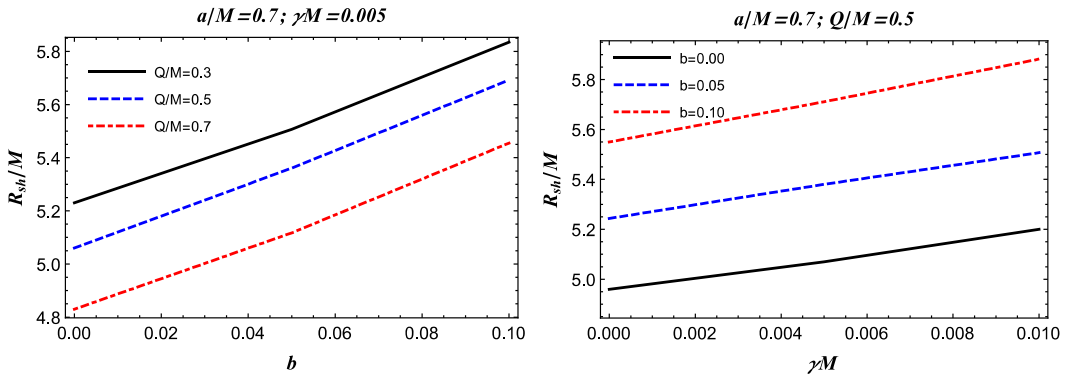

Figure 9: Radius of shadow (Atamurotov et al. EPJC 2022).

of the black hole, per unit mass using the expression given as (Atamurotov et al. 2022)

$$d_{\rm sh} = \frac{D\theta}{M} \tag{54}$$

The diameter of the shadow can then be obtained from the expression $d^{\rm theo}_{\rm sh} = 2R_{\rm sh}$. Thereby, the diameter of the image of the shadow cast by the black hole is $d^{\rm M87*} = (11 \pm 1.5)M$ for the supermassive black hole M87* and $d^{\rm Sgr\ A*} = (9.5 \pm 1.4)M$ for the supermassive black hole Sgr A* at the cetre of the Milky way galaxy. taking in account the data released by the EHT collaboration, we have the constraints on the parameters b and γ for the supermassive black holes, one at the centre of the galaxy M87 and the other at the centre of the Milky way galaxy. For fixed values of the spin a and charge Q of the KNKL black hole, we show our results in the Tables 1. We observe that the upper limit of the CS parameter b increases when the quintessence parameter γ decreases. This study of constraining the two parameters b and γ, for the KNKL black hole, suggests that the effect of the SC may be stronger then the effect of the quintessence on the spacetime geometry of the KNKL black hole (Atamurotov et al. EPJC 2022).

Equatorial and polar quasinormal modes (QNMs) and their relation with typical shadow radius. In this section we explore the relation between the typical shadow radius and QNMs. This correspondence is interesting and can be tested in the near future. In particular we know

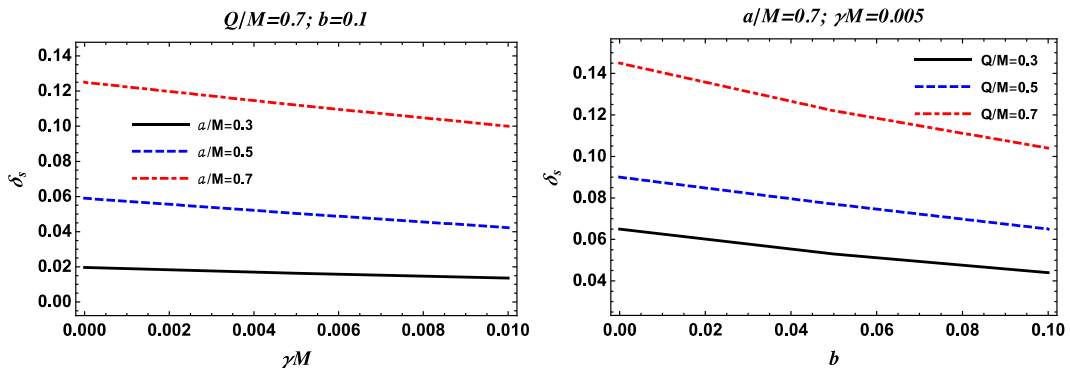

Figure 10: Distortion parameter of the black hole shadow.

Table 1: The upper values of γ and a are tabulated for the supermassive black holes in thegalaxy M87* and the Sgr A*. Note that we set $M = 1$.

	Estimated values of parameters for M87* black hole					
Parameters	$Q = 0.0$ and $a = 0.5$			$Q = 0.5$ and $a = 0.5$		
b	0.0000	0.0200	0.0400	0.0000	0.0200	0.0400
γ	0.0358	0.0297	0.0235	0.0435	0.0386	0.0339
	Estimated values of parameters for Sgr A* black hole					
Parameters	$Q = 0.0$ and $a = 0.5$			$Q = 0.5$ and $a = 0.5$		
b	0.0000	0.0200	0.0345	0.0000	0.0200	0.0400
γ	0.0110	0.0050	0.0000	0.0201	0.0154	0.0104

that QNMs are modes related to ringdown phase of the black hole and can be given in terms of the real and imaginary part as follows $\omega = \omega_{\Re} - i\omega_{\Im}$ while the shadow radius is relevant for testing General Relativity(GR) in the strong gravity regime using supermassive black holes. It has been shown that for asymptotically flat and static metrics there is a relation between angular velocity and real part of QNMs. In particular one can then easily relate the shadow radius and the real part of QNMs in terms of the relation

$$R_{sh} = \frac{l+\frac{1}{2}}{\omega_{\Re}} \tag{55}$$

Note, however, that this relation can be violated in in modified theories of gravity like Einstein-Lovelock theory. It was shown that the QNM frequency in the Eikonal limit reads

$$\omega_{QNM} = \left(l + \frac{1}{2}\right)\Omega_R - i\gamma_L\left(n + \frac{1}{2}\right) \tag{56}$$

where

$$\Omega_R = \Omega_\theta + \frac{m}{l+\frac{1}{2}}\Omega_{prec} \tag{57}$$

in which Ω_θ gives the orbital frequency in the polar direction. Moreover Ω_{prec} is known as the Lense-Thiring precision frequency of the orbit plane and γ_L is the Lyapunov exponent of the orbit. It is well known that apart from the mass of the black hole (which is proportional to the shadow radius), due to the black hole spin the shadow gets distorted and the apparent shape of the shadow depends on the viewing angle. Therefore it is not possible in general to find a closed form or analytical expression for the shadow radius.

· Case I: Viewing angle $\theta_0 = \pi/2$

Let us consider here the special case with the viewing angle $\theta_0 = \pi/2$. Moreover, we consider equatorial orbit which can be used to compute the typical shadow radius. To do so, we use the fact that the Lense-Thiring precision frequency is related to the orbital frequency and Keplerian frequency via

$$\Omega_{\text{prec}} = \pm\Omega_\phi \mp \Omega_\theta \tag{58}$$

with

$$\Omega_\phi = \frac{-\partial_r g_{t\phi} \pm \sqrt{(\partial_r g_{t\phi})^2 - (\partial_r g_{tt})(\partial_r g_{\phi\phi})}}{\partial_r g_{\phi\phi}}. \tag{59}$$

One can apply the same approach as the WKB analysis for Kerr quasinormal modes, then by writing $2\int_{-\theta}^{\theta} \sqrt{\Theta} d\theta = 2\pi(L - |L_z|)$, which physically can be viewed as the Bohr-Sommerfeld Condition and can be compare with the eigenvalue problem in the θ direction for the Kerr quasinormal modes. It was argued that

$$\mathcal{K} + L_z^2 \simeq L^2 - \frac{a^2E^2}{2}\left(1 - \frac{L_z^2}{L^2}\right) \tag{60}$$

and now if we divide the last equation by E^2, we can obtain

$$\eta + \xi^2 \simeq \frac{L^2}{E^2} - \frac{a^2}{2}\left(1 - \frac{L_z^2}{L^2}\right). \tag{61}$$

At this point we can make use of the correspondence

$$L_z \quad \Leftrightarrow m \tag{62}$$

$$E \quad \Leftrightarrow \omega_{\Re} \tag{63}$$

$$L \quad \Leftrightarrow l + \frac{1}{2} \tag{64}$$

where one has $\omega_{\Re} = L\Omega_R$. In the limit $m = l >> 1$, also known as the Eikonal limit, we have $\mu = m/(l + 1/2) = 1$ with

$$\Omega_{prec} = \Omega_{\phi} - \Omega_{\theta} \tag{65}$$

one can then ind

$$\Omega_R = \Omega_{\theta} + \Omega_{\text{prec}} = \Omega_{\phi}. \tag{66}$$

In other words, these QNMs are related to the Kepler frequency which can be written as (Atamurotov eta al. EPJC 2022)

$$\omega_{\Re}^{\pm} = \left(l + \frac{1}{2}\right) \frac{-\partial_r g_{t\phi} \pm \sqrt{\left(\partial_r g_{t\phi}\right)^2 - \partial_r g_{tt}\, \partial_r g_{\phi\phi}}}{\partial_r g_{\phi\phi}}, \tag{67}$$

provided $m = l >> 1$. We use the following definition to specify the typical shadow radius

$$\bar{R}_{sh} := \frac{1}{2}\left(\alpha^{+}\left(r_{ph}^{+}\right) - \alpha^{-}\left(r_{ph}^{-}\right)\right) \tag{68}$$

where $\alpha^{\pm}\left(r_{ph}\right) = \pm\sqrt{f(r_0)}\xi$ and $\eta\left(r_{ph}^{\pm}\right) = 0$. Now if we use Eq. (61) it follows that

$$\xi^{\pm} = \pm\sqrt{\frac{\left(l+\frac{1}{2}\right)^2}{\omega_{\Re}^2\left(r_{ph}^{\pm}\right)} - \frac{a^2}{2}(1-\mu^2)} \tag{69}$$

Combining these equation we arrive at

$$\begin{aligned} \bar{R}_{sh} \quad &= \frac{\sqrt{f(r_0)}}{2}\sqrt{\frac{\left(l+\frac{1}{2}\right)^2}{\omega_{\Re}^2\left(r_{ph}^{+}\right)} - \frac{a^2}{2}(1-\mu^2)} \\ &+ \frac{\sqrt{f(r_0)}}{2}\sqrt{\frac{\left(l+\frac{1}{2}\right)^2}{\omega_{\Re}^2\left(r_{ph}^{-}\right)} - \frac{a^2}{2}(1-\mu^2)} \end{aligned} \tag{70}$$

where

$$f(r_0) = 1 - b - \frac{2M}{r} + \frac{Q^2}{r^2} - \gamma r^{-3\omega_q - 1}\Big|_{r_0} \tag{71}$$

and r_0 is the location of the observer. In other words due to the CS parameter the spacetime topology is globally conical and not asymptotically flat hence the shadow radius measured by the distant observer is modified. The correspondence is precise if we consider the eikonal limit, that is, if we set $\mu = \pm 1$ (namely [$(m = \pm l)$], yielding

$$\bar{R}_{sh}(\mu = \pm 1) = \left(l + \frac{1}{2}\right)\frac{\sqrt{f(r_0)}}{2}\left(\frac{1}{\omega_{\Re}\left(r_{ph}^{+}\right)} - \frac{1}{\omega_{\Re}\left(r_{ph}^{-}\right)}\right) \tag{72}$$

We can obtain the static case when $\omega^{+} = -\omega^{-} = \omega_{\Re}$ yielding

$$\bar{R}_{sh} = \sqrt{f(r_0)}\,\frac{l+\frac{1}{2}}{\omega_{\Re}} \tag{73}$$

We see that for asymptotically flat spacetime $f(r_0) \to 1$ and the last equation reduces to Eq. (27). Using the metric functions and after some algebraic

manipulation in the Eikonal limit we can use Eq. (67) which can be further simplified as follows (Atamurotov et al. EPJC 2022)

$$\omega_{\Re}^{\pm}=\left(l+\frac{1}{2}\right)\frac{1}{a\pm\sqrt{\frac{2r_{ph}^{\pm}}{f'(r)|_{r_{ph}}^{\pm}}}} \tag{74}$$

We can rewrite the typical shadow radius equation, to obtain a simple equation

$$\bar{R}_{sh}=\frac{\sqrt{2f(r_0)}}{2}\left(\sqrt{\frac{r_{ph}^{+}}{f'(r)|_{r_{ph}^{+}}}}+\sqrt{\frac{r_{ph}^{-}}{f'(r)|_{r_{ph}^{-}}}}\right). \tag{75}$$

The last equation is nothing but the result which was obtained previously in Ref. (Atamurotov et al. EPJC 2022), where the points $r_{\mathrm{p}\overline{\mathrm{h}}}^{\pm}$ were determined by solving (Atamurotov et al. EPJC 2022)

$$r_{ph}^{2}-\frac{2r_{ph}}{f'(r)|_{r_{ph}^{\pm}}}f\left(r_{ph}\right)\mp 2a\sqrt{\frac{2r_{ph}}{f'(r)|_{r_{ph}}}}=0. \tag{76}$$

In Table 2 we present the numerical values for the equatorial QNMs of the KNKL black hole for a given domain of parameters. With the increase of l we normally expect the precision to increase.

· Case II: Viewing angle $\theta_0 = 0$ & $\theta_0 = \pi$

Our second example is to consider the polar orbit $\theta = 0$ along with the viewing angle for the observer: $\theta_0 = 0$ & $\theta_0 = \pi$. For the polar orbit, we know that the azimuthal angular momentum is zero, i.e., $L_z = 0$. Using the circular geodesics i.e., $r^{\cdot 2}$, it follows that

$$(r^2+a^2)^2-[r^2f(r)+a^2]R_s^2=0, \tag{77}$$

Table 2: Numerical values of the real part of QNMs for equatorial modes and polar modes. We have set $M = 1$, $Q/M = 0.5$, $a/M = 0.5$, $\gamma = 0.001$, $\omega_q = -2/3$ and $b = 0.001$ (Atamurotov et al. EPJC 2022).

	Equatorial modes		Polar modes
l	$\omega_{\Re}^{+}$	$\omega_{\Re}^{-}$	$\omega_{\Re}$
1	0.394368035	-0.250600581	0.306612155
2	0.657280058	-0.417667636	0.511020260
3	0.920192081	-0.584734690	0.715428363
4	1.183104105	-0.751801745	0.919836467
5	1.446016128	-0.918868799	1.124244572
6	1.708928152	-1.085935854	1.328652675
7	1.971840175	-1.253002909	1.533060779
8	2.234752199	-1.420069964	1.737468883
9	2.497664222	-1.587137018	1.941876987
10	2.760576245	-1.754204073	2.146285091

along with

$$4r(r^2+a^2)-2rf(r)R_s^2-r^2f'(r)R_s^2=0, \tag{78}$$

in which we have the impact parameter $R^2_s = K/E^2 + a^2$. Now by using Eq. (77) we obtain

$$R_s^{\pm}=\pm\frac{a^2+r^2}{\sqrt{r^2f(r)+a^2}}\Big|_{ph} \tag{79}$$

For the typical shadow radius we assume the following definition $\bar{R}_{sh}:=(\sqrt{f(r_0)}R_s^{+}-\sqrt{f(r_0)}R_s^{-})/2$, yielding

$$\bar{R}_{sh}=\sqrt{f(r_0)}\,\frac{a^2+r^2}{\sqrt{r^2f(r)+a^2}}\Big|_{ph} \tag{80}$$

where r_{ph} can be found by solving the relation

$$\left(a^2+r_{ph}^2\right)^2-\frac{4[r_{ph}^2f(r_{ph})+a^2](a^2+r_{ph}^2)}{r_{ph}f'(r_{ph})+2f(r_{ph})}=0. \tag{81}$$

Using Eq. (32) and taking $L_z = 0$, for the typical shadow radius we obtain

$$\bar{R}_{sh}=\sqrt{f(r_0)}\sqrt{\frac{(l+1/2)^2}{\omega_{\Re}^2(r_{ph})}+\frac{a^2}{2}} \tag{82}$$

One can easily observe that for the nonrotating case the shadow radius reduces to Eq. (45) as we expect. On the other hand if we combine Eqs.(45) and (52) the real part of QNMs can be expressed as follows

$$\omega_{\Re}=\left(l+\frac{1}{2}\right)\sqrt{\frac{2(r^2f(r)+a^2)}{2(a^2+r^2)^2-a^2(r^2f(r)+a^2)}}\Big|_{r=r_{ph}} \tag{83}$$

Finally, in Table 2, we have presented the numerical values for the polar QNMs. We expect that with the increase of l the precision of the numerical values for the QNMs frequency increases.

Shadow cast by the Kerr-Newman-Kiselev-Letelier black hole in the presence of plasma.

In GR mostly the influence of the medium on the light rays passing through it is neglected. Nonetheless, for instance the Solar corona influences the travel time of the radio signals and also their angle of deflection very close to the Sun. This phenomena suggests the presence of a medium which can give us some nontrivial physics. Therefore, it is of interest to study the astrophysically relevant processes like black hole shadow in the presence of a plasma medium. Consequently in this section we investigate the shadow cast by the KNKL black hole in a plasma medium.

Dynamics of photon in a plasma medium.

Here we use the the Hamiltonian for the light ray moving around a black hole which is surrounded by plasma to obtain the equation of motion in the following form (Atamurotov et al., PRD 2021):

$$\mathcal{H} = \frac{1}{2}\left[g^{\mu\nu}p_\mu p_\nu + \omega_{\mathrm{p}}(x)^2\right] \tag{84}$$

where the electron plasma frequency ω_{p} is defined as

$$\omega_p(x)^2 = \frac{4\pi e^2}{m_e}N_e(x) \tag{85}$$

with the charge and mass of electron as e and m_{e}, respectively. The number density of electrons is N_{e}.

In the case of photon the Hamilton-Jacobi equation is given as

$$\mathcal{H}\left(x, \frac{\partial S}{\partial x}\right) = 0 \tag{86}$$

Here we adopt the method of separation of variables and write the action in the following separable form

$$S = -\omega_0 t + p_\phi \phi + S_r(r) + S_\theta(\theta), \tag{87}$$

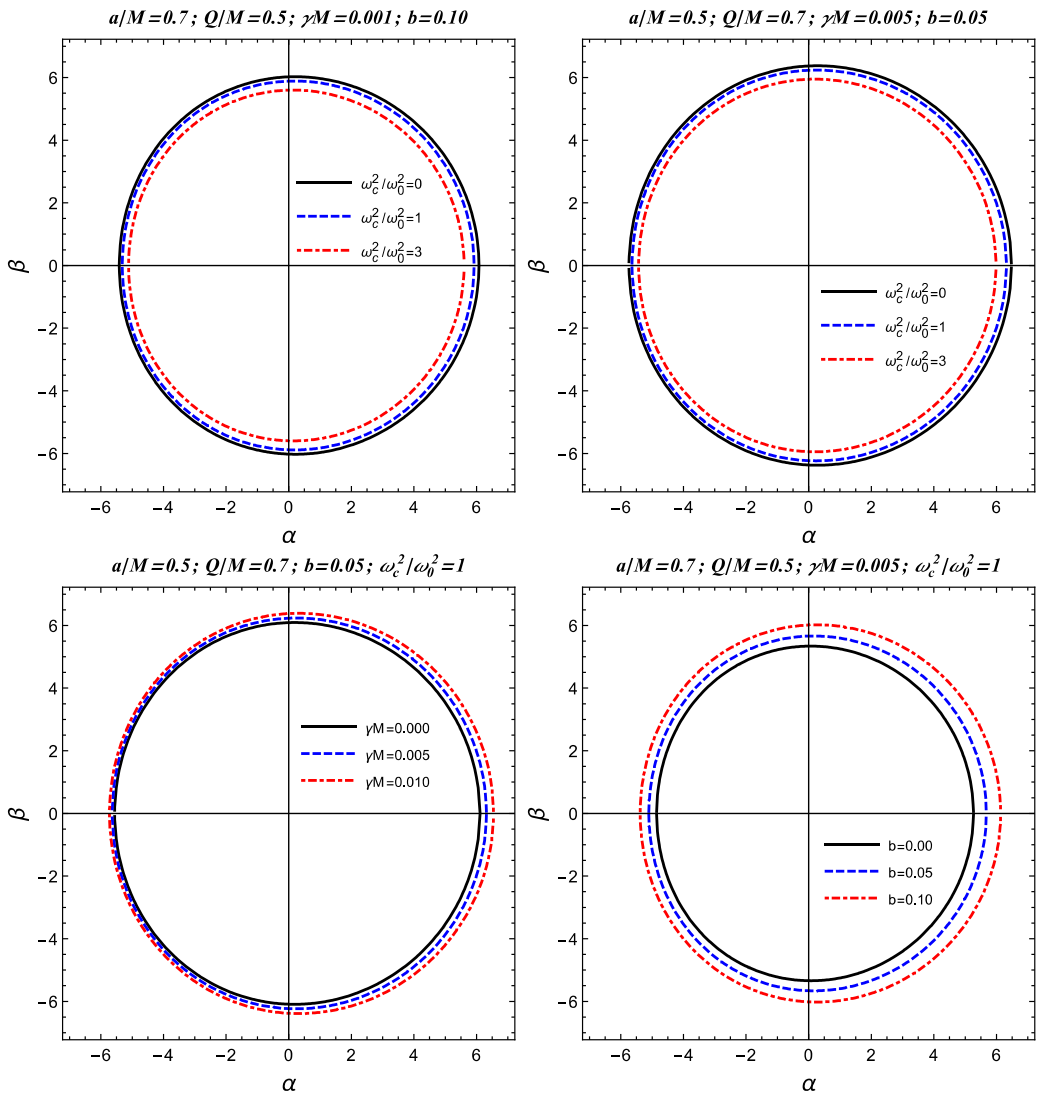

Figure 11: Shadow of the KNKL black hole in the presence of plasma (Atamurotov et al., EPJC 2022)

where the angular momentum and energy of the particle are p_ϕ, ω_0, which are the conserved quantities. Recently, it is presented and discussed for the rotating black hole, that the plasma frequency can be written in the following form (Badia and Eiroa, PRD 2021):

$$\omega_p(x)^2 = \frac{h(r)+g(\theta)}{\rho^2} \tag{88}$$

where the functions$h(r)$ and $g(\theta)$ are related to the radial and the angular parts, respec-tively. We use (87) and (88) into Eq. (86) and get the following expression

$$0 = \frac{a^2\Delta\sin^2\theta-(r^2+a^2)^2}{\Delta}\omega_0^2 + \frac{4aMre^{-l/r}}{\Delta}\omega_0 p_\phi + \Delta(S_r')^2 + (S_\theta')^2 + \frac{\Delta-a^2\sin^2\theta}{\Delta\sin^2\theta}p_\phi^2 + h(r) + g(\theta), \tag{89}$$

in the KNKL black hole spacetime with a plasma medium. Next we use the Carter constant K to separate the equation into the the following two parts as

$$(S_\theta')^2 + \left(a\omega_0 \sin\theta - \frac{p_\phi}{\sin\theta}\right)^2 + g(\theta) \quad = \mathcal{K} \tag{90}$$

$$\frac{1}{\Delta} - \Delta(S_r')^2 \left((r^2 + a^2)\omega_0 - a p_\phi\right)^2 - h(r) \quad = \mathcal{K} \tag{91}$$

Using the Eq. (89) we can get the equation of motion in the spacetime of the KNKL blackhole with the plasma medium as

$$\rho^2 \frac{dt}{d\tau} \quad = a\left(p_\phi - a\omega_0 \sin^2\theta\right) + \frac{r^2 + a^2}{\Delta} P(r), \tag{92}$$

$$\rho^2 \frac{dr}{d\tau} \quad = \pm\sqrt{\mathcal{R}}, \tag{93}$$

$$\rho^2 \frac{d\theta}{d\tau} \quad = \pm\sqrt{\Theta}, \tag{94}$$

$$\rho^2 \frac{d\phi}{d\tau} \quad = \frac{p_\phi}{\sin^2\theta} - a\omega_0 + \frac{a}{\Delta} P(r), \tag{95}$$

where $P(r)$ is given by

$$P(r) = (r^2 + a^2)\omega_0 - a p_\phi, \tag{96}$$

the functions R and Θ are related to the radial and angular equations of motion, respectively, and are expressed as

$$\mathcal{R} \quad = P(r)^2 - \Delta\left[\mathcal{Q} + \left(p_\phi - a\omega_0\right)^2 + h(r)\right] \tag{97}$$

$$\Theta \quad = \mathcal{Q} + \cos^2\theta\left(a^2\omega^2 - p_\phi^2 \sin^{-2}\theta\right) - g(\theta) \tag{98}$$

where $Q = K - (p_\phi - a\omega_0)^2$.

Shadow of the Kerr-Newman-Kiselev-Letelier black hole in the presence of plasma. To discuss the shadows of black holes we evaluate the boundary of the circular light rays. We use the conditions given as $R = 0 = R'$ to obtain the constants of motion in terms of the radius r of the circular orbits of photons as

$$\mathcal{Q} \quad = \frac{\left(a p_\phi - \omega_0(a^2 + r^2)\right)^2}{\Delta} - \left(p_\phi - a\omega_0\right)^2 - h(r) \tag{99}$$

$$p_\phi \quad = \frac{\omega_0}{a}\left[r^2 + a^2 - \frac{\Delta}{a\Delta'}\left(\sqrt{4r^2 - \frac{h'(r)\Delta'(r)}{\omega_0}} + 2r\right)\right]. \tag{100}$$

Now we use the celestial coordinates to present the silhouette of the shadow cast by black hole in the presence of plasma. It can be represented in the following form

$$\alpha = -\frac{p_\phi}{\omega_0 \sin\theta_0}\sqrt{f(r_0)}, \tag{101}$$

$$\beta = \pm\frac{\sqrt{f(r_0)}}{\omega_0}\sqrt{Q + \cos^2\theta_0\left(a^2\omega_0^2 - \frac{p_\phi^2}{\sin^2\theta_0}\right) - g(\theta_0)} \tag{102}$$

To consider the size and the shape, as functions of the spacetime parameters, we will consider the well-known case of the dust that is at rest at infinity and was first used by Shapiro, for the plasma in our current analysis. In the rotating spacetime the mass density, and by Eq. 132, the squared plasma frequency, go as $r^{-3/2}$, being independent of θ to a very good approximation. However, such a plasma distribution cannot be put into the separable form given by Eq. 88. Therefore, we take the frequency to have an additional angular dependency by choosing as :

$$h(r) = \omega_c^2\sqrt{M^3 r} \tag{103}$$

$$g(\theta) = 0, \tag{104}$$

from that

$$\omega_p^2 = \omega_c^2\frac{\sqrt{M^3 r}}{r^2 + a^2\cos^2\theta} \tag{105}$$

where ω_c is a constant and M represents the mass of the black hole.

We combine Eqs. (101), (102), (103) and (104), in the equatorial plane to get the shadow cast by the KNKL black hole and the plots in the Fig. 11 show the shadow of the black hole for the different values of the spacetime and the plasma parameters. From the Fig. 11, we observe that with an increase in the plasma parameter the size of the shadow of the KNKL black hole decreases, for fixed values of all other spacetime parameters. Further we see that the shadow of the KNKL black hole increase for the increasing values of the parameter γ and b, if we keep the plasma parameter and the other spacetime parameters fixed. Hence the presence of plasma shrinks the shadow cast by the KNKL black hole. Further, the nature of both the parameters γ and b is still repulsive even in the presence of the plasma medium (Bambi, PRD 2013).

Let us consider a rather simple accretion model which consists of an infalling gas onto a black hole in the presence of axion-plasmon medium. Although, the realistic picture is rather complicated and depends on a number of ingredients such as the size and the shape of the accretion model, or the distribution of the magnetic fields around the black hole. We are going to use the numerical technique known as the Backward Raytracing in order to find the apparent shadow due to the infalling and radiation gas. The first quantity that we need to define the specific intensity $I_{\nu 0}$ observed far away from the black hole given by the following expression (Bambi, PRD 2013)

$$I_{obs}(\nu_{obs}, X, Y) = \int_{\gamma} \mathrm{g}^3 j(\nu_e) dl_{\mathrm{prop}} \tag{106}$$

where $g = \nu_{\mathrm{obs}}/\nu_{\mathrm{e}}$ is the redshift factor and ν_{e} gives the photon frequency which is measuredin the rest-frame of the emitter. To calculate the total flux one can use the relation

$$F_{obs}(X, Y) = \int_{\gamma} I_{obs}(\nu_{obs}, X, Y) d\nu_{obs} \tag{107}$$

The radiating gas is in a free fall so that its four-velocity components are given by

$$u_e^t = \frac{1}{f(r)}, u_e^r = -\sqrt{1 - f(r)}, u_e^\theta = u_e^\phi = 0. \tag{108}$$

In order to compute the total flux we also need to determine the relation between theradial and time components of the photon four-velocity which is given by the relation

$$k^r = \pm k^t f(r) \sqrt{f(r)\left(\frac{1}{f(r)} - \frac{b^2}{r^2}\right)}. \tag{109}$$

The physical meaning of the signs +(−) in the above equation is the following: The photon can either approach or recedes from the black hole. Note that the impact parameter$b$ encodes the axion-plasmon effect and it reads (Atamurotov et al., PRD 2021)

$$b = r \sqrt{\frac{1}{f(r)} - \frac{\omega_{\mathrm{p}}^2(r)}{\omega_0^2}\left(1 + \frac{\tilde{B}^2}{1 - \tilde{\omega}_\varphi^2}\right)}. \tag{110}$$

We can also use the redshift function g which can be calculated also by the relation

$$\mathrm{g} = \frac{k_\alpha u_o^\alpha}{k_\beta u_e^\beta} \tag{111}$$

In our accretion model we shall apply one more assumption, namely we are going to use a monochromatic and a $1/r^2$ radial profile for the specific emissivity given by the equation

$$j(\nu_e) \propto \frac{\delta(\nu_e - \nu_\star)}{r^2} \tag{112}$$

in which δ is the Dirac delta function. We can express the proper length in terms of therelation

$$dl_{\mathrm{prop}} = k_\alpha u_e^\alpha d\lambda = -\frac{k_t}{\mathrm{g}|k^r|} dr \tag{113}$$

Finally, we can rewrite the total flux given by Eq. (107) after we integrate the intensity overall the observed frequencies, that is, we can write

$$F_{obs}(X, Y) \propto -\int_{\gamma} \frac{\mathrm{g}^3 k_t}{r^2 k^r} dr \tag{114}$$

We closely follow the numerical technique presented in (Atamurotov, PRD 2021) and the resulting shadow images of the black hole with axion-plasmon effects are depicted in Fig. 12. In particularwe have considered a uniform plasma medium and the power law plasma medium. We can clearly see the difference in the intensities as well as the shadow radii compared to the vacuum case when seen by an observer located far away. For the case of

uniform plasma the effect is stronger. The difference in the intensities observed far away from the black hole is explained by the fact that the deflection angle of light is affected by plasma. Since the deflection angle increases for the uniform plasma, the intensity will be smaller at infinity since more photons will be captured by the black hole. In the present work we have integrated numerically from the photon sphere, although there is a small contribution, or practically a neglecting effect, coming from the region between the horizon and the photon sphere.

Part III

Particle acceleration. Consider the action which leads to the field equations of Einstein- Born-Infeld (EBI) gravity and is obtained when the gravitational field is coupled to a non-linear Born-Infeld electrodynamics in (3 + 1) dimensions reads

$$I = \int d^4x\sqrt{-g}\left(\frac{R}{16\pi G} + \mathcal{L}(\mathcal{F})\right) \tag{115}$$

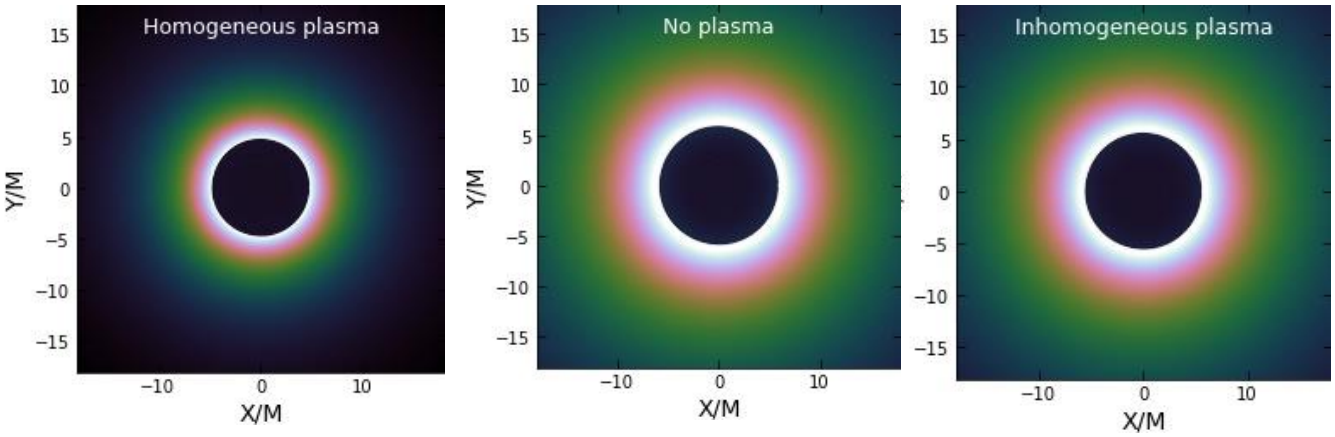

Figure 12: Shadow images for a black hole is a plasma medium and in absence of plasma.

where R is the scalar curvature and $g = \det|g_{\mu\nu}|$. The Lagrangian $L(F)$ is defined as

$$\mathcal{L}(\mathcal{F}) = \frac{\beta^2}{4\pi G}\left(1 - \sqrt{1 + \frac{2\mathcal{F}}{\beta^2}}\right) \tag{116}$$

$\mathcal{F} = \frac{1}{4}F_{\mu\nu}F^{\mu\nu}$, $F_{\mu\nu}$ indicates the electromagnetic field-tensor. The symbol β is the Born-Infeld parameter, equal to the maximum value of electromagnetic field intensity. The Einstein field equations and the electromagnetic field equations are constructed out of (115), respectively, as

$$R_{\mu\nu} - \frac{1}{2}g_{\mu\nu}R = kT_{\mu\nu}, \tag{117}$$

$$\nabla_\mu\left(F^{\mu\nu}\mathcal{L}_{,\mathcal{F}}\right) = 0. \tag{118}$$

The energy-momentum $T_{\mu\nu}$ reads

$$T_{\mu\nu} = \mathcal{L} g_{\mu\nu} - F_{\mu\eta} F_{\nu}^{\eta} \tag{119}$$

$L_{,F}$ represents the partial derivative of L with respect to F. The spacetime of a static andspherically symmetric compact object with mass *M* and a nonlinear electromagnetic source in the EBI postulated theory has been foremostly investigated by Hoffmann. The metricfor EBI space-time is expressed as

$$ds^2 = -f(r)dt^2 + f(r)^{-1}dr^2 + r^2(d\theta^2 + \sin^2\theta d\phi^2)$$
$$f(r) = \left(1 - \frac{2GM}{r} + \frac{Q^2(r)}{r^2}\right) \tag{120}$$

whereas, $Q^2(r)$ is a unique composition of the black hole's charge *Q*, the Born-Infeld param-eter β and *r*.

$$Q^2(r) = \frac{2\beta^2 r^4}{3}\left(1 - \sqrt{1 + \xi^2(r)}\right) + \frac{4Q^2}{3} F\left(\frac{1}{4}, \frac{1}{2}, \frac{5}{4}, -\xi^2(r)\right), \tag{121}$$

here, F denotes the Gauss hypergeometric function and the parameter $\xi^2(r)$ is characterized by $Q^2/(\beta^2 r^4)$.

Now we make an inclusive analysis to probe the acceleration of particles in the EBI gravitybackground. We shall precisely study the centre-of-mass (CM) energy produced due to a two-particle collision near the horizon considering an extremal and a non-extremal chargedblack hole. We put forth the scenario where two nonrelativistic particles initially located at infinity fall freely towards the black hole and ultimately encounter a massive collision near the horizon. Here, we made a unique choice for the collision point because particles falling in from infinity appear with an infinite blue-shift at the horizon and hence are considered to produce an arbitrarily large amount of energy.

We consider motion of a time-like particle with a rest mass m_0 in the equatorial plane $\theta = \pi/2$ where the polar velocity, $\dot{\theta}$ becomes zero. The generalized momenta of the particlein the spacetime of a rotating charged black hole is expressed in the form,

$$P_t = g_{tt}\dot{t} + g_{t\phi}\dot{\phi} \tag{122}$$
$$P_\phi = g_{\phi\phi}\dot{\phi} + g_{t\phi}\dot{t} \tag{123}$$

where P_t and P_ϕ are the constants of motion. Basically, the two quantities P_t and P_ϕ cor- respond to the particleâs energy $\boldsymbol{E}$ and the angular momentum $\boldsymbol{L}$, respectively, acting along the axis of symmetry. The overdot denotes differentiation with respect to the proper time τ. The equations of motion of a massive particle are calculated from (122,123) along with the normalization condition $u_\mu u^\mu = -m^2$, given as below

$$\dot{t} = \frac{1}{r^2}\left[\frac{(a^2+r^2)}{\Delta}(E(a^2+r^2)-aL) + a(L-aE)\right], \quad (124)$$

$$\dot{\phi} = \frac{1}{r^2}\left[\frac{a}{\Delta}(E(a^2+r^2)-aL) + (L-aE)\right], \quad (125)$$

$$\dot{r} = \pm\frac{\sqrt{(aL-(a^2+r^2)E)^2 - \Delta(m_0^2 r^2 + (L-aE)^2)}}{r^2}. \quad (126)$$

The + and − signs of (126) refer respectively, to the outgoing and incoming geodesics. In order to understand the motion of the test particle in the vicinity of EBI gravity thoroughly we must evaluate the effective potential, which is straightforwardly worked out using (126).

$$\frac{1}{2}\dot{r}^2 + V_{\text{eff}} = 0, \quad (127)$$

$$V_{\text{eff}} = -\frac{(aL-(a^2+r^2)E)^2 - \Delta(m_0^2 r^2 + (L-aE)^2)}{2r^4}. \quad (128)$$

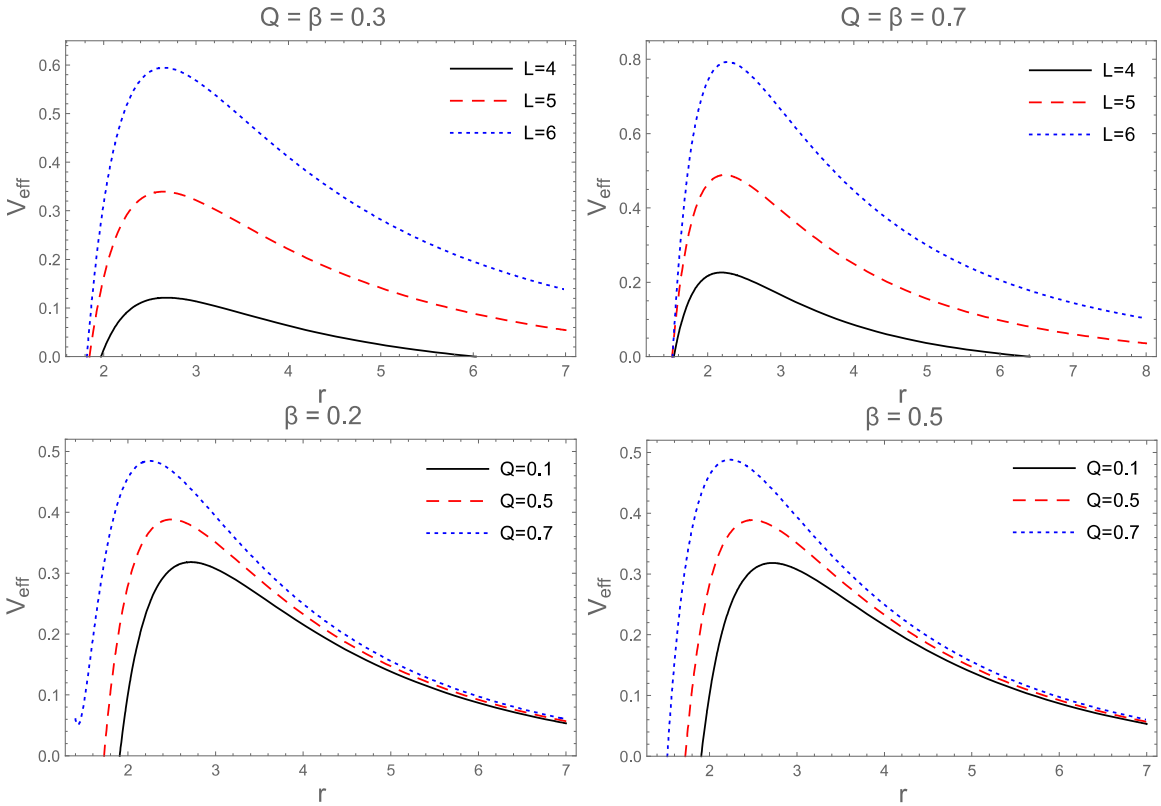

Figure 13: Effective potential is plotted as a function of *r*.

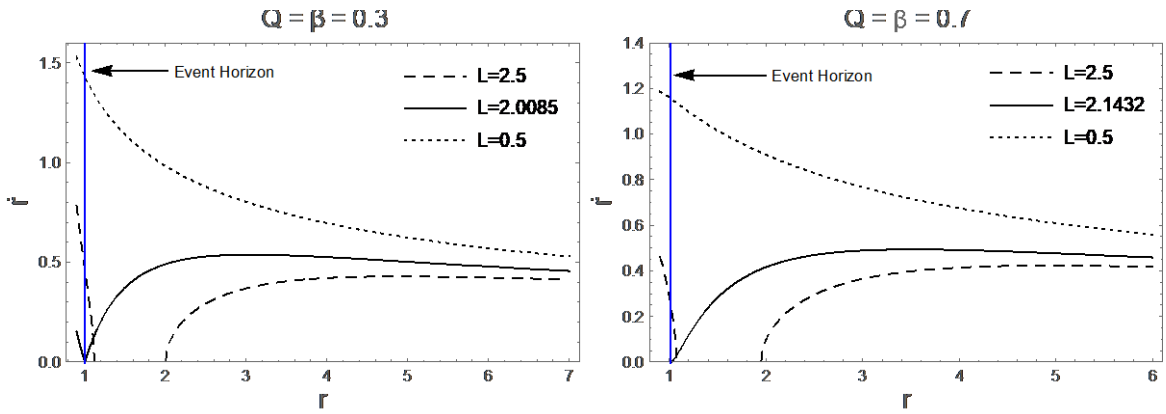

Figure 14: The variation of $\dot{r}$ with respect to the radial coordinate.

When an accelerated particle reaches the black hole, it can most probably continue its motion in the spacetime gravity. In Fig. (13) the effective potential is shown by varying the angular momentum of the incoming test particle for a fixed $Q = \beta$. It is viewed that the potential barrier rises for the larger values of L interpreting that a boosted particle can quickly start circling the black hole. Also, the feasibility of a particle's motion in the black hole surround- ings is increased if the electric field intensity attains its maximum strength.

The magnitude of a particle's momentum plays a vital role to perceive its geodesics in the gravitational space-time. Thus one may get the critical value of the angular momentum from (124) when $r \to r_H^E$, i.e, $L_c = (a^2 + (r_H^E)^2)E/a$.

Fig. (14) gives a comprehensible demonstration of the geodesics in EBI space-time. The particle with L < Lc is always captured by the black hole gravity and falls exactly at the horizon if L = Lc, however, when L > Lc the geodesics never fall into the black hole.

The solution to the simultaneous equations ∂_rVeff = ∂^2Veff = 0 defines the innermost stable circular orbit rISCO of the particle. Fig. (15) illustrates the r_{ISCO} for a static non-rotating EBI gravity by varying the Born-Infeld parameter and charge Q of the black hole. It is observed that the radius of the orbits becomes smaller as β and Q increases, however the decrease is seen to be relatively higher in case of the black hole's charge. More precisely we can say that the charge of the EBI black hole besides its infinite gravity significantly enhances its ability to grasp the incoming particle in its vicinity and by increasing the amount of charge the ISCO as a result comes closer to the black hole. This behaviour is reminiscent of what has been investigated for the Kerr-Newman spacetime in.

Near Horizon collision. Now we analyze the ultrahigh energy produced as a result of a two-particle collision near the horizon of EBI black hole. We consider particles with the same mass m0 and different four-velocities u^1 and

u^2. The CM energy Ec.m of collision between two particles at the radial coordinate r is given by the following expression (Banados et al., PRD 2009),

$$E_{\text{c.m}} = m_0\sqrt{2}\sqrt{1 - g_{\mu\nu}u_1{}^{\mu}u_2{}^{\nu}}. \quad (129)$$

By substituting (124-126) in the above mentioned energy frame we get

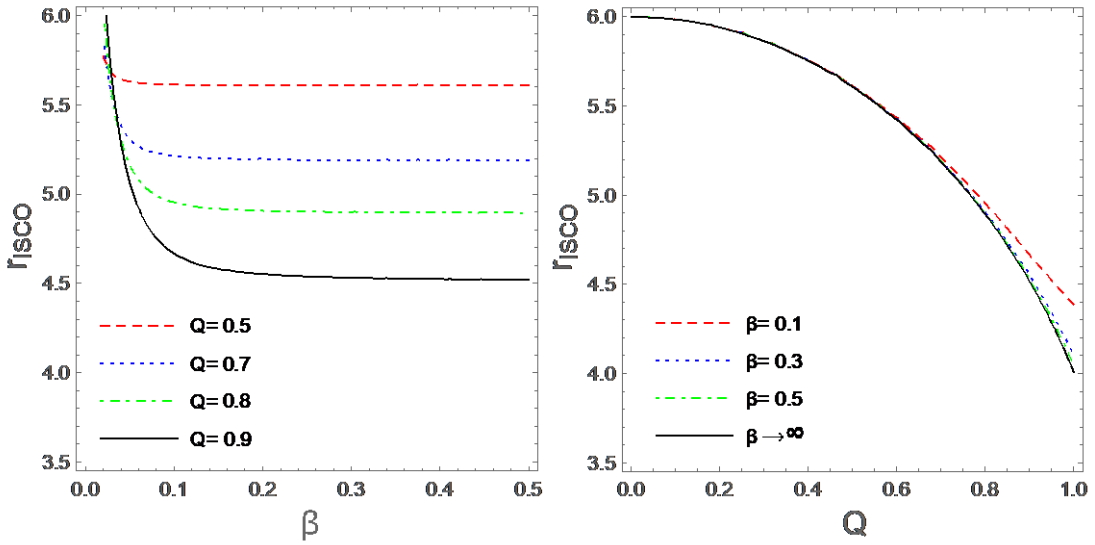

Figure 15: The inner most stable circular orbits by varying the Born-Infeld parameter β and charge Q for a static non-rotating EBI black hole.

$$\frac{E^2_{\text{c.m}}}{2m_0^2} = -\frac{\mathcal{K}}{r^2\Delta}, \quad (130)$$

Table 3: The limiting values of the angular momentum for different extremal cases of a rotating EBI black hole.

Q	β	$Q(r)_{\text{E}}$	a_{E}	r_{H}^{E}	L_1	L_2
0	0	0	1	1	-4.82843	2
0.2	0.2	0.19792	0.98021707	1.00141	-4.80013	2.00327
0.3	0.3	0.296864	0.95491506	1.00304	-4.76386	2.0085
0.4	0.4	0.39579	0.91832659	1.00512	-4.71127	2.01845
0.5	0.5	0.494701	0.86903103	1.00751	-4.64012	2.03709
0.6	0.6	0.593595	0.80470045	1.01008	-4.54673	2.07259
0.7	0.7	0.692477	0.72132723	1.01274	-4.42477	2.1432

Table 4: The limiting values of the angular momentum for different non-extremal cases of a rotatingEBI black hole (Babar, PRD 2021)

Q	β	a	r_{H}^{-}	r_{H}^{+}	L_1	L_2
0.2	0.2	0.9	0.663948	1.38792	-4.74224	2.56572
0.3	0.3	0.8	0.632149	1.52037	-4.64939	2.78645
0.4	0.4	0.7	0.638054	1.59260	-4.54509	2.93519
0.5	0.5	0.6	0.653747	1.62586	-4.42765	3.04241
0.6	0.6	0.5	0.674623	1.62645	-4.29465	3.11902
0.7	0.7	0.3	0.686800	1.65050	-4.04668	3.33159

where K is given as below,

$$\begin{aligned}\mathcal{K} \quad &= -2r^4 + 2r^3 - r^2(2a^2 + Q^2(r) - L_1L_2) \\ &-2a^2r + 2r[a(L_1 + L_2) - L_1L_2] \\ &+Q^2(r)(a - L_1)(a - L_2) \\ &+\sqrt{(a^2 + r^2 - aL_1)^2 - \Delta[r^2 + (a - L_1)^2]} \\ &\times \sqrt{(a^2 + r^2 - aL_2)^2 - \Delta[r^2 + (a - L_2)^2]}\end{aligned} \tag{131}$$

In our discussion, the participating particles have the same intrinsic identities and are mainly distinguished by their angular momenta L_1 and L_2. Here, for the sake of simplicity, weshall take the conserved energies $E_1/m_0=E_2/m_0=1$. It is worth mentioning that an arbitrarily high amount of energy is obtained when the test particle approaching the back hole has the critical angular momentum L_c. The limiting values of the angular momentum along with the corresponding spin parameters and the horizons for the *extremal* and *non-extremal* EBI space-time are presented, respectively, in the Tables (3,4). The $E_{c.m}$ generated as a result of collision near the horizon of an extremal black hole for different values of $Q = \beta$ is shown in Fig. (16). Quite similar to a charged Kerr-Newman gravity, the CM energy instantaneously diverges near the EBI horizon whenever the incoming particle is equipped with the critical parameters of the motion, on the other hand, the particles admitting $L < L_c$ contribute only a finite $E_{c.m}$. Nonetheless, if we consider a collision in a non-extremal space-time background, we attain a limited $E_{c.m}$ irrespective of the event's location, see Fig. (17).

Thermodynamics. In this part of our work, we consider the action for $f(Q)$ gravity, which is given by

$$S = \int \sqrt{-g}d^4x \left[\frac{1}{2}f(Q) + \lambda_\alpha^{\beta\mu\nu}R^\alpha_{\beta\mu\nu} + \lambda_\alpha^{\mu\nu}T^\alpha_{\mu\nu} + L_m\right] \tag{132}$$

where determinant of $g_{\mu\nu}$ is denoted by g, $f(Q)$ is the function of non-metricity Q, $\lambda^{\beta\mu\nu}$ are the multiplier for the Lagrangian, and L_m denotes the matter Lagrangian density. Now, we consider the solution of field equations of $f(Q)$ gravity as a 4-dimensional spherical symmetric and stationary spacetime for the ansatz $f(Q) = Q + \alpha Q^2$, where the coupling constant is denoted with α. The respective line element of black hole in the modified $f(Q)$ gravity is written as

$$ds^2 = g_{tt}dt^2 - g_{rr}dr^2 - r^2d\theta^2 - r^2\sin^2\theta d\phi^2 \tag{133}$$

here the respective metric component ($g_{tt} = 1/g_{rr}$) is defined as [26]

$$g_{tt} = -\frac{\alpha c_2 + \alpha^2(c_3 - 16(3c_6 + c_7)m^2) + 2m}{r} - \frac{(\alpha^2\mu)\log\left(\frac{r}{R}\right)}{r} + 1, \tag{134}$$

with real integrating constants c_1, c_2, c_3 and c_4. Here, m represents the mass of Schwarzschild black hole. Here, the coupling constant is denoted with α and its values must be follows the requirement $|\alpha| < 1$ for the physically acceptable configuration. In this manuscript, we also considered the values of α according to the required range as $|\alpha| < 1$. In order to get a dimensionless argument in the logarithm, a new scale parameter introduced as $\mu = 48m^2c_7$ and a scale R is used to shift the constant $c_6 \rightarrow c_6 - 48m^2c_7 \log(R)$. For $\alpha = 0$, it is reduced to Schwarzschild solution in GR.

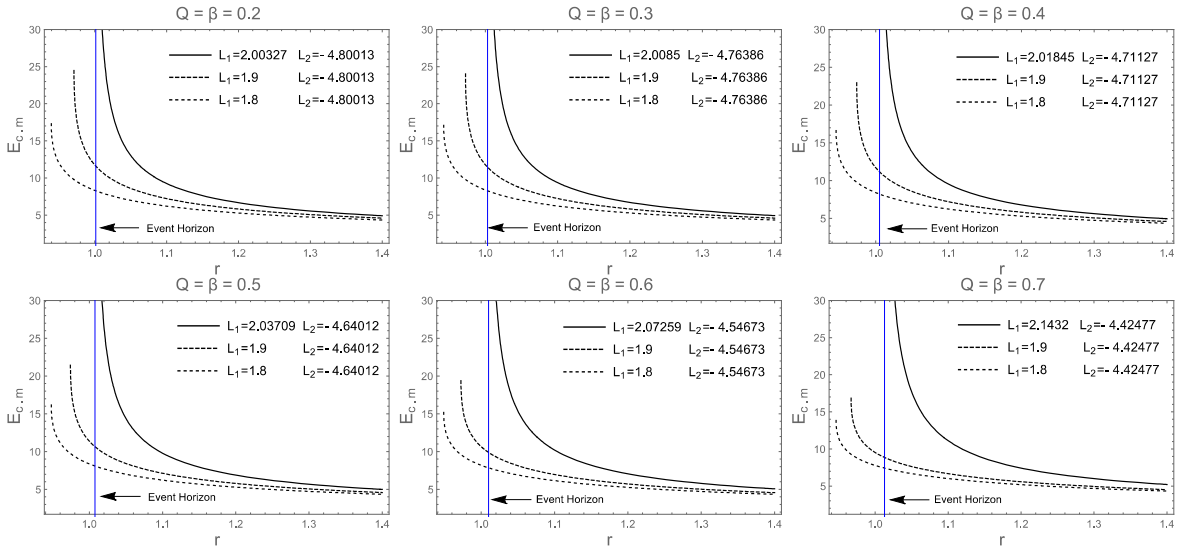

Figure 16: The center-of-mass energy $E_{\text{c.m}}$ dependence of the radial coordinate r for an extremal black hole.

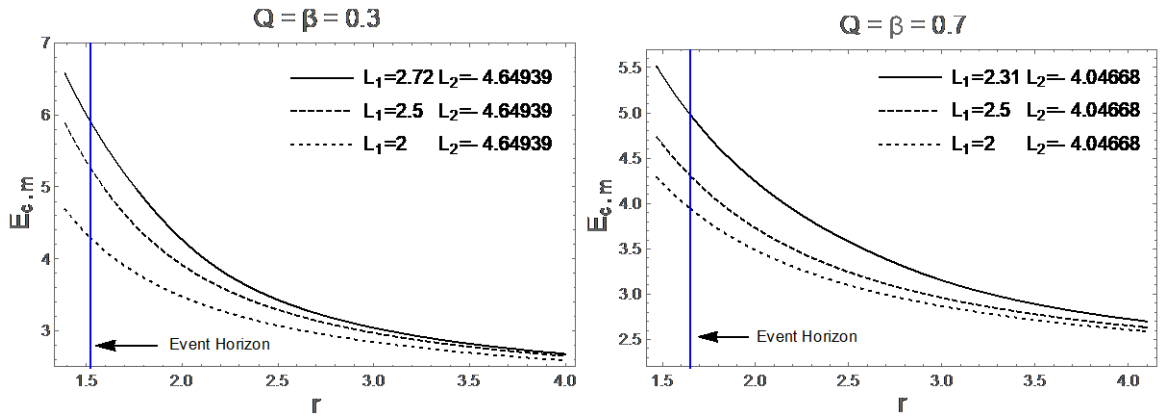

Figure 17: The center-of-mass energy $E_{\text{c.m}}$ dependence of the radial coordinate r for a non- extremal black hole.

The line element given in Eq. (133) with the metric function defined in Eq. (134) is not an exact solution of the theory, it is only a perturbed solution. In this regard, we rewrite the metric function as

$$\mathcal{J}(r) = g_{\text{tt}}|_{\alpha=0} + \alpha\epsilon g_{\text{tt},\alpha} + \alpha^2\epsilon^2 g_{\text{tt},\alpha\alpha}, \tag{135}$$

where $\epsilon \ll 1$ is a tracking parameter. We consider the derivative of the metric function with respect to coupling constant α up to second-order terms. Hence, the

corresponding metric function as a solution of considered geometry with above defined ansatze become

$$\mathcal{J}(r) = 1 - \frac{2m}{r} + \frac{\alpha\epsilon}{r}\left(-2\alpha(c_3 - 16(3c_6 + c_7)m^2) - c_2 - 2\alpha\mu\log\left(\frac{r}{R}\right)\right) + \frac{\alpha^2\epsilon^2}{r}\left(-2(c_3 - 16(3c_6 + c_7)m^2) - 2\mu\log\left(\frac{r}{R}\right)\right) \quad (136)$$

For $\alpha = 0$, it is reduced to Schwarzschild solution in GR and the correction terms might lead to deviations from the Schwarzschild solution at large value of r. By taking $J(r) = 0$, we calculate the position of event horizon in the following form

$$r_h = 2m + \alpha\epsilon\left(Re^{-\frac{c_2}{2\alpha\mu} - \frac{c_3}{\mu} + \frac{16(3c_6+c_7)m^2}{\mu}}\right) + \alpha^2\epsilon^2\left(Re^{\frac{16(3c_6+c_7)m^2}{\mu} - \frac{c_3}{\mu}}\right). \quad (137)$$

Fig. (18) shows the graphical behavior of the metric function for different values of physical parameters. It is noted that the metric function shows symmetric behavior about positive and negative values of coupling constant α. The behavior of the metric function moves from negative to positive as r and α increase while α increases either negatively or positively. The position of event horizon is increased as the mass of black hole increases. TheLeft and right plots of Fig. (19) show the graphical behavior of the position of the event horizon for different values of the mass of Schwarzschild black hole.

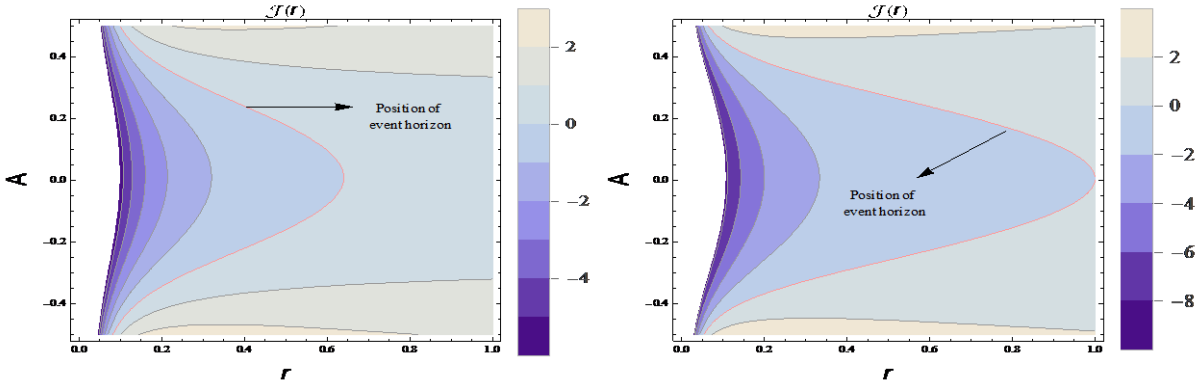

Figure 18: Contour plots of metric function verses coupling constant α and radial coordinate r.

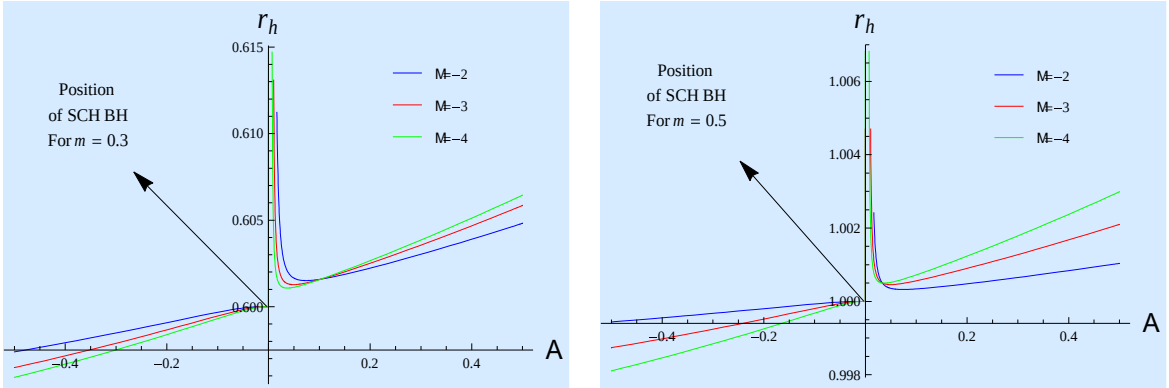

Figure 19: Plots of event horizon verses couplingconstant α.

Here, it is very interesting to mention that the position of Schwarzschild event horizon ($r_h = 2m$) is recovered for $\alpha = 0$,i.e., for $m = 0.3$ and 0.5, we get $r_h = 0.6$ and $r_h = 1$, respectively. It is noted that the event horizon increases as α increases positively. Now, we calculate the thermodynamical quantities of considered black hole, i.e.,Hawking temperature in terms of the mass of black hole and heat capacity. These quantities are used to explore the thermodynamically stable characteristics of the black hole structure. For this purpose, we put J $(r) = 0$, then we get black hole mass in terms of r_h is given as

$$m = \frac{\frac{1}{2}\sqrt{128\alpha^2\left(3c_6+c_7\right)\epsilon(\epsilon+1)\left(\alpha\epsilon\left(2\alpha c_3(\epsilon+1)+c_2\right)+2\alpha^2\mu\epsilon(\epsilon+1)\log\left(\frac{r_h}{R}\right)-r\right)+4}+1}{32\alpha^2\left(3c_6+c_7\right)\epsilon(\epsilon+1)}. \tag{138}$$

Black hole surface gravity ($k = 0.5\, d\mathcal{J}(r)/dr$)is used to determine the Hawking temperature (Hawking, Nature 1974) For the considered structure, it has the following form

$$\kappa = \frac{\alpha\epsilon\left(2\alpha(\epsilon+1)\left(c_3-16\left(3c_6+c_7\right)m^2\right)+c_2\right)+2\left(\alpha^2\mu(-\epsilon)(\epsilon+1)+m+\alpha^2\mu\epsilon(\epsilon+1)\log\left(\frac{r_h}{R}\right)\right)}{2r_h^2}.$$

Hence, we get the Hawking temperature ($\mathbb{T} = k/2\pi$) as

$$\mathbb{T} = \frac{\alpha\epsilon(2\alpha(\epsilon+1)(c_3-16(3c_6+c_7)m^2)+c_2)+2\left(\alpha^2\mu(-\epsilon)(\epsilon+1)+m+\alpha^2\mu\epsilon(\epsilon+1)\log\left(\frac{r_h}{R}\right)\right)}{4\pi r_h^2}. \tag{139}$$

The left plot of Fig. (20) represents the Hawking temperature and it is found that T decreasesas α increases both positively/negatively and decreases for large black holes. Temperature shows symmetric behavior for positive and negative values of coupling constant α.

The entropy of the system is calculated through area entropy relationship of Bekenstein. It is given as

$$\mathbb{S} = \int_0^{2\pi}\int_0^{\pi}\sqrt{g_{\theta\theta}g_{\phi\phi}}d\theta d\phi = \pi r_h^2. \tag{140}$$

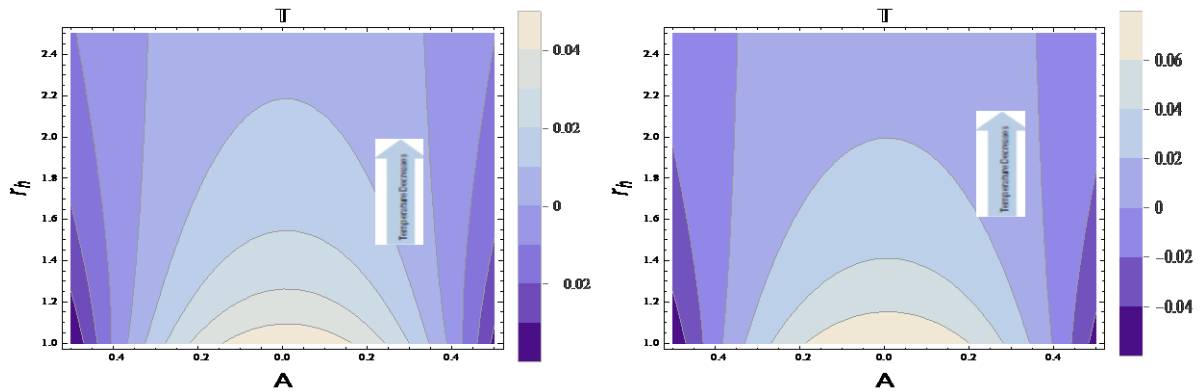

Figure 20: Graphical behavior of Hawking temperature versus r_h and α.

CONCLUSIONS

The following conclusions have been presented on the basis of research carried out on the topic of "Astrophysical processes around compact objects in plasma environment":

1. It has been justified that the size of the horizon of the Kerr–Newman–Kiselev–Letelier black hole increases with the increase of the parameters of quintessence and cloud string. With the increase in the value of the quintessence and cloud string parameters the unsuitability of the photon circular orbits also decreases. It has been also shown that the distortion parameter of shadow decreases with the increase in quintessence and cloud string parameters. The upper limits on the cloud string and quintessence parameters are evaluated using a detailed comparison with the recent observational data from EHT collaboration.
2. The cloud string parameter has been proven to accelerate the Hawking radiation process. It has been proven that with the increase of perfect fluid dark matter parameter, charge and rotation parameter the peak of the effective potential is shifted towards the central object. It has been observed that the size of the black hole shadow decreases with the increase in value of the perfect fluid dark matter parameter as well as the black hole's charge along with a distortion in the shape of the shadow. Accordingly, the size of Einstein rings decreases with the increase of the perfect fluid dark matter parameter.
3. It has been demonstrated that the size of the black hole shadow decreases with increasing axion-plasmon for a distant observer. It is demonstrated that the effects of a homogeneous plasma on the radius of the photon sphere as well as on the radius of the shadow of the black hole are more pronounced than the effects of an inhomogeneous plasma. It has been also stated that for a homogeneous plasma, the deflection angle increases as the axion frequency increases.
4. It has been shown that the singular isothermal sphere deflection angle is greater to a certain extent than that of the non-singular isothermal sphere, even though the difference could be regarded as negligible. It has been stated that the photons deviate at a larger angle when uniform plasma walls are in the black hole. It has been further shown that the effect of plasma results in the increase of the photon sphere radius, the deflection angle and the strong deflection coefficients.
5. It is also shown that with increasing black hole spin the impact of plasma on strong gravitational lensing becomes smaller as the spin parameter increases in the prograde orbit.
6. It has been found that the Hawking temperature of a black hole increases as the coupling parameter of the teleparallel gravity decreases. It has been shown that with increasing the nonlinear charge and coupling parameter the efficiency of accretion decreases. The radiation flux decreases at the singularity and has a maximum position away from the singularity in the vicinity of the strong field.

НАУЧНЫЙ СОВЕТ DSc.03/31.03.2022.T/FM.10.04 ПО ПРИСУЖДЕНИЮ УЧЕНЫХ СТЕПЕНЕЙ ПРИ ИНСТИТУТЕ ФУНДАМЕНТАЛЬНЫХ И ПРИКЛАДНЫХ ИССЛЕДОВАНИЙ, «ТИИИМСХ» НАЦИОНАЛЬНЫЙ ИССЛЕДОВАТЕЛЬСКИЙ УНИВЕРСИТЕТ

ИНСТИТУТЕ ФУНДАМЕНТАЛЬНЫХ И ПРИКЛАДНЫХ ИССЛЕДОВАНИЙ

АТАМУРОТОВ ФАРРУХ ШУХРАТОВИЧ

АСТРОФИЗИЧЕСКИЕ ПРОЦЕССЫ В ОКРЕСТНОСТИ КОМПАКТНЫХ ОБЪЕКТОВ В ПЛАЗМЕННОЙ СРЕДЕ

01.03.01 – Астрономия
01.04.02 – Теоретическая физика
(физико-математические науки)

ПРЕДСТАВЛЕНИЕ
по присуждению ученой степени доктора наук (DSc) на основе научных публикаций без диссертации

Ташкент – 2023

Тема диссертации доктора наук (DSc) по физико-математическим наукам зарегистрирована в Высшей аттестационной комиссии при Министерстве высшего образования, науки и инноваций Республики Узбекистан под номером B2023.2.DSc/FM224.

Работа выполнена в институте фундаментальных и прикладных исследований при НИУ “ТИИМСХ”.

Представление на трех языках (узбекский, английский, русский (резюме)) размещен на веб-странице Научного совета (www.ifar.uz) и Информационно-образовательном портале «Ziyonet» (www.ziyonet.uz).

Научные консультанты: **Абдужаббаров Ахмаджон Адилжанович**
доктор физико-математических наук, профессор

Ахмедов Бобомурат Жураевич
доктор физико-математических наук, профессор

Представление научного исследования состоится «**01**» **августа 2023 года в 17^{00} часов** на заседании Научного Совета **DSc.03/31.03.2022.T/FM.10.04** по защите диссертаций на соискание ученых степеней при Институте фундаментальных и прикладных исследований, “ТИИИМСХ” Национальный Исследовательский университет по адресу: 100000, г. Ташкент, Qori Niyaziy Street 39, Институт фундаментальных и прикладных исследований, Зал 108; Тел.: 71 237-09-61; email: info@ifar.uz.

С представлением научного исследованияможно ознакомиться в Информационно-ресурсном центре при Институте фундаментальных и прикладных исследований, “ТИИИМСХ” Национальный Исследовательский университет (регистрационный номер ____) (Адрес: 100000, г. Ташкент, Qori Niyaziy Street 39, Институт фундаментальных и прикладных исследований, Зал 205; Тел.: 71 237-09-61).

Представление научного исследования разослано «____» _____ 2023 г.
(протокол рассылки № 49 от __ _____ 2023 г.).

А.Р. Хаётов
Заместитель председателя
Научного совета по присуждению
ученых степеней, д.ф.-м.н., профессор

Э. Х. Каримбаев
ученый секретарь Научного совета
по присуждению ученых степеней
доктор философии (PhD) ф.-м.н.

ВВЕДЕНИЕ (Аннотация к представлению)

Целью исследования является разработка и усовершенствование модели динамики фотонов и слабого гравитационного линзирования вокруг компактного объекта в присутствии плазмы, ограничения на параметры гравитационных моделей с помощью наблюдений.

Задачи исследования:

изучить движения фотона и связанных с ним явлений тени черной дыры в пространстве-времени черной дыры Керра – Ньюмена – Киселева – Летелье;

исследование влияние параметра облака струны и параметра квинтэссенции на движение фотона и тень черной дыры;

исследование эффективного потенциала фотона при наличии параметров квинтэссенции и облачной струны;

получить верхние пределы на параметры облачной струны и квинтэссенции в случае черной дыры Керра–Ньюмена–Киселева–Летелье;

изучить влияние спина и заряда черной дыры Керра-Ньюмена-Киселева-Летелье на скорость излучения энергии;

изучить влияние параметра облачной струны на процесс излучения Хокинга;

проанализировать влияние параметра темной материи идеальной жидкости на динамику фотонов и связанные с ними процессы вокруг черной дыры;

изучить скорость излучения при наличии параметра темной материи идеальной жидкости и нелинейного заряда;

проанализировать влияние аксион-плазмона на динамику фотонов вокруг невращающейся черной дыры;

изучить влияние однородной и неоднородной плазмы на движение фотонов и гравитационное линзирование вокруг гравитирующих объектов;

провести анализ явления линзирования слабого поля на фоне гравитирующих объектов, окруженных однородной плазмой, сингулярной изотермической сферой и неособой изотермической сферой;

исследовать поведение температуры Хокинга для телепараллельной гравитации;

проанализировать влияние нелинейного заряда и параметра связи в нелинейной электродинамике, связанной с общей теорией относительности, на эффективность аккреции;

Объектом исследования являются астрофизические компактные объекты, фотоны, плазменная среда.

Предметом исследования являются теоретические модели исследования динамики фотонов вблизи компактных гравитационных объектов в присутствии плазмы, численные и аналитические методы решения дифференциальных уравнений.

Методами исследования являются методы вычислительной математики, методы теоретической астрофизики, современные методы математической физики, аналитические и численные методы расчета дифференциальных уравнений для поля и движения частиц.

Научная новизна исследования заключается в следующем:

Показано, что размер горизонта черной дыры Керра-Ньюмена-Киселева-Летелье увеличивается с увеличением параметров квинтэссенции и облачной струны.

Анализ эффективного потенциала фотона показал, что он уменьшается с увеличением значений параметров квинтэссенции и облачной струны. С ростом значений параметров квинтэссенции и облачной струны непригодность круговых орбит фотонов также уменьшается.

Показано, что параметр облачной струны ускоряет процесс излучения Хокинга. Показано, что с увеличением параметра темной материи идеальной жидкости, параметра заряда и вращения пик эффективного потенциала смещается влево.

Показано, что скорость излучения выше при малом значении как параметра темной материи идеальной жидкости, так и заряда. Было показано, что размер тени черной дыры уменьшается с увеличением аксион-плазмона для большого расстояния наблюдателя, и, что интересно, это было показано ранее и для случая неоднородной плазмы.

Показано, что для однородной плазмы угол отклонения увеличивается с увеличением частоты аксиона. Показано, что угол отклонения сингулярной изотермической сферы в некоторой степени больше, чем у неособой изотермической сферы, хотя различие можно было бы считать незначительным.

Показано, что фотоны отклоняются на больший угол, когда однородная плазма стенок в черной дыре. Далее было показано, что влияние плазмы приводит к увеличению радиуса фотонной сферы, угла отклонения и сильных коэффициентов отклонения.

Показано, что температура Хокинга увеличивается с уменьшением параметра связи телепараллельной гравитации. Показано, что с увеличением нелинейного заряда и параметра связи эффективность аккреции снижается.

Практические результаты исследования следующие:

Показано, что параметр искажения тени уменьшается с увеличением параметров квинтэссенции и облачной струны. Было показано, что тень, отбрасываемая быстровращающейся и сильно заряженной черной дырой, будет более искаженной. Это наблюдение может быть полезным для оценки значений спина a и заряда черных дыр.

Показано, что размер тени в случае невращающейся черной дыры уменьшается с увеличением значения параметра темной материи идеальной жидкости, а также заряда черной дыры.

Используя данные коллаборации Event Horizon Telescope, получены верхние пределы на параметры облачной струны и квинтэссенции в случае черной дыры Керра-Ньюмена-Киселева-Летелье.

Показано, что размер колец Эйнштейна уменьшается с увеличением параметра темной материи идеальной жидкости.

Достоверность результатов исследований обеспечивается применением современных апробированных методов математической физики, вычислительной математики и релятивистской астрофизики. Результаты были получены строго в рамках математического аппарата общей теории относительности и теоретической физики. Также используются современные численные и аналитические методы расчета, результаты сравниваются с имеющимися данными наблюдений и результатами других авторов. Структурированные выводы диссертации соответствуют основным правилам астрофизики компактных объектов.

Научная и практическая значимость результатов исследования. Научная значимость результатов исследования заключается в том, что анализ тени, отбрасываемой быстровращающейся и заряженной черной дырой, может быть полезен для оценки значений спина a и заряда черных дыр.

Практическая значимость результатов исследований заключается в том, что они могут сыграть роль в получении верхних пределов и ограничений на параметры облачной струны и квинтэссенции в рамках модифицированной теории гравитации.

Внедрение результатов исследования. На основе разработанных теоретических моделей динамики фотонов вокруг компактных объектов в присутствии плазмы:

научные результаты, полученные в отношении движения фотонов, были использованы учеными из Фуданьского университета (FU) в Шанхае (справочник FU, Китай, 7 июля 2023 г.);

результаты по гравитационному линзированию вокруг компакта использовались в работах зарубежных исследователей, в зарубежных журналах с высоким импакт-фактором (Physical Review D, 2023, Volume 107, Issue 12, article id.124003, Web-Sc, IF: 5.407 Ежемесячные уведомления Королевского астрономического общества, том 521, выпуск 1, стр. 708-716, Web-Sc, IF: 4.8, Physics of the Dark Universe, том 41, номер статьи 101249, Web-Sc, IF: 5.5 ; The European Physical Journal C, том 83, выпуск 5, номер статьи 426, Web-Sc, IF: 4.4; The European Physical Journal Plus, том 138, выпуск 3, номер статьи 192, Web-Sc, IF: 3.4. Журнал космологии и физики астрочастиц, том 2021, выпуск 10, номер 013, 26 стр, Web-Sc, IF: 7.28), чтобы описать влияние плазмы на движение фотонов вокруг компактных объектов.

Публикация результатов исследований. Результаты исследования доктора наук представлены в 24 рецензируемых статьях, опубликованных в престижных научных журналах, рекомендованных Высшей

аттестационной комиссией при Министерстве высшего образования, науки и инноваций Республики Узбекистан.

ВЫВОДЫ

На основе исследований, проведенных по теме «Астрофизические процессы вокруг компактных объектов в плазменной среде», сделаны следующие выводы:

1. Показано, что размер горизонта черной дыры Керра-Ньюмена-Киселева-Летелье увеличивается с увеличением параметров квинтэссенции и облачной струны. С увеличением значения параметров квинтэссенции и облачной струны непригодность круговых орбит фотонов также уменьшается. Показано также, что параметр искажения тени уменьшается с увеличением параметров квинтэссенции и облачной струны. Верхние пределы параметров цепочки облаков и квинтэссенции оцениваются с использованием подробного сравнения с последними данными наблюдений коллаборации EHT.
2. Показано, что параметр облачной струны ускоряет процесс излучения Хокинга. Доказано, что с увеличением параметра темной материи идеальной жидкости, параметра заряда и вращения пик эффективного потенциала смещается в сторону центрального объекта. Было замечено, что размер тени черной дыры уменьшается с увеличением значения параметра темной материи идеальной жидкости, а также заряда черной дыры вместе с искажением формы тени. Соответственно размер колец Эйнштейна уменьшается с увеличением параметра темной материи идеальной жидкости.
3. Продемонстрировано, что размер тени черной дыры уменьшается с увеличением аксиона-плазмона для удаленного наблюдателя. Показано, что влияние однородной плазмы на радиус фотонной сферы, а также на радиус тени черной дыры выражено сильнее, чем влияние неоднородной плазмы. Было также заявлено, что для однородной плазмы угол отклонения увеличивается с увеличением частоты аксиона.
4. Показано, что угол отклонения сингулярной изотермической сферы в некоторой степени больше, чем у неособой изотермической сферы, хотя различие можно было бы считать незначительным. Установлено, что фотоны отклоняются на больший угол, когда в черной дыре находятся однородные плазменные стенки. Далее было показано, что влияние плазмы приводит к увеличению радиуса фотонной сферы, угла отклонения и сильных коэффициентов отклонения.

5. Также показано, что с увеличением спина черной дыры влияние плазмы на сильное гравитационное линзирование становится меньше по мере увеличения параметра спина на прямой орбите.
6. Обнаружено, что температура Хокинга черной дыры увеличивается с уменьшением параметра связи телепараллельной гравитации. Показано, что с увеличением нелинейного заряда и параметра связи эффективность аккреции снижается. Поток излучения убывает на сингулярности и имеет максимальное положение вдали от сингулярности в окрестности сильного поля.

E'LON QILINGAN ISHLAR RO'YXATI
СПИСОК ОПУБЛИКОВАННЫХ РАБОТ
LIST OF PUBLISHED WORKS

Included in PhD Dissertation

1. Atamurotov F., Abdujabbarov A., Ahmedov B., Shadow of rotating non-Kerr black hole // Physical Review D, Volume 88, Issue 6, article id.064004 (2013) (№1 Web of Science, IF: 5.407).
2. Abdujabbarov A., Atamurotov F., Kucukakca Y., Ahmedov B., Camci U., Shadow of Kerr-Taub-NUT black hole // Astrophysics and Space Science, Volume 344, Issue 2, pp.429-435 (2013) (№1 Web of Science, IF: 1.9)
3. Atamurotov F., Ahmedov B., Shaymatov S., Formation of black holes through BSW effect and black hole-black hole collisions // Astrophysics and Space Science, Volume 347, Issue 2, pp.277-281 (2013) (№1 Web of Science, IF: 1.9).
4. Atamurotov F., Abdujabbarov A., Ahmedov B., Shadow of rotating Hořava-Lifshitz black hole // Astrophysics and Space Science, Volume 348, Issue 1, pp.179-188 (2013) (№1 Web of Science, IF: 1.9).
5. Shaymatov S., Atamurotov F., Ahmedov B., Isofrequency pairing of circular orbits in Schwarzschild spacetime in the presence of magnetic field // Astrophysics and Space Science, Volume 350, Issue 1, pp.413-419 (2014) (№1 Web of Science, IF: 1.9).
6. Papnoi U., Atamurotov F., Ghosh S. G., Ahmedov B., Shadow of five-dimensional rotating Myers-Perry black hole // Physical Review D, Volume 90, Issue 2, id.024073 (2014) (№1 Web of Science, IF: 5.407).
7. Abdujabbarov A., Atamurotov F., Dadhich N., Ahmedov B., Stuchlik Z., Energetics and optical properties of 6-dimensional rotating black hole in pure Gauss-Bonnet gravity // The European Physical Journal C, Volume 75, article id.399, 11 pp. (2015) (№1 Web of Science, IF: 4.4).
8. Atamurotov F., Ahmedov B., Abdujabbarov A., Optical properties of black holes in the presence of a plasma: The shadow // Physical Review D, Volume 92, Issue 8, id.084005 (2015) (№1 Web of Science, IF: 5.407).
9. Hakimov A., Atamurotov F., Gravitational lensing by a non-Schwarzschild black hole in a plasma // Astrophysics and Space Science, Volume 361, article id.112, 7 pp. (2016) (№1 Web of Science, IF: 1.9).
10. Abdujabbarov A., Atamurotov F., Dadhich N., Ahmedov B., Stuchlik Z., Horizon structure of rotating Einstein-Born-Infeld black holes and shadow // The European Physical Journal C, Volume 76, Issue 5, article id.273, 16 pp. (2016) (№1 Web of Science, IF: 4.4).
11. Abdujabbarov A., Ahmedov B., Dadhich N., Atamurotov F., Optical properties of a braneworld black hole: Gravitational lensing and retrolensing // Physical Review D, Volume 96, Issue 8, id.084017 (2017) (№1 Web of Science, IF: 5.407).

I bo'lim (part I; I часть)

1. Ditta A., Tiecheng X., Mumtaz S., Atamurotov F., Mustafa G., Abdujabbarov A., Testing metric-affine gravity using particle dynamics and photon motion // Physics of the Dark Universe, Volume 41, article id. 101248 (2023) (№1 Web of Science, IF: 5.5).
2. Ditta A., Tiecheng X., Atamurotov F., Mustafa G. Aripov M., Particle dynamics and weak gravitational lensing around nonlinear electrodynamics black hole // Chinese Journal of Physics, Vol. 83, pp. 664-679 (2023) (№1 Web of Science, IF: 5.0).
3. Ditta A., Tiecheng X., Ali R., Atamurotov F., Mahmood A., Mumtaz S., Thermodynamic stability of the regular charged torus-like black hole // Annals of Physics, Volume 453, article id. 169326 (2023) (№1 Web of Science, IF: 3.0).
4. Mustafa G., Atamurotov F., Ghosh S. G., Structural properties of generalized embedded wormhole solutions via dark matter halos in Einsteinian-cubic-gravity with quasi-periodic oscillations // Physics of the Dark Universe, Volume 40, article id. 101214 (2023) (№1 Web of Science, IF: 5.5).
5. Javed F., Mustafa G., Mumtaz S., Atamurotov F., Thermal analysis with emission energy of perturbed black hole in f(Q) gravity // Nuclear Physics B, Volume 990, article id. 116180 (2023) (№1 Web of Science, IF: 2.8).
6. Ghorani E., Pulice B., Atamurotov F., Rayimbaev J., Abdujabbarov A., Demir D., Probing geometric proca in metric-palatini gravity with black hole shadow and photon motion // The European Physics Journal C, Volume 83, Issue 4, article id. 318 (2023) (№1 Web of Science, IF: 4.4).
7. Atamurotov F., Jamil M., Jusufi K., Quantum effects on the black hole shadow and deflection angle in the presence of plasma // Chinese Physics C, Volume 47, Issue 3, id. 035106, 11p (2023) (№1 Web of Science, IF: 2.944).
8. Mustafa G., Hussain I., Atamurotov F., Liu W. M., Imprints of dark matter on wormhole geometry in modified teleparallel gravity // The European Physics Journal Plus, Volume 138, Issue 2, article id. 166 (2023) (№1 Web of Science, IF: 3.4).
9. Atamurotov F., Hussain I., Mustafa G., Ovgun A., Weak deflection angle and shadow cast by the charged-Kiselev black hole with cloud of strings in plasma // Chinese Physics C, Volume 47, Issue 2, id. 025102, 23p (2023) (№1 Web of Science, IF: 2.944).
10. Atamurotov F., Hussain I., Mustafa G., Jusufi K., Shadow and quasinormal modes of the Kerr-Newman-Kiselev-Letelier black hole // The European Physics Journal C, Vol. 82, Issue 9, article id. 831 (2022) (№1 Web of Science, IF: 4.4).
11. Ditta A., Tiecheng X., Mustafa G., Yasir M., Atamurotov F., Thermal stability with emission energy and Joule-Thomson expansion of regular BTZ-like black hole // The European Physics Journal C, Volume 82, Issue 8, article id. 756 (2022) (№1 Web of Science, IF: 4.4).

12. Atamurotov F., Ghosh S. G., Gravitational weak lensing by a naked singularity in plasma // The European Physics Journal Plus, Volume 137, Issue 6, article id. 662 (2022) (№1 Web of Science, IF: 3.4).
13. Papnoi U., Atamurotov F., Rotating charged black hole in 4 D Einstein-Gauss-Bonnet gravity: Photon motion and its shadow // Physics of the Dark Universe, Volume 35, article id. 100916 (2022) (№1 Web of Science, IF: 5.5).
14. Atamurotov F., Papnoi U., Jusufi K., Shadow and deflection angle of charged rotating black hole surrounded by perfect fluid dark matter // Classical and Quantum Gravity, Volume 39, Issue 2, id. 025014, 20 pp (2022) (№1 Web of Science, IF: 3.5).
15. Atamurotov F., Abdujabbarov A., Han W. B., Effect of plasma on gravitational lensing by a Schwarzschild black hole immersed in perfect fluid dark matter // Physical Review D, Volume 104, Issue 8, article id.084015 (2021) (№1 Web of Science, IF: 5.407).
16. Atamurotov F., Jusufi K., Jamil M., Abdujabbarov A., Azreg-Ainou M., Axion-plasmon or magnetized plasma effect on an observable shadow and gravitational lensing of a Schwarzschild black hole // Physical Review D, Volume 104, Issue 6, article id.064053 (2021) (№1 Web of Science, IF: 5.407).
17. Babar G. Z., Atamurotov F., Babar A. Z., Gravitational lensing in 4-D Einstein-Gauss-Bonnet gravity in the presence of plasma // Physics of the Dark Universe, Volume 32, article id. 100798 (2021) (№1 Web of Science, IF: 5.5).
18. Babar G. Z., Atamurotov F., Ul Islam Sh., Ghosh S. G., Particle acceleration around rotating Einstein-Born-Infeld black hole and plasma effect on gravitational lensing // Physical Review D, Volume 103, Issue 8, article id.084057 (2021) (№1 Web of Science, IF: 5.407).
19. Atamurotov F., Abdujabbarov A., Rayimbaev J., Weak gravitational lensing Schwarzschild-MOG black hole in plasma // The European Physics Journal C, Volume 81, Issue 2, article id. 118 (2021) (№1 Web of Science, IF: 4.4).
20. Abdujabbarov A., Rayimbaev J., Atamurotov F., Ahmedov B., Magnetized Particle Motion in γ-Spacetime in a Magnetic Field // Galaxies, Volume 8, Issue 4, p76 (2020) (№1 Web of Science, IF:2.5).
21. Babar G. Z., Babar A. Z., Atamurotov F., Optical properties of Kerr-Newman spacetime in the presence of plasma // The European Physics Journal C, Volume 80, Issue 8, article id. 761 (2020) (№1 Web of Science, IF: 4.4).
22. Atamurotov F., Alloqulov M., Abdujabbarov A., Testing the Einstein-Æther gravity: particle dynamics and gravitational lensing // The European Physics Journal Plus, Volume 137, Issue 5, article id. 634 (2022) (№1 Web of Science, IF: 3.4).
23. Atamurotov F., Sarikulov F., Abdujabbarov A., Ahmedov B., Gravitational weak lensing by black hole in Horndeski gravity in presence of plasma // The European Physics Journal Plus, Volume 137, Issue 3, article id. 336 (2022) (№1 Web of Science, IF:3.4).

24. Abdujabbarov A., Rayimbaev J., Turimov B., Atamurotov F., Dynamics of magnetized particles around 4-D Einstein Gauss–Bonnet black hole // Physics of the Dark Universe, Volume 30, article id. 100715 (2020) (№1 Web of Science, IF: 5.5).

“Fan va innovatsiyalar” xalqaro ilmiy jurnali (International scientific journal “Science and Innovation”) tahririyatida tahrirdan o‘tkazilib, o‘zbek, ingliz va rus tillaridagi matnlari o‘zaro muvofiqlashtirildi (20.07.2023).

№ 1400

Bosishga ruxsat etildi: 20.07.2023
Bichimi: 60x84 $^{1}/_{16}$ «Times New Roman»
Garniturada raqamli bosma usulda bosildi.
Shartli bosma tabog‘i 5,75 Adadi 100. Buyurtma: № 49/3
«Innovatsion rivojlanish nashriyot-matbaa uyi »
bosmaxonasida chop etildi.
100174, Toshkent sh., Olmazor tumani Universitet ko‘chasi, 7-uy.